PB-240 398

COMPACT SAMPLING SYSTEM FOR COLLECTION OF PARTICULATES FROM STATIONARY SOURCES

Carl G. Ringwall

General Electric Company

Prepared for:

National Environmental Research Center

April 1974

DISTRIBUTED BY:

NTIS
National Technical Information Service
U. S. DEPARTMENT OF COMMERCE

TECHNICAL REPORT DATA

(Please read Instructions on the reverse before completing)

1. REPORT NO. EPA-650/2-74-029	2.	PB 240 398
4. TITLE AND SUBTITLE Compact Sampling System for Collection of Particulates from Stationary Sources		5. REPORT DATE April, 1974
		6. PERFORMING ORGANIZATION CODE
7. AUTHOR(S) Carl G. Ringwall		8. PERFORMING ORGANIZATION REPORT NO.
9. PERFORMING ORGANIZATION NAME AND ADDRESS General Electric Company P.O. Box 431, Bldg. 37 Schenectady, New York 12301		10. PROGRAM ELEMENT NO. 1AA010
		11. CONTRACT/GRANT NO. 68-02-0546
12. SPONSORING AGENCY NAME AND ADDRESS EPA, Chemistry & Physics Laboratory National Environmental Research Center Research Triangle Pk., N.C. 27711		13. TYPE OF REPORT AND PERIOD COVERED Final Report
		14. SPONSORING AGENCY CODE

15. SUPPLEMENTARY NOTES

16. ABSTRACT

This report summarizes the work performed on a program to design, fabricate, and evaluate a controller for automatically sensing and maintaining isokinetic conditions at the inlet of a particulate sampling nozzle.

The key components developed on the program were the gas velocity sensor and a fluidic control amplifier. The sensor concept is based on a static pressure differential between the free air stream and the nozzle inlet. The fluidic control amplifier which interfaces directly with the sensor provides the control to automatically maintain isokinetic conditions.

Field tests were performed on the engineering prototype system at both oil-fired and coal-fired power plant installations. Results of these tests showed that the sensor and controller can function with no degradation in performance under the adverse environment of representative power plant stacks. Temperatures up to 205°C and solid particulate concentrations of 3.50 grams per cubic meter were encountered during the field testing.

Reproduced by
NATIONAL TECHNICAL
INFORMATION SERVICE
US Department of Commerce
Springfield, VA. 22151

PRICES SUBJECT TO CHANGE

17. KEY WORDS AND DOCUMENT ANALYSIS

a. DESCRIPTORS	b. IDENTIFIERS/OPEN ENDED TERMS	c. COSATI Field/Group
Isokinetic Sampling Automatic Isokinetic Sampling EPA Train Sampling Stationary Source SAmpling	Pollution Monitoring Particulates Stack Monitoring Mass Concentration	

18. DISTRIBUTION STATEMENT Release Unlimited	19. SECURITY CLASS *(This Report)* Unclassified	21. NO. OF PAGES 108
	20. SECURITY CLASS *(This page)* Unclassified	22. PRICE $5.25/2.25

EPA Form 2220-1 (9-73)

EPA-650/2-74-029

COMPACT SAMPLING SYSTEM FOR COLLECTION OF PARTICULATES FROM STATIONARY SOURCES

by

Carl G. Ringwall

General Electric Company
P.O. Box 43, Bldg. 37
Schenectady, N. Y. 12301

Contract No. 68-02-0546
Program Element No. 1A1010

Project Officer: John W. Davis

Chemistry and Physics Laboratory
National Environmental Research Center
Research Triangle Park, N. C. 27711

Prepared for

OFFICE OF RESEARCH AND DEVELOPMENT
ENVIRONMENTAL PROTECTION AGENCY
WASHINGTON, D.C. 20460

April 1974

i a

This report has been reviewed by the Environmental Protection Agency and approved for publication. Approval does not signify that the contents necessarily reflect the views and policies of the Agency, nor does mention of trade names or commercial products constitute endorsement or recommendation for use.

TABLE OF CONTENTS

Section		Page
1	INTRODUCTION	1-1
2	RESULTS, CONCLUSIONS AND RECOMMENDATIONS	2-1
	2.1 Results	2-1
	2.2 Conclustions	2-2
	2.3 Recommendations	2-3
3	TECHNICAL DISCUSSION	3-1
	3.1 Function Description of Automatic Sampler	3-1
	3.2 Sensors	3-4
	3.3 Hardware Development	3-10
	3.3.1 Flow Control Valve	3-10
	3.3.2 Fluidic Control Amplifier	3-12
	3.3.3 Flow Rate and Flow Totalizing	3-21
	3.3.4 Vacuum Pump Selection	3-22
	3.4 Hardware Description	3-22
	3.5 System Setup and Operation	3-28
4	TEST PROGRAM	4-1
	4.1 Dynamic Laboratory Tests	4-1
	4.2 Steady-State Tests	4-3
	4.3 Field Tests	4-15
	4.3.1 Preliminary Field Test	4-15
	4.3.2 Field Test on Engineering Prototype	4-23
	APPENDIX I	A-1
	Sensor Test Results	A-1
	Differential Static Sensor	A-1
	Co-Flow Sensor	A-3
	Cross-Flow Sensor	A-17
	APPENDIX II	A-25
	Controller Parts Identification	A-25

LIST OF FIGURES

Number	Title	Page
3-1	Block Diagram of Sampler	3-2
3-2	Control Model of Sampling Case	3-3
3-3	Transfer Characteristics of Sampling Case	3-5
3-4	Block Diagram of Controller and Sampling Case	3-6
3-5	Sensor Configurations	3-8
3-6	Flow Control Valve Characteristics	3-11
3-7	Control Valve Schematic	3-13
3-8	Throttle Valve Response	3-14
3-9	Steady-State Characteristics of Control Valve	3-15
3-10	Sensor-Amplifier Interface	3-17
3-11	Fluidic Amplifier Schematic	3-19
3-12	Fluidic Amplifier Characteristics	3-20
3-13	Sample Case Flow Vs. Vacuum	3-23
3-14	Functional Block Location	3-24
3-15	Fluidic Controller and Sampling Case	3-25
3-16	$\frac{1}{4}$ Inch Sampling Nozzle and Sensor	3-26
3-17	3/8 Inch Sampling Nozzle and Sensor	3-27
3-18	Fluidic Controller	3-29
3-19	Control Console	3-30
3-20	Pump and Flow Meter	3-31
4-1	Dynamic Test Setup	4-2
4-2	Dynamic Response at Various Gain Settings	4-4
4-3	Dynamic Response - 20 Ft/Sec	4-5
4-4	Dynamic Response - 80 Ft/Sec	4-6
4-5	Steady-State Controller Error-3/8 Inch Nozzle	4-7
4-6	Steady-State Controller Error-$\frac{1}{4}$ Inch Nozzle	4-8
4-7	Controller Error Vs. Supply Pressure	4-10
4-8	Controller Error Vs. Velocity for ±20% Supply Variation	4-11
4-9	Sampling Error Vs. Filter Pressure Drop-3/8 Inch Nozzle	4-12
4-10	Steady-State Calibration-3/8 Inch Nozzle	4-13
4-11	Steady-State Calibration-$\frac{1}{4}$ Inch Nozzle	4-14
4-12	3/8 Inch Diameter Sampling Nozzle	4-17

LIST OF FIGURES (cont.)

Number	Title	Page
4-13	¼ Inch Diameter Sampling Nozzle	4-18
4-14	Calibration Runs-3/8 Inch Diameter Nozzle	4-19
4-15	Calibration Runs-¼ Inch Diameter Nozzle	4-20
4-16	3/8 Inch Nozzle	4-21
4-17	¼ Inch Nozzle	4-22
4-18	Velocity Ratio Vs. Time on Coal-Fired Installation	4-25
4-19	Fluidic Controller Output Pressure Vs. Time	4-26
A-1	Differential Static Sensor Configurations	A-1
A-2	Differential Static Sensor Characteristics-3/8 Inch Nozzle	A-4
A-3	Differential Static Sensor Characteristics-¼ Inch Nozzle	A-5
A-4	Effect of Non-Isokinetic Probe Flow on Static Differential Sensor Reading	A-6
A-5	Static Sensor Noise	A-7
A-6	Co-Flow Sensor Gain	A-8
A-7	Co-Flow Sensor Noise	A-9
A-8	Co-Flow Sensor Gain/Null Bias Ratio	A-10
A-9	Difference in Two Co-Flow Sensor Indications	A-11
A-10	Co-Flow Sensor Noise Vs. Bandwidth	A-12
A-11	Velocity Acceleration at Nozzle Inlet	A-13
A-12	Velocity Acceleration at Nozzle Inlet	A-14
A-13	Co-Flow Sensor Output Vs. Velocity	A-15
A-14	Cross-Flow Signal Upstream Receiver	A-18
A-15	Cross-Flow Signal Downstream Receiver	A-19
A-16	Velocity Deceleration at Inlet	A-20
A-17	Velocity Deceleration at Inlet	A-21
A-18	Velocity Deceleration at Inlet	A-22
A-19	Cross-Flow Sensor Noise Vs. Bandwidth	A-24
A-20	Fluidic Controller-Front Face	A-26
A-21	Fluidic Controller-Back Face	A-27
A-22	Control Console Connectors	A-28
Table 1	Controller Gain Setting	3-33
Table 2	Parts Identification	A-29
Table 3	Inlet-Outlet Connectors	A-30

ENGLISH TO METRIC CONVERSIONS

English Units	Metric Units
SCFM	28.317 Liters/min
PSI	6895 Newtons/meter^2
ft	3.048(10^{-1}) meter
ft^3	2.831(10^{-2}) meter^3
#/in	175.125 Newtons/meter
in/sec	2.54(10^{-2}) meters/sec
psi/ft/sec	22622 Newton sec/meter^3
in^2	6.45(10^{-4}) meter^2
#/in^3	61023.4 Newtons/meter^3
sec/in^2	1550 sec/meter^2
inches H_2O	249.1 Newtons/meter^2

ABSTRACT

This report summarizes the work performed on a program to design, fabricate, and evaluate a controller for automatically sensing and maintaining isokinetic conditions at the inlet of a particulate sampling nozzle.

The key components developed on the program were the gas velocity sensor and a fluidic control amplifier. The sensor concept is based on a static pressure differential between the free air stream and the nozzle inlet. The fluidic control amplifier which interfaces directly with the sensor provides the control to automatically maintain isokinetic conditions.

Field tests were performed on the engineering prototype system at both oil-fired and coal-fired power plant installations. Results of these tests showed that the sensor and controller can function with no degradation in performance under the adverse environment of representative power plant stacks. Temperatures up to 205°C and solid particulate concentrations of 3.50 grams per cubic meter were encountered during the field testing.

1. INTRODUCTION

This report summarizes all work under Contract 68-02-0546, Compact Sampling System for Collection of Particulates from Stationary Sources. An engineering prototype system capable of automatically maintaining isokinetic sampling conditions that can be interfaced with presently available air pollution control sampling trains and Beta gauge monitors was designed, fabricated and tested.

The specific design goals for the system are:

- Isokinetic sampling of gas streams having velocities in the range of 20 to 150 feet per second.
- Isokinetic sampling of gas streams having temperatures of -1°C to 535°C.
- A sampling rate of 0.5 to 20 standard cubic feet per minute.
- A response time capable of following flow fluctuations of ±10% with a period of 30 to 120 cycles per minute.
- Automatic control of the sampling rate.
- Totaling automatically the total gas sample flow.
- Provide a visual output reading.
- Electrical outputs to accommodate continuous recording of sampling rate.

2. RESULTS, CONCLUSIONS AND RECOMMENDATIONS

2.1 Results

The engineering prototype system developed on this program meets all of the design objectives, with the exception of the sampling rate of 0.5 to 20 scfm. Presently available APCO sampling trains limit the maximum sampling rate to approximately 2.0 scfm. This limitation is due to the impedance of the particulate collecting filter and the standard impingers used in the sampling train. The sensor and automatic controller are compatible with the specified sampling rate if used with a sampling unit capable of sustaining the flow rate. High volume air samplers are commercially available and can satisfy the maximum specified flow.

The key components developed on the program are the gas velocity sensor and the fluidic controller required to automatically maintain isokinetic sampling. The developed sensor is based on measuring the differential static pressure between the free air stream and sampling nozzle inlet. This sensor was selected over two other potential candidates, the cross-flow and co-flow sensor, on the basis of signal-to-noise ratio.

The automatic controller was designed as an integral component of a modified commercial sampling case with no change in outline dimension. The weight of the sampling case was increased by 4 pounds or approximately a 15% increase.

Operation of the controller requires minimal operator training. Prior to starting a sampling test, the controller gain control is set to correspond to a tabulated setting. This setting is a function of the pressure differential across the S-type pitot tube on the probe. One additional operation is required to remove system bias. The bias is removed by adjusting a regulator to obtain a specified reading on a pressure gauge. No further adjustments are necessary if the velocity of the sampled gas is in the range of 15 to 40 ft/sec. For the higher velocity ranges one additional step by the operator is required to compensate for a sensor bias. After the probe has been inserted in the gas stream, the flow corresponding to isokinetic conditions is determined using measured gas temperature and velocity as input parameters. The bias control on the controller is then adjusted until the system flow rate meter corresponds to the calculated flow.

The flow totalizing function of the controller utilizes a mass flow meter and an electromechanical counter. Visual readout of sampling rate and totalized flow are provided as well as an electrical output of sampling rate. The flow meter is a true mass flow meter and does not require correction factors for gas temperature or absolute pressure.

Results of the field tests demonstrated that the sensors and controller can function in an adverse environment with no degradation of performance. Isokinetic sampling was controlled to an accuracy of 5% in gas temperatures to 205°C and solid particulate concentration as high as 3.52 grams per cubic meter.

2.2 Conclusions

The following specific conclusions can be drawn from the results of this program:

- Automatic control of sampling rate will significantly increase accuracy and repeatability of sampling. Large and erratic variations in stack velocity were observed during the field tests. Establishing a time average of isokinetic flow requires an operator judgment factor. This factor is a variable, depending on the operator, the environmental stresses present during the test, and the physiological state of the operator during the test. The automatic control will, to a large extent, overcome the effects of these variables.

- Fluidic amplification of the sensor error signals provides a reliable and economical technique for implementing the automatic controller. In the lower band of the specified velocity range fluidics is considered the only practical technique for reliably sensing and amplifying the small error signals. At 20 feet per second and a gas temperature of 535°C, differential pressures of less than 0.005 inches of water must be sensed and accurately controlled. Commercially available electromechanical pressure transducers have adequate sensitivity and are excellent laboratory instruments; however, they are subject to excessive null shift with temperature changes and with abuse, and are not attractive for a field type operation.

- The limiting source of error in the automatic controller is in the sensor. The error is introduced by losses associated with the protective shrouding enclosing the free air stream sensor. This error can be partially compensated for by a controller adjustment. The compensation imposes an additional burden on the operator in that isokinetic sampling flow must be determined.

  The error of the fluidic amplifier and other control components is less than ±2%.

- Contamination of the sensor and associated fluidic amplifiers can be prevented by backflushing the sensor ports with clean air. Location of the sensor ports relative to the overall probe geometry is also a significant factor in achieving insensitivity to contamination.

- Test and evaluation of three sensor configurations, the cross-flow sensor, the co-flow sensor, and the differential static pressure sensor, showed that only the differential static sensor has sufficiently high signal-to-noise ratio to meet the design goals on system bandwidth.

2.3 Recommendations

The specific design goal which had the greatest impact on the overall system design was the specified capability of following 2 Hz perturbations in the gas velocity. This requirement eliminated both the cross-flow and co-flow sensors because of inadequate signal-to-noise ratio in the system bandpass.

With the exception of the bandwidth requirement, the co-flow sensor is attractive for this application and would have been the logical sensor choice. Both the controller hardware and the setup and operating procedure could be significantly simplified by utilizing this sensor. The gain of this sensor is independent of velocity and an order of magnitude higher than the static probe in the low velocity range. In addition, shrouding losses can be negated by a coarse adjustment of sensor flow. These characteristics eliminate the need for presetting gain as a function of the S-type pitot reading as well as the determination and adjustment for isokinetic sampling flow.

In view of these observations, the following recommendations are made:

- The bandwidth required of a particulate sampling system should be re-evaluated.

At the extremes of the solid particulate spectrum, i.e., the large, heavy particles where the sampling nozzle is a 100% efficient impact probe(1) and for the fine particles where the gas stream lines are followed, the only prerequisite for the sampling system is ability to maintain an average isokinetic velocity to obtain totalized flow from which a determination of particulate concentration can be made. There would be no errors introduced by the controller's inability to track rapid perturbations.

In the mid-range of the spectrum there is a potential error source because of the unsymmetrical relationship between sampling error and positive or negative errors in sampling velocities. This relationship has been verified experimentally and theoretically(2) and becomes significant for very large deviations from isokinetic conditions. Within the design goal range of ±10% deviations from nominal isokinetic velocities, the dissymmetry is minimal.

The investigation of sampling error vs. bandwidth could be approached from both theoretical considerations and empirical testing completely divorced from the hardware developed on the current program.

- If a reduction in system bandwidth to approximately 0.2 Hz or lower appears feasible, then a retrofit of the engineering prototype unit to include co-flow sensors is recommended. This retrofit would require fabrication and replacement of the sampling nozzles and minor modification to the fluidic controller.

- If the system bandwidth cannot be reduced, the only alternative is the sensor delivered with the prototype system. A modest test program should then be initiated to further reduce the sensor error.

3. TECHNICAL DISCUSSION

3.1 Functional Description of Automatic Sampler

A simplified block diagram of the sampler is shown in Figure 3.1. The free air stream velocity (V_R) is converted to pressure by the free air stream sensor. This pressure is compared to the output of a similar sensor located in the inlet of the sampling nozzle. The resultant pressure error signal is amplified and adjusts the suction on the vacuum pump to give the required nozzle inlet velocity (V_N).

The closed loop transfer function for the simplified block diagram is given by:

$$(1)\quad \frac{V_N}{V_R} = \frac{K_R G}{1+K_N G}$$

If $K_N G \gg 1$ and identical sensors are used for free air stream and nozzle inlet velocity, then $K_R = K_N$.

$$(2)\quad \frac{V_N}{V_R} \approx 1$$

Providing the free air stream sensor satisfies the criteria for isokinetic sensing, then isokinetic gas velocities will be maintained at the inlet of the sampling nozzle. The accuracy of the controller is directly related to the loop gain ($K_N G$), as shown in equation (1). To maintain isokinetic velocities to an error of less than 5% requires a loop gain greater than 20.

A control model of the sampling case is shown in Figure 3-2. The open loop transfer functions for the model representing the complete sampling train is given by:

$$(3)\quad TF = \frac{G\varepsilon^{-s\tau}}{\rho A\left[RR_1C_1C_2S^2 + (R_1C_2+RC_2)S+1\right](1+TS)}$$

$$\approx \frac{G\varepsilon^{-s\tau}}{\rho A\left[1+(R_1C_2 + RC_1 + RC_2)S\right]\left[1+\frac{RR_1C_1C_2S}{(R_1C_2+RC_1+RC_2)}\right](1+TS)}$$

where:

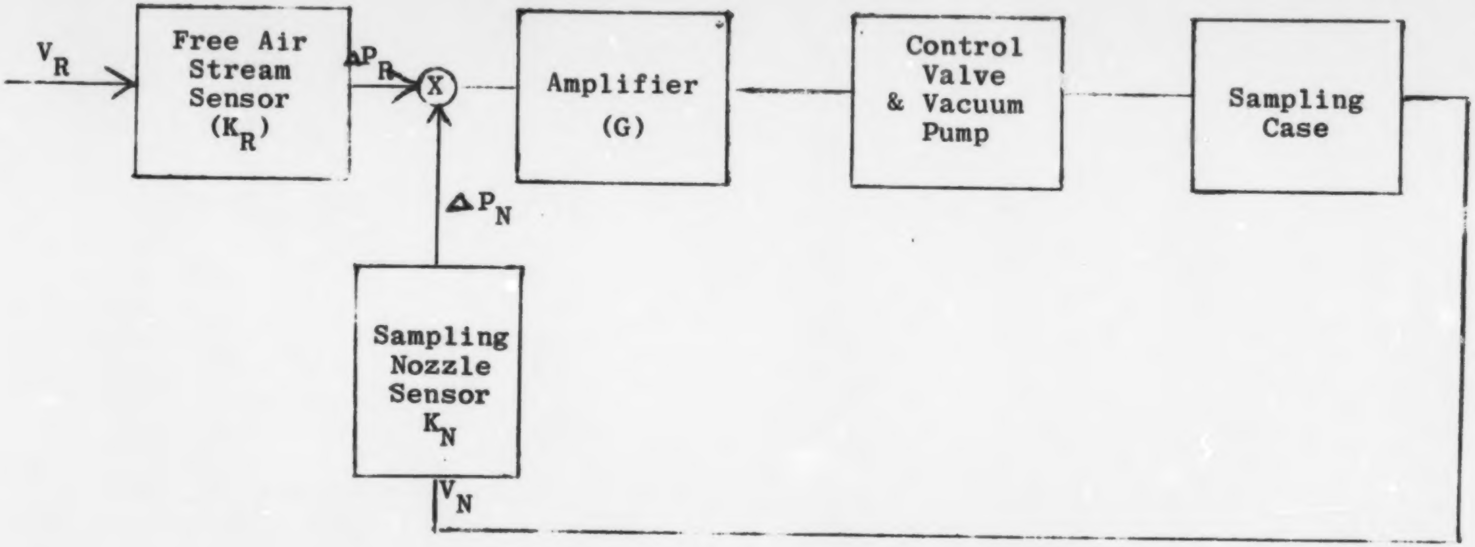
V_R
Free Air Stream Sensor (K_R)
ΔP_R
X
ΔP_N
Amplifier (G)
Control Valve & Vacuum Pump
Sampling Case
Sampling Nozzle Sensor K_N
V_N

Figure 3-1. Block Diagram of Sampler

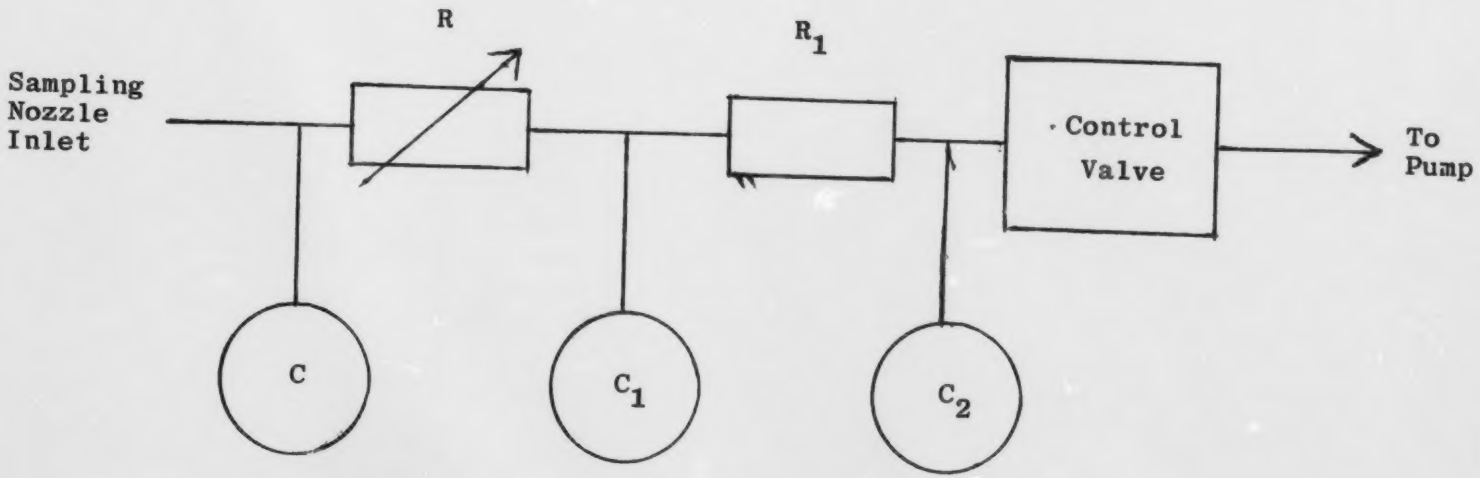

Figure 3-2. Control Model of Sampling Case

G = gain of forward loop - #/sec/in/sec

A = cross-sectional area of sampling probe - in^2

ρ = density of sampled gas - $\#/in^3$

T = time constant of control valve - sec

τ = transport lag - sec

C = capacitance between sampling nozzle and filter

C_1 = capacitance between filter and first impinger - in^2

C_2 = capacitance of impinger section - in^2

R = filter restriction - sec/in^2

R_1 = impinger restriction - sec/in^2

The closed loop transfer function relating the sampling nozzle inlet velocity to free air stream velocity is given by:

$$(4)\quad \frac{V_S}{V_R} = \frac{G\varepsilon^{-s\tau}(1 + CRS)}{(\rho A+G^{-s\tau})\left[\frac{\rho ARR_1C_1C_2TS^3}{\rho A+G\varepsilon^{-s\tau}} + \frac{\rho A\left[R_1C_2T+RC_2T+RR_1C_1C_2\right]S^2}{\rho A + G\varepsilon^{-s\tau}} + \frac{\rho A(T+R_1C_2+RC_2)\ S + 1}{\rho A + G\varepsilon^{-s\tau}}\right]}$$

Equation (4) indicates that to maintain isokinetic conditions in the sampling nozzle, the gain (G) in units of mass flow (#/sec) per in/sec of velocity error must be much greater than the product of gas density and sampling nozzle area (ρA).

A measured attenuation and phase plot of a commercially available sampling case is shown in Figure 3.3. The characteristics include the flow modulating valve designed for the loop and a representative 10-foot length of signal transmission line. With the system gain set for 20 ρA, the crossover is a 5 Hz with a negative phase margin of 20 degrees. Stable operation of this loop will require frequency shaping of the signal. A lag-lead circuit is used to lower the open loop crossover to 2.5 Hz, while still maintaining adequate steady-state gain. In addition to the lag-lead, a lead circuit is required to get adequate phase margin.

Figure 3-4 is a block diagram of the system as implemented.

3.2 Sensors

The gas velocity sensor is the key component in the automatic sampling control loop. It is exposed to a severe environment with temperatures as high as 535°C, along with heavily contaminated gases. In addition to sensing gas velocity, one

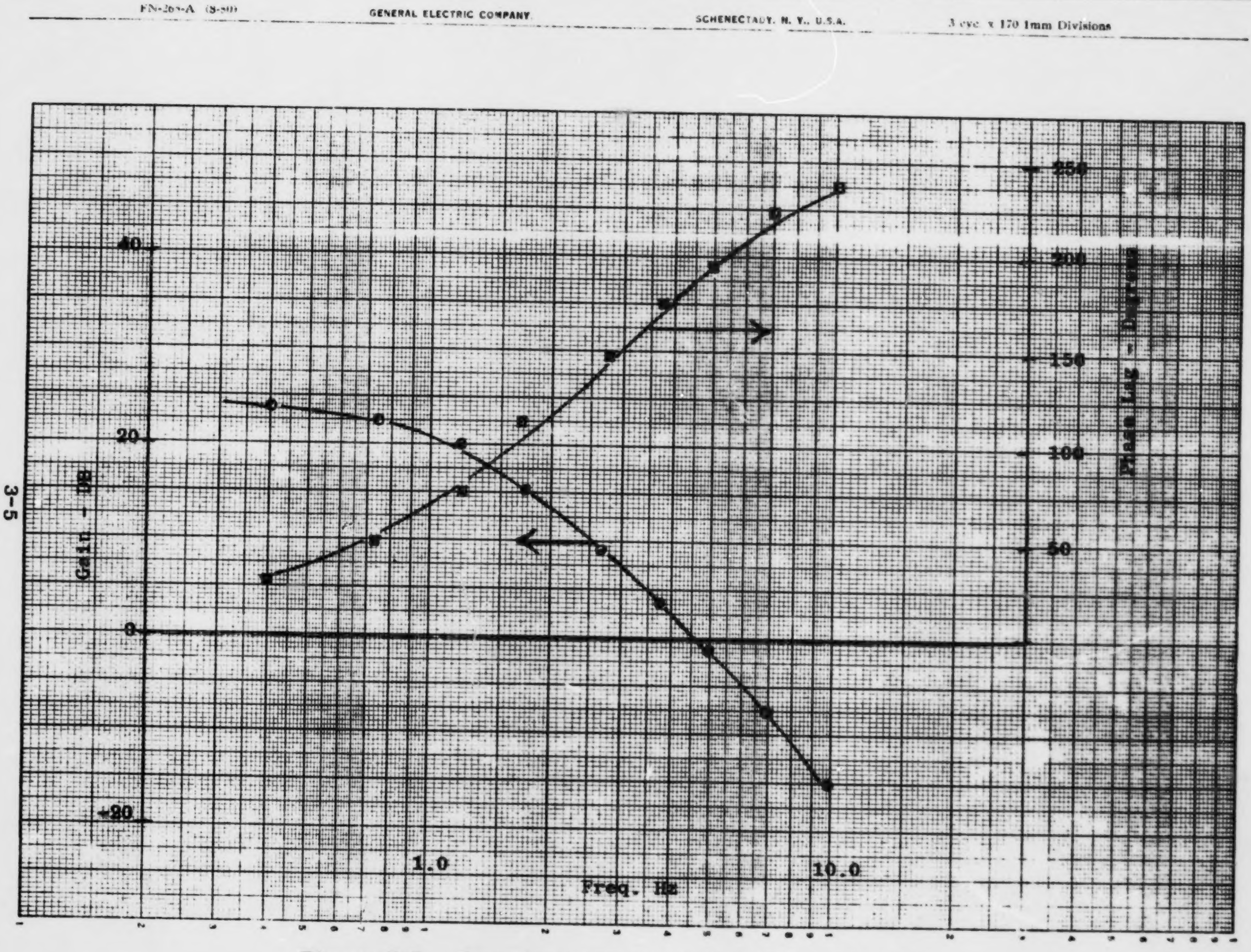

Figure 3-3. Transfer Characteristic of Sampling Case

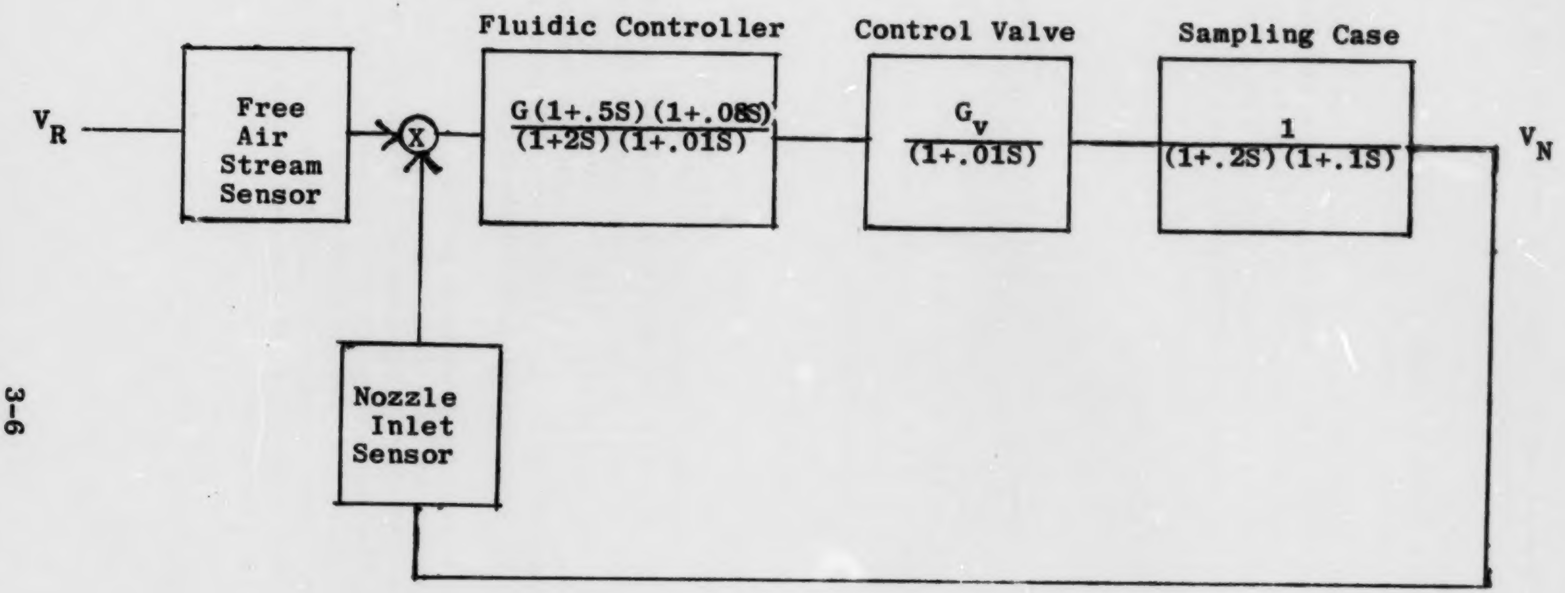

Figure 3-4. Block Diagram of Controller and Sampling Case

additional constraint is imposed on the sensor in this application--isokinetic conditions must be satisfied on the reference sensor (free air stream sensor).

Three fluidic sensor configurations were tested and evaluated on the program. They were:

a) Cross-flow sensor
b) Parallel or co-flow sensor
c) Differential static pressure sensor

Figures 3-5a, b and c are schematics illustrating the fundamental operating principle of each sensor. The cross flow sensor shown in Figure 3-5a utilizes a jet directed at two receivers. The axis of the nozzle forming the jet is perpendicular to the free air stream velocity vector. The angular displacement of the jet axis from the nozzle axis is given by:

$$(5) \quad \phi = \tan^{-1} \frac{M_s}{M_j}$$

Where M_s is the momentum imparted to the jet from the free air stream and M_j is the momentum of the power jet. If the receivers are positioned to give a linear relationship between differential pressure and jet angle, then the output of the sensor is proportional to the square of the free air stream velocity and the sensor gain is directly proportional to the free air stream velocity. To a first order approximation, the sensor gain ($\Delta P/\Delta V_s$) is independent of the jet velocity; however, the maximum range of the sensor is directly dependent on jet velocity.

The co-flow sensor shown in Figure 3-5b utilizes a jet directed at a single receiver with the jet axis parallel to the free air stream velocity vector. Interaction between the free air stream and the jet at the jet boundary imparts a portion of the free air stream velocity to the jet. The change in recovered pressure at the receiver is linearily related to free air stream velocity providing the incremental velocity imparted to the jet is small compared to the nominal free jet velocity. Sensor gain and maximum range are directly related to jet velocity.

The differential static pressure probe shown in Figure 3-5c compares the static pressure in the free air stream to the static pressure at the inlet to the sampling nozzle. When the static pressures are equalized the velocity at the inlet to the sampling nozzle will be equal to the free air stream velocity. In contrast to the other two sensors, this sensor is not an absolute velocity sensor -- it can sense only equality of gas velocities in a common duct. The sensor gain is given by:

$$(6) \quad \frac{\Delta P}{\Delta V} = \frac{1}{2} \rho (V_s + V_f)$$

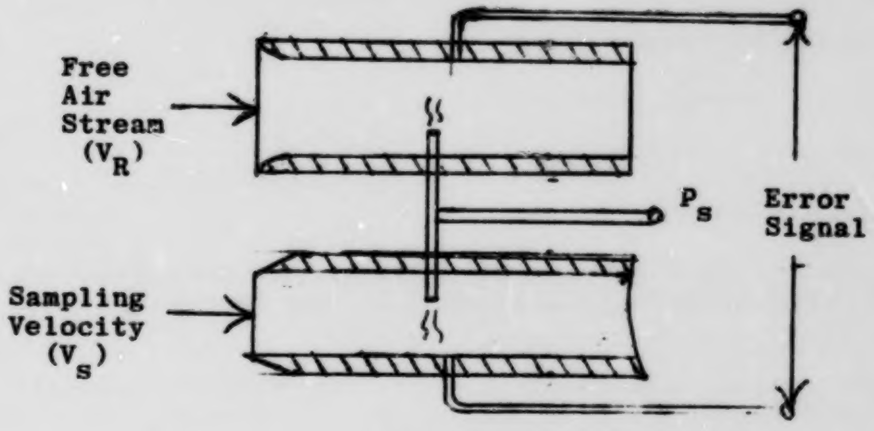

a. Cross-flow Sensor

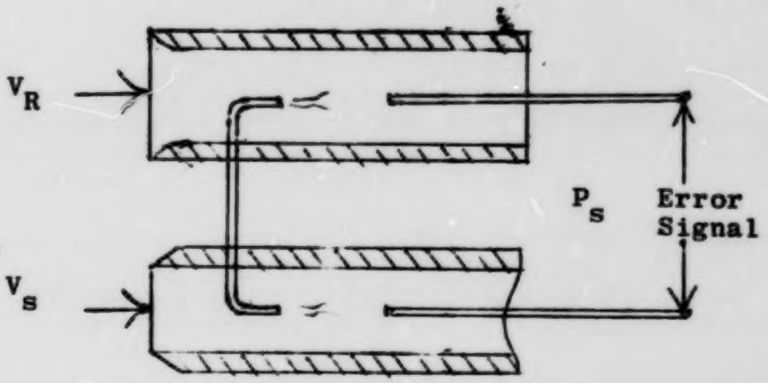

b. Co-flow Sensor

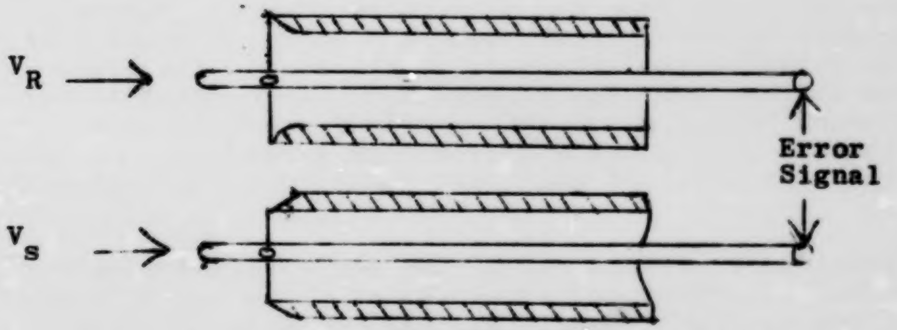

c. Differential Static Sensor

Figure 3-5. Sensor Configurations

where:

ρ = density of gas

V_s = velocity at sampling nozzle inlet

V_f = free air stream velocity

ΔV = $(V_s - V_f)$

ΔP = output of sensor

At near isokinetic conditions at the inlet to the sampling nozzle, $V_s \approx V_f$ and the gain becomes proportional to the free air stream velocity.

In the initial phases of the program, primary emphasis was placed on the development of the cross-flow sensor. Because of the relatively high supply pressures used on the sensor, along with the capability of operating with back pressured receivers, it appeared to offer the greatest potential for successful operation in a contaminated environment. In addition, there was considerable background experience on application of the sensor as an anemometer. A sensor with satisfactory gain and range characteristics was developed on the program. However, the developed sensor failed to meet the criteria for maintaining isokinetic characteristics at the free air stream sensor.

In addition, the signal-to-noise ratio of the sensor was not acceptable. Noise saturation of the signal amplifier stages occurred when operating at the required steady-state gain and bandwidth. The sensor was abandoned for these reasons.

The development effort was next directed at the co-flow sensor. As a preliminary step it was established that this sensor could meet the criteria for maintaining isokinetic characteristics with a practical hardware configuration. The developed sensor had excellent characteristics from the standpoint of scale factor, range and constancy of scale factor over the complete range. The signal-to-noise ratio of the sensor is comparable to the cross-flow sensor and was not adequate to meet the system requirements. This sensor, though rejected for this particular application, would be the logical choice for a system with a bandwidth on the order of 0.2 Hz (an order of magnitude lower than the contract requirements).

The specific configuration of the differential static pressure probe was conceived and developed concurrently with the development of the co-flow sensor. Initial tests on the sensor concept showed a signal-to-noise ratio of about an order of magnitude higher than the other sensors and that isokinetic conditions could be maintained at the free air stream sensor. For these reasons this sensor was selected as the prime sensor for further development.

Test results on the three sensor configurations are reported in Appendix I.

3.3 Hardware Development

A prime objective in the layout of the system was to minimize the weight and physical size of the flue mounted sampling case. Existing units are already heavy and quite difficult to maneuver while inserting the probe into the three-inch sampling ports which are typical on existing installations.

The basic control circuit consisting of the sensor, flow control valve, and amplifiers must be located on the sampling case. This is predicated by a consideration of signal transport -- the transport lag associated with the vacuum line in the umbilical cord connecting the sampling case to the ground-based central unit must be eliminated from the control loop. This cord can range from 25 to 100 feet in length and may introduce transport lags in excess of 0.1 sec. Stabilizing a control loop with a 2 Hz bandwidth would be very difficult with transport lags of this magnitude.

The physical location of the flow rate and flow totalizing meters will depend on the configuration of the flow control valve. Flow in the sample collecting nozzle can be controlled by a throttling valve placed in series with the nozzle and the vacuum pump or by a bypass valve around the pump.

With a throttle control valve, the flow in the umbilical cord is equal to the sampled flow and the flow rate and flow totalizer meters can be located at the pump end of the umbilical cord. On the other hand, with a bypass valve, the flow in the umbilical cord is equal to the sampled flow plus the bypass flow. With this configuration, the flow meters must be inserted between the sampling nozzle and the control valve. In the case of the automatic control loop, this dictates that the flow meters also be stack mounted.

Both system configurations and a definition of signal shaping and gain required in the remaining control loop depend on the control valve; hence, it was the first of the control elements developed.

3.3.1 Flow Control Valve

Figure 3-6 is a plot of flow through the sampling nozzle as a function of control valve area for both the throttling valve and the bypass valve. The flow characteristics were determined for two values of sampling case impedance. The solid curves represent a pressure drop of 7.0 psi at a flow of 1.5 scfm; while the dashed curves are for a 7.0 psi drop at 0.5 scfm. For a given valve area, the flow control range is somewhat higher with the throttle valve as compared to the bypass valve. The major difference between the two approaches is the control range where the valve becomes non-linear. The throttle valve becomes non-linear in the maximum flow range, whereas the bypass valve is non-linear in the minimum flow range.

100X140 7/100 Inch Divisions

GENERAL ELECTRIC COMPANY, SCHENECTADY, N. Y., U.S.A.

FN-521-B (8-50)

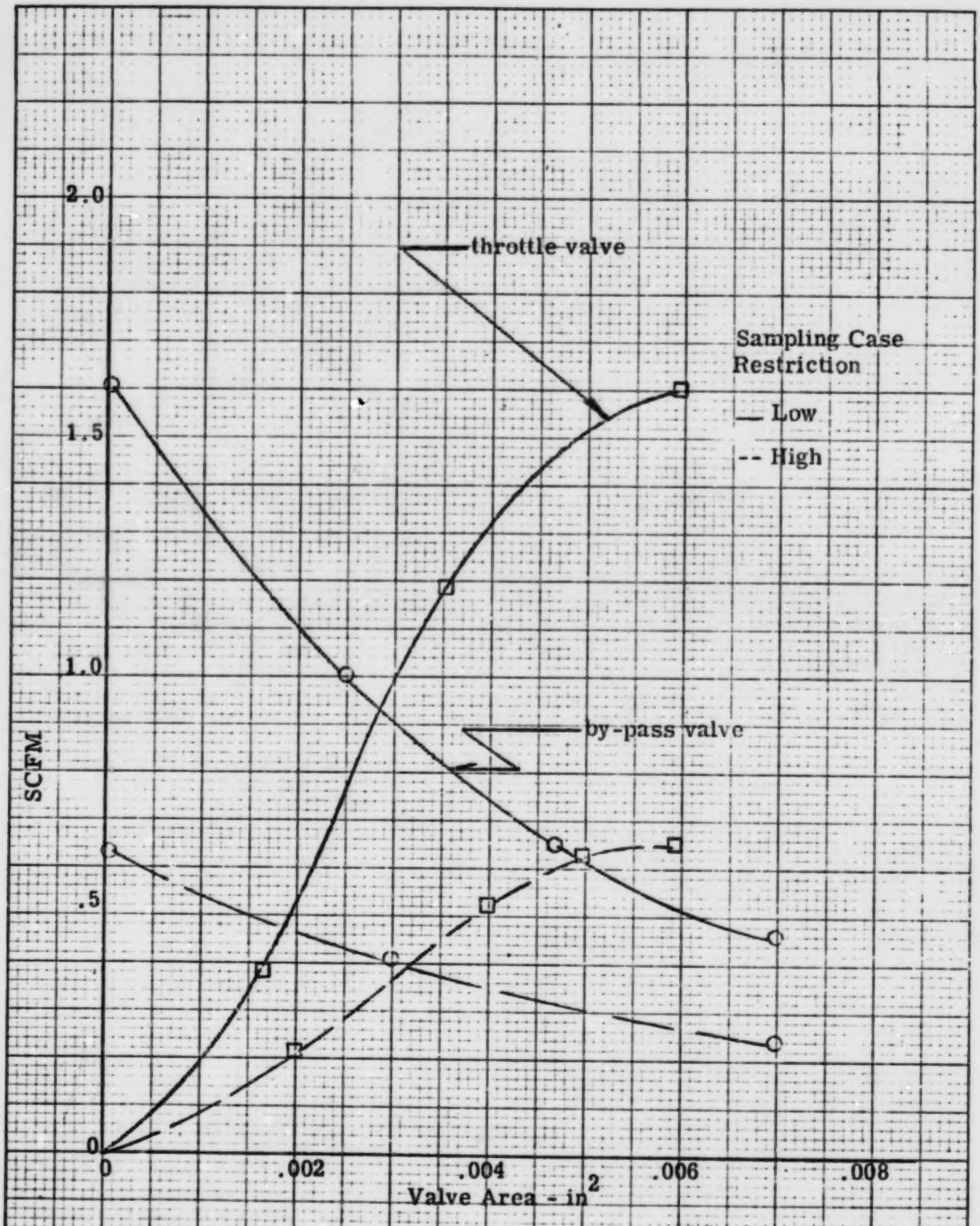

Figure 3-6. Flow Control Valve Characteristics

From the standpoint of control characteristics, either configuration can be adapted to the system. The bypass valve maintains a relatively constant flow at low suction at the inlet to the vacuum pump; hence is conducive to long life and also minimizes pump leakage flow as compared to the throttling valve. These inherent advantages of the bypass valve over the throttling valve were not considered of sufficient significance as compared to the disadvantage of stack-mounted flow meters. On this basis, the throttling valve configuration was selected.

Figure 3-7 is a schematic of the control valve. Flow is throttled by a spring-loaded poppet valve. The poppet is actuated through a bellows seal by a pressure differential across a flexible diaphragm.

Figure 3-8 shows the frequency response characteristic of the valve. The valve has the characteristic of a simple time constant of 0.01 second.

A plot of the steady-state control characteristics of the valve is shown in Figure 3-9. The valve goes through its full control range with a control pressure change of 1.5 psi. Gain of the valve is 1.4 scfm per psi when inserted in the sampling case.

3.3.2 Fluidic Control Amplifier

The fluidic control amplifier completes the interface between the differential static velocity error sensor and the control valve. The prime prerequisites of the amplifier are:

- To make a satisfactory interface with the sensor, the amplifier must be capable of establishing a local reference slightly positive relative to the stack static pressure. This gives an outflow of clean air from the amplifier through the sensor ports and thus prevents contamination of the amplifier and the sensor.

- The threshold of the amplifier must be well below 0.01 inches of water. This is the magnitude of error signal produced at 20 ft/sec gas velocity and a ten percent error in velocity.

- The steady-state gain must be sufficiently high to maintain isokinetic conditions as flow impedance of the sampling case changes with filter loading.

- Amplifier must provide the proper signal frequency shaping to stabilize the overall control loop.

- To interface with the control valve the output driver amplifier must have high flow capability to insure adequate bandwidth in the control valve.

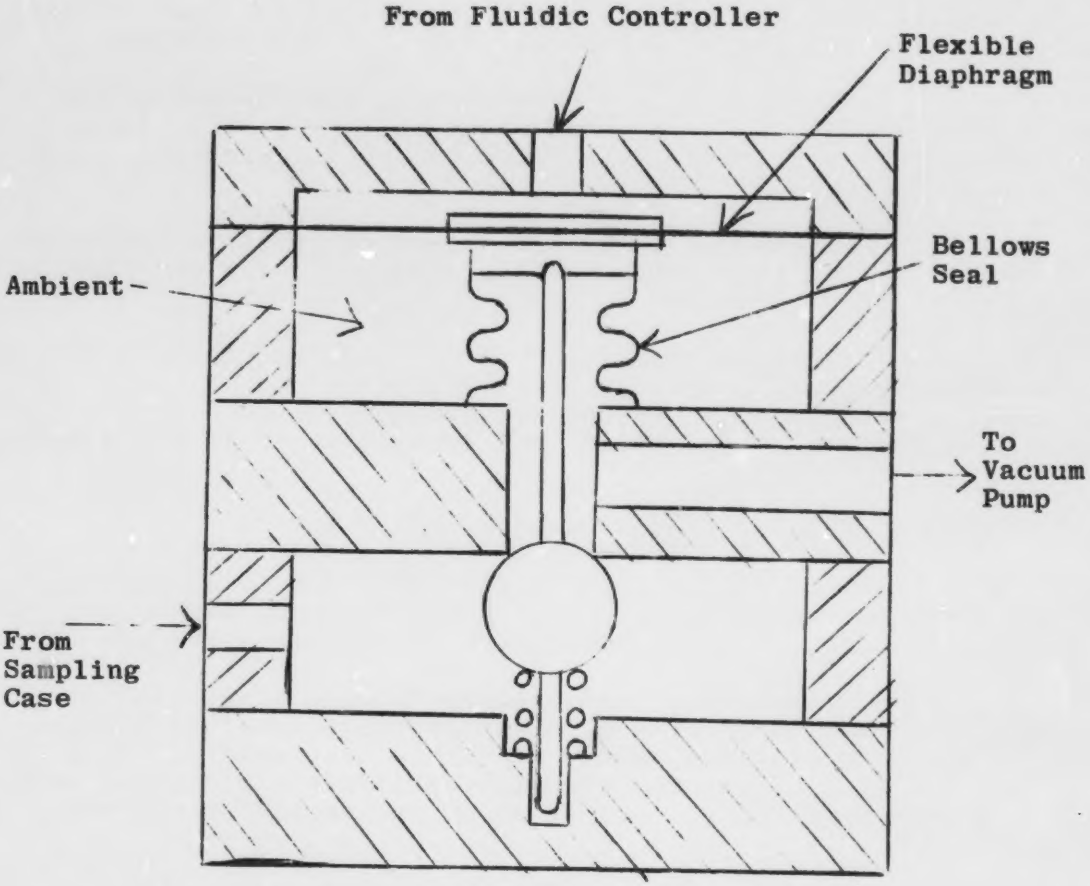

Figure 3-7. Control Valve Schematic

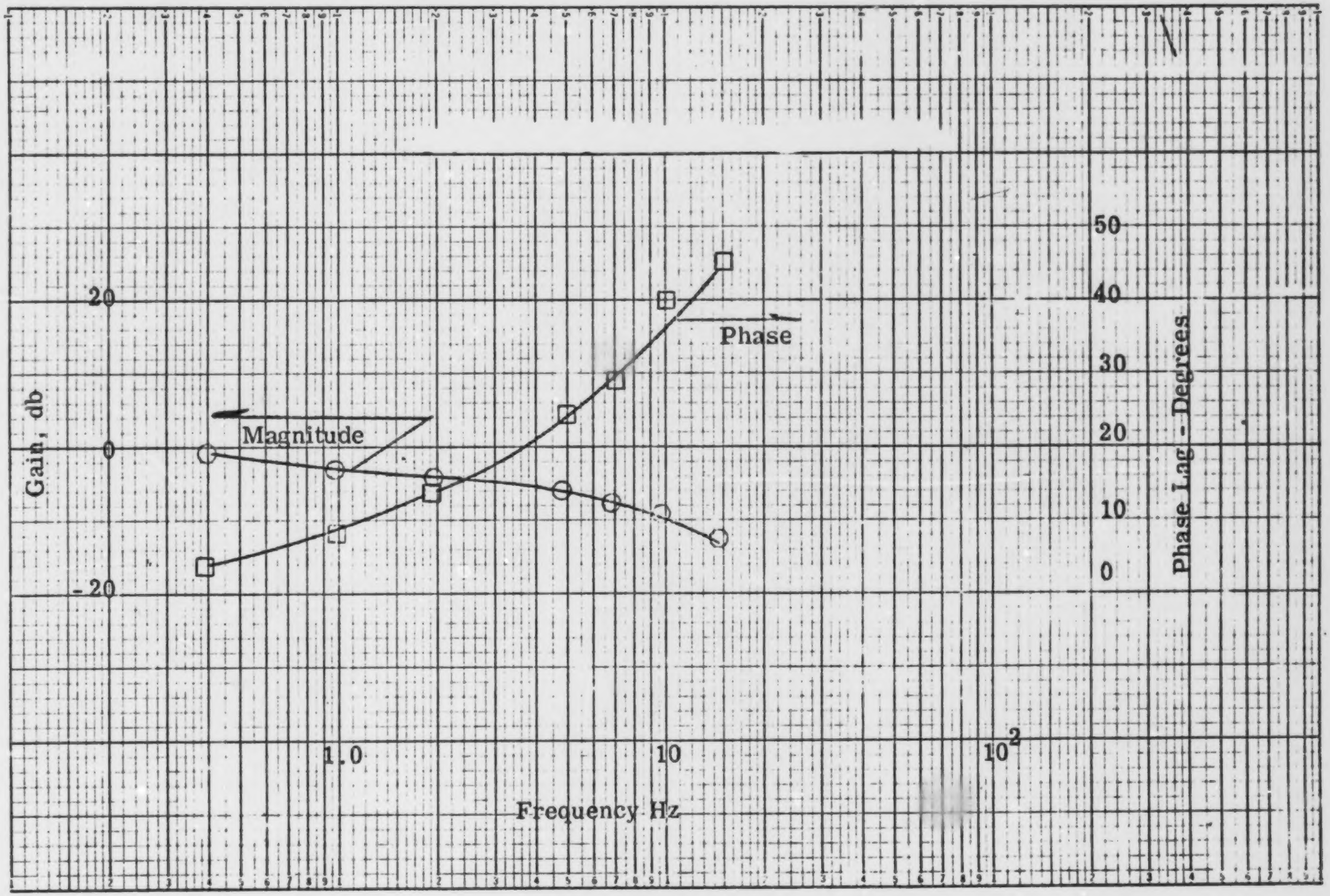

Figure 3-8. Throttle Valve Response

180x250 1mm Divisions

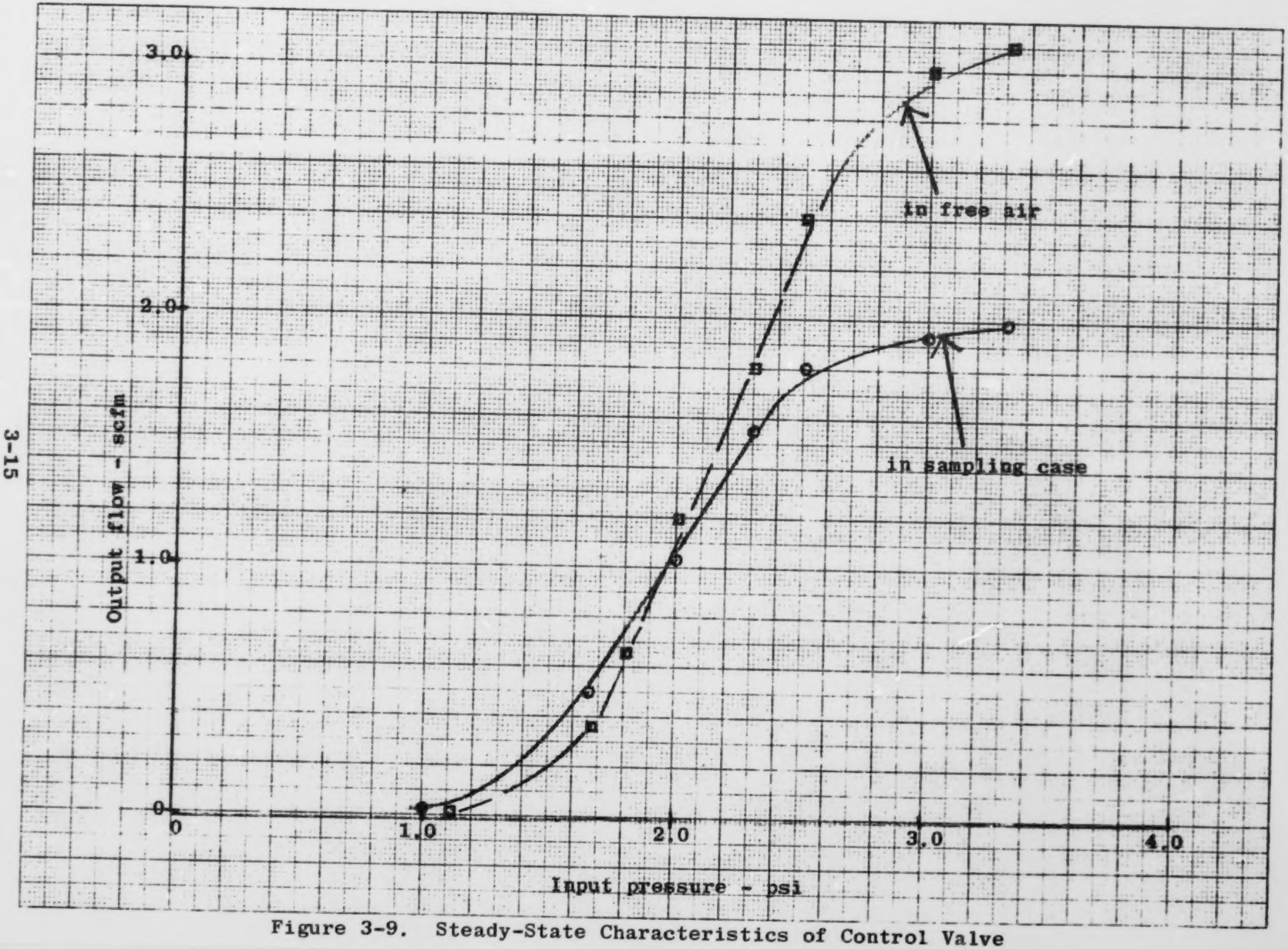

Figure 3-9. Steady-State Characteristics of Control Valve

Figure 3-10 illustrates the method of interfacing with the sensor. The input stage is a proportional fluidic amplifier whose supply for the jet nozzle is derived from a relatively high pressure and a flow restrictor. The spill-over flow from the jet (i.e., all flow not exiting through the receiver) is collected and vented to the stack through the stack static reference tube. The flow impedance of the reference tube and the magnitude of flow, as determined by the flow restrictor, determines the pressure in the amplifier vent region relative to the stack static. In the developed amplifier these parameters were fixed to establish a pressure level at the amplifier of a positive 0.5 inches of water relative to the static pressure of the stack. This pressure level also insures an outflow of clean supply air from the amplifier control ports and sensor ports.

The steady-state gain requirements of the controller can be determined by reference to equation (4) in section 3. The steady-state ratio of the sampled velocity to reference velocity is given by:

$$(7) \quad \frac{V_S}{V_R} = \frac{G}{\rho A + G}$$

To maintain the velocity error of less than 5% requires that $V_S/V_R > .95$ and the nominal value of G must be greater than 20 ρA. Using a typical sampling nozzle area of 0.1 in^2 and a density based on air at 30F, $\rho A = 4.6/10^6$ #/in.

The nominal gain must then be:

$$G = 20 \rho A = \frac{9.2}{10^5} \text{ \#/sec/in/sec} = \frac{9.2}{10^5} \text{ \#/in}$$

Referring to Figure 3-9, the gain of the valve is 1.4 scfm/psi or $63/10^6$ #/sec/in/H_2O.

At a nominal gas velocity of 20 ft/sec, the sensor gain is $8.7/10^4$ inches of water per in/sec velocity error. The product of sensor and valve gain is then approximately $5.5/10^8$ #/in. To obtain the required gain of $9.2/10^5$ requires a pressure amplification between the sensor and the flow valve of 1600.

Another argument for determining the steady-state gain can be based on full utilization of the flow control valve range to accommodate increased filter loading. Referring to Figure 3-9 it is apparent that the linear range of the control valve is traversed with a pressure change of 0.8 psi (22.25 inches of water). If this range is to be traversed with a 5% velocity error at 20 ft/sec, the pressure gain must be 2225. This latter criterion was used in establishing the final amplifier configuration.

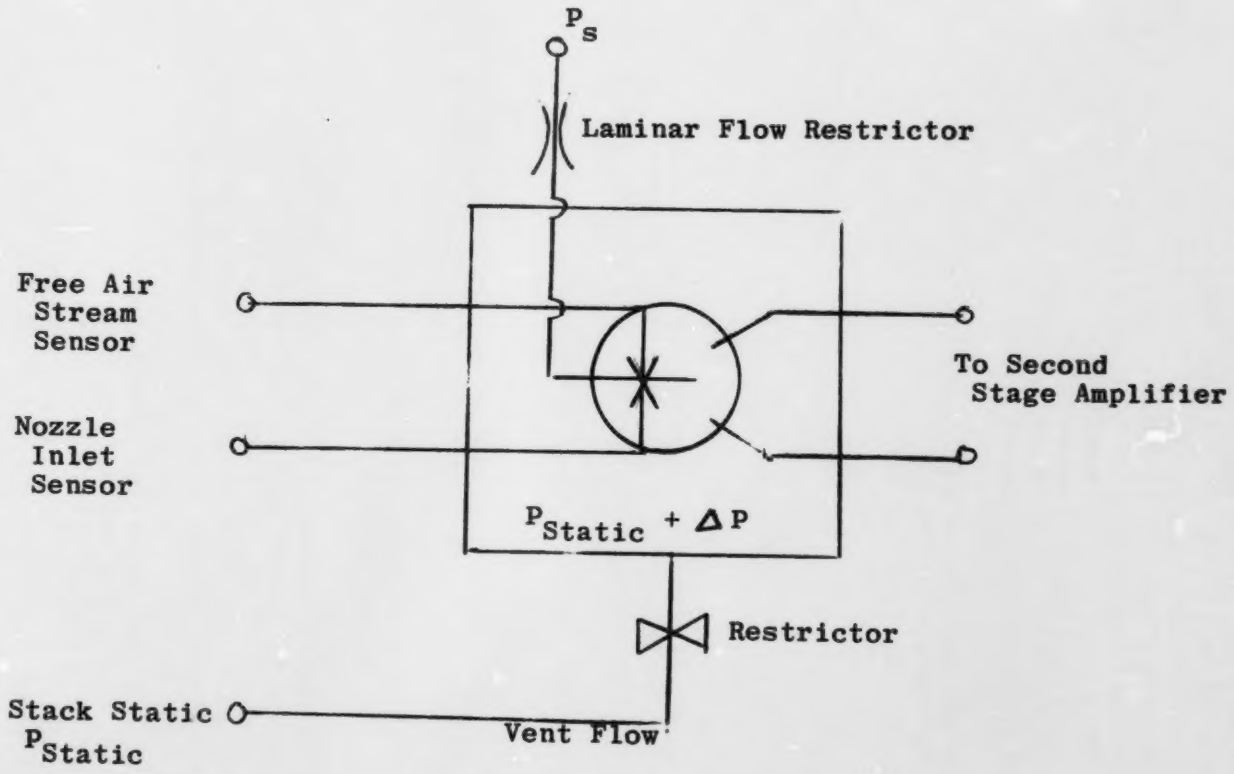

Figure 3-10. Sensor-Amplifier Interface

Figure 3-11 is a schematic of the developed amplifier, including signal shaping networks. The input amplifier is followed by four cascaded stages of proportional amplifiers. These amplifiers are miniature amplifiers (0.01 x 0.01 inch power nozzle) and provide a maximum pressure gain of 2000. A dual variable resistor is used between the third and fourth stages to reduce the gain to accommodate the change in gain characteristics of the velocity sensor with velocity and also the area differences of sampling nozzles. A pair of fixed resistors bypass the input ports to the fourth stage. These resistors can be switched in or out to accommodate very high velocities and small sampling nozzles.

The output of the fifth stage goes through a passive lag-lead circuit. This circuit has a lag break at 0.5 rad/sec and a lead at 2.0 rad/sec and serves the function of lowering the system crossover frequency to 2.5 Hz (12.3 rad/sec). Without this lag-lead circuit the system crossover when the steady-state gain requirements are satisfied is 5.0 Hz. The accumulated phase lag from the control valve, the signal transport lag and the sampling case characteristic made it virtually impossible to stabilize the system at 5 Hz crossover.

The signal is next processed in a lead-lag circuit. This function is implemented with five cascaded stages of proportional amplifiers with feedback to give the signal shaping. The lead break of this amplifier occurs at 12 rad/sec with the lag at 90 rad/sec. The function of the lead-lag is to provide adequate positive phase margin at the system crossover. Two additional input resistors are provided on the lead-lag circuit. These resistors function as a summing junction, whereby a bias signal can be inserted to offset bias introduced by circuit or sensor dissymetries. This bias control can also be used to establish control values of V_S/V_F greater than unity if so desired.

The last three stages following the lead-lag circuit function as flow amplifiers. The pressure gain of the cascaded stages is 2.5 with a flow gain of 50. The output stage is sized to obtain a 0.01 second time constant on the control valve.

The resistors associated with the supply are used to establish the supply pressure levels required for the cascaded stages. All circuit elements are protected from contamination entering through the supply by three integral filters, shown on the schematic. In addition to these filters, a primary filter for all supply air to the controller is located in the ground-based control console.

The gain vs. frequency characteristic of the amplifier is plotted in Figure 3-12. In the frequency range of 0 to 10 Hz, the characteristics are dictated by the overall loop requirements on steady-state accuracy and bandwidth. At the higher frequencies, the gain can be rolled off to attenuate high frequency noise components. It is apparent from Figure 3-12 that even with the maximum high frequency roll off, the amplifier will

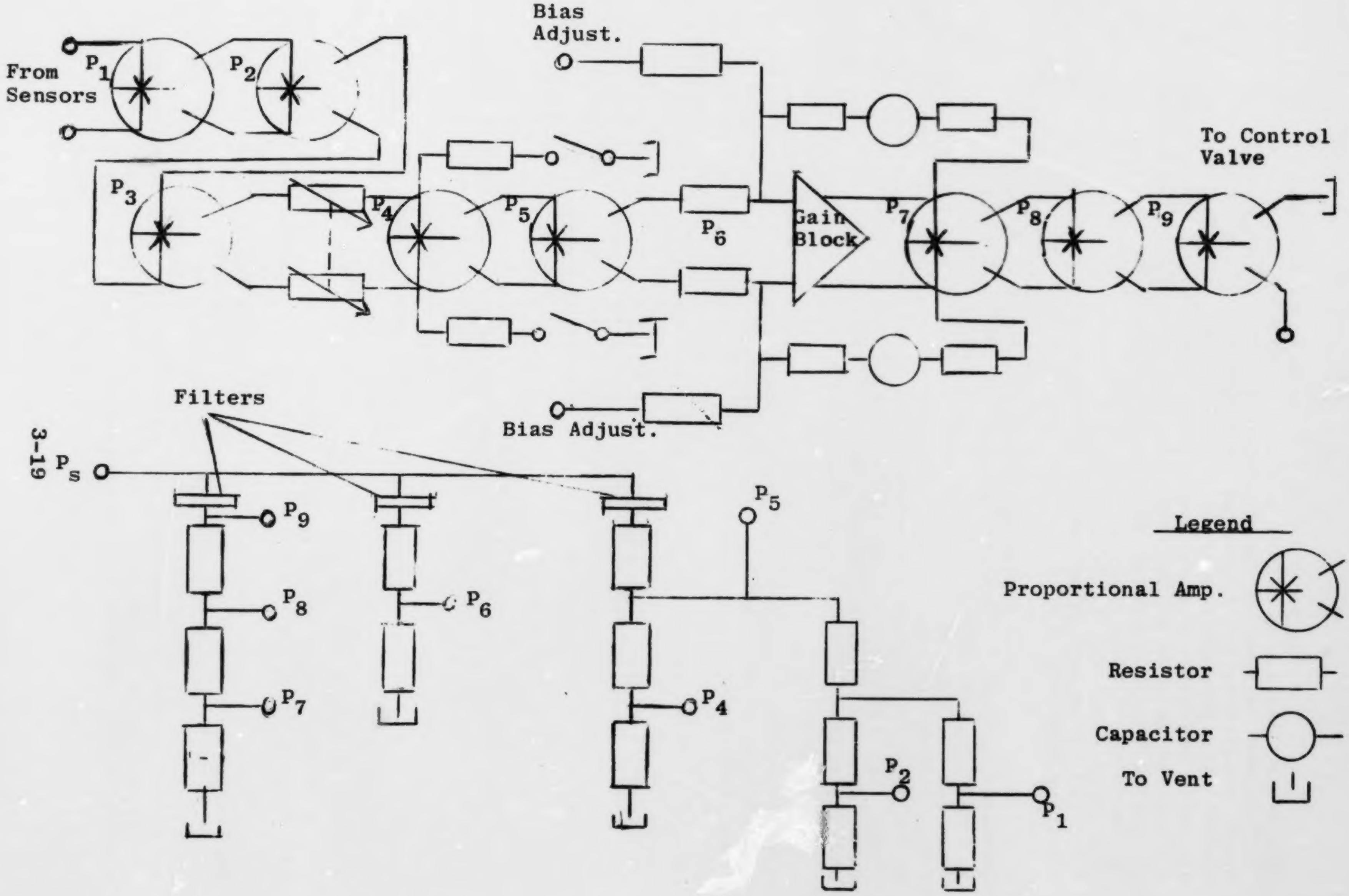

Figure 3-11. Fluidic Amplifier Schematic

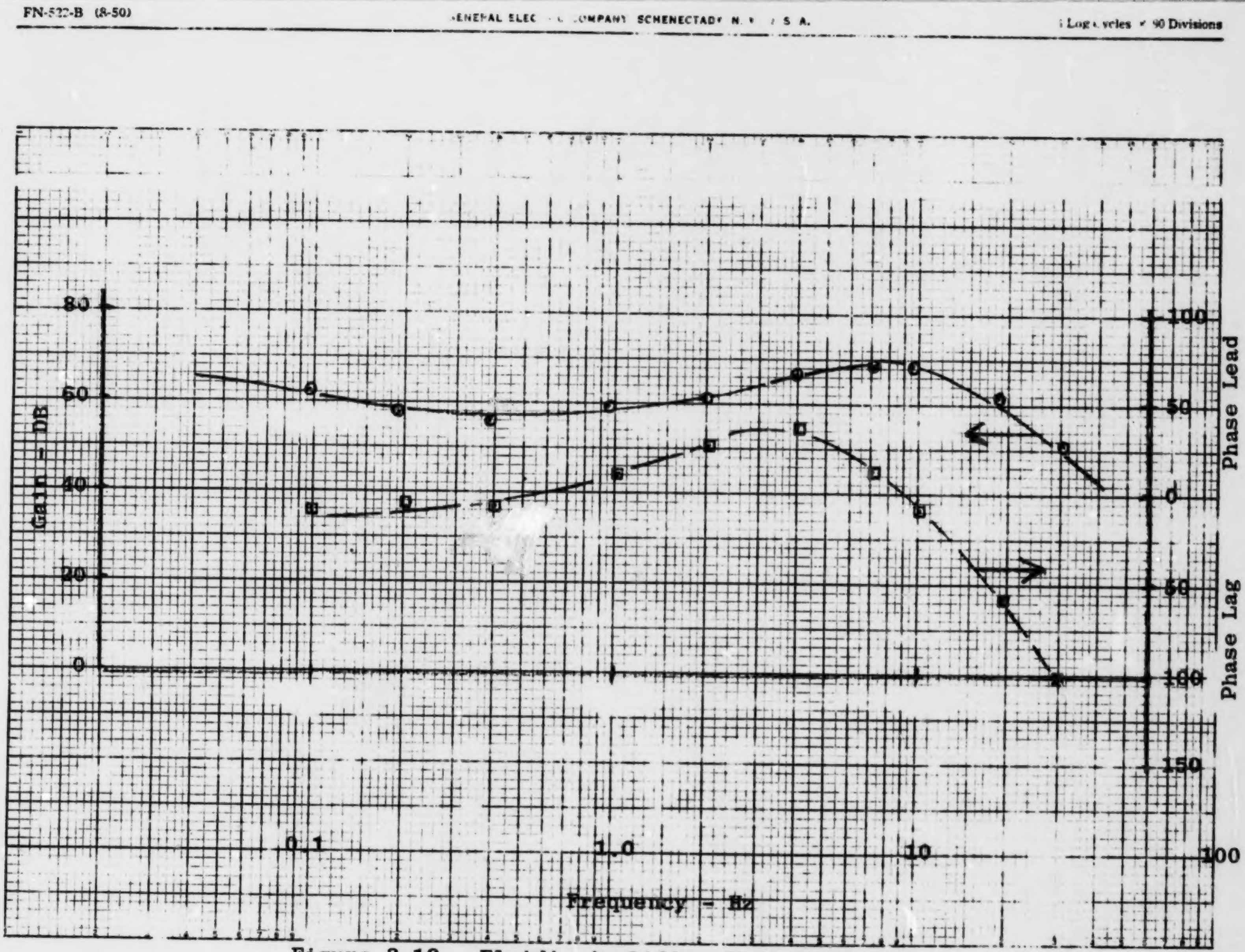

Figure 3-12. Fluidic Amplifier Characteristics

have a relatively broad bandwidth with a high average gain, and will be vulnerable to saturation by broadband noise. This high gain-bandwidth product severely limits the maximum tolerable sensor noise. This product can be roughly approximated by an average gain equal to the steady-state gain with a bandwidth of 70 Hz. Considering the previously determined minimum gain requirement of $9.2/10^5$ #/in and a valve with a flow control range of approximately $2.2/10^3$ #/sec (2 scfm), then the velocity error required to saturate the system is:

$$V_{\varepsilon} = \frac{2.2}{10^3} \frac{(10^5)}{(9.2)} = 24 \text{ in/sec}$$

As a rule of thumb, peak-to-peak noise of approximately one half the saturation level can be tolerated on the output. If the sensors have a noise source with a Gaussian distribution, as typical on all sensors investigated in this program, the ratio of peak-to-peak noise to RMS is 6:1. This requirement translates into a maximum RMS noise of 4 in/sec measured with a 70 Hz bandpass filter. Measured sensor noise on both the co-flow and cross-flow sensors is an order of magnitude greater than this (see Appendix I). Application of these sensors will require a severe compromise on gain or bandwidth. For example, a 2:1 gain reduction in conjunction with a 10:1 bandwidth reduction would be required.

3.3.3 Flow Rate and Flow Totalizing

The differential static pressure sensor selected introduces negligible diluent flow into the sample. This permits the use of standard commercially available flow meters. A Hasting-Raydist mass flow meter was selected for the flow rate measuring function. This is a true mass flow meter and can be located at either the suction or exhaust side of the vacuum pump. In this application the meter is located in the suction side of the pump to eliminate errors due to pump leakage.

The meter has a relatively long time constant (1-2 sec). This is not considered detrimental in a system where flow rate is controlled automatically in that the prime function of the flow meter is to get a reasonable time average. Electrical outputs suitable for remote recordings are provided on the meter.

Flow totalizing is also done with a commercially available totalizer. The totalizer accepts the analog output of the flow rate meter, makes an analog-to-frequency conversion, and accumulates pulses on an electromechanical counter.

Both the flow rate and totalizer functions have been integrated into the ground-based control console.

3.3.4 Vacuum Pump Selection

One of the objectives of the program was to provide for sampling rates of 0.5 to 20 scfm. The upper limit of 20 scfm cannot be achieved with currently available APCO particulate sampling systems with which the developed system must interface. The upper flow limit is limited by the filter restriction and impingers in the sampling train and above a certain limit is independent of pump capacity and sampling nozzle area.

The criteria used to size the pump for this program was to select a pump with adequate capacity so that the maximum flow is limited by the APCO sampling case and not by the pump.

Figure 3-13 is a plot of sampling flow vs. pump vacuum. It is apparent that vacuums greater than 8 psi do not significantly increase the sampling flow. On the basis of this curve, the pump is selected with sufficient capacity to provide the flow at a vacuum of 8 psi. A pump with a 7 scfm capacity at zero vacuum was selected.

3.4 Hardware Description

Figure 3-14 is a schematic identifying the location of the primary components supplied on the engineering prototype system. The blocks identified with either the sampling case or control console are integral parts of these units.

The sampling case is shown in Figure 3-15. This unit contains the standard impingers, filters, and filter ovens required to conduct sampling tests as specified in the Federal Register. Volume 36, No. 247, Pt. II.

The automatic controller is located inside the sampling case in a rectangular enclosure between the filter oven and the ice bath container for the impingers. The flow control valve is located in back of the controller. Heat transfer from the filter oven will maintain the air temperature around the control unit and valve at approximately 10°C above the ambient air temperature. This is an ideal temperature range for both the controller and the valve.

Three pneumatic lines go from the controller out to the sampling end of the probe. Flexible Tygon tubing is used inside the sampling case to connect the stainless steel tubing at the sampling case end of the probe to AN couplings. The flexible tubing permits rotation of the sampling probe through an angle of 360°. The three connectors, two for the velocity sensor and one for stack static reference, are shown on the left side of Figure 3-15. The stainless steel tubes are attached to the outer jacket of the probe and the two signal lines terminate in an AN connector at the sample nozzle end of the probe as shown in Figure 3-16. Figure 3-17 is a closeup view of the sampling nozzle and sensor. The static pressure ports for the sampling nozzle are drilled in

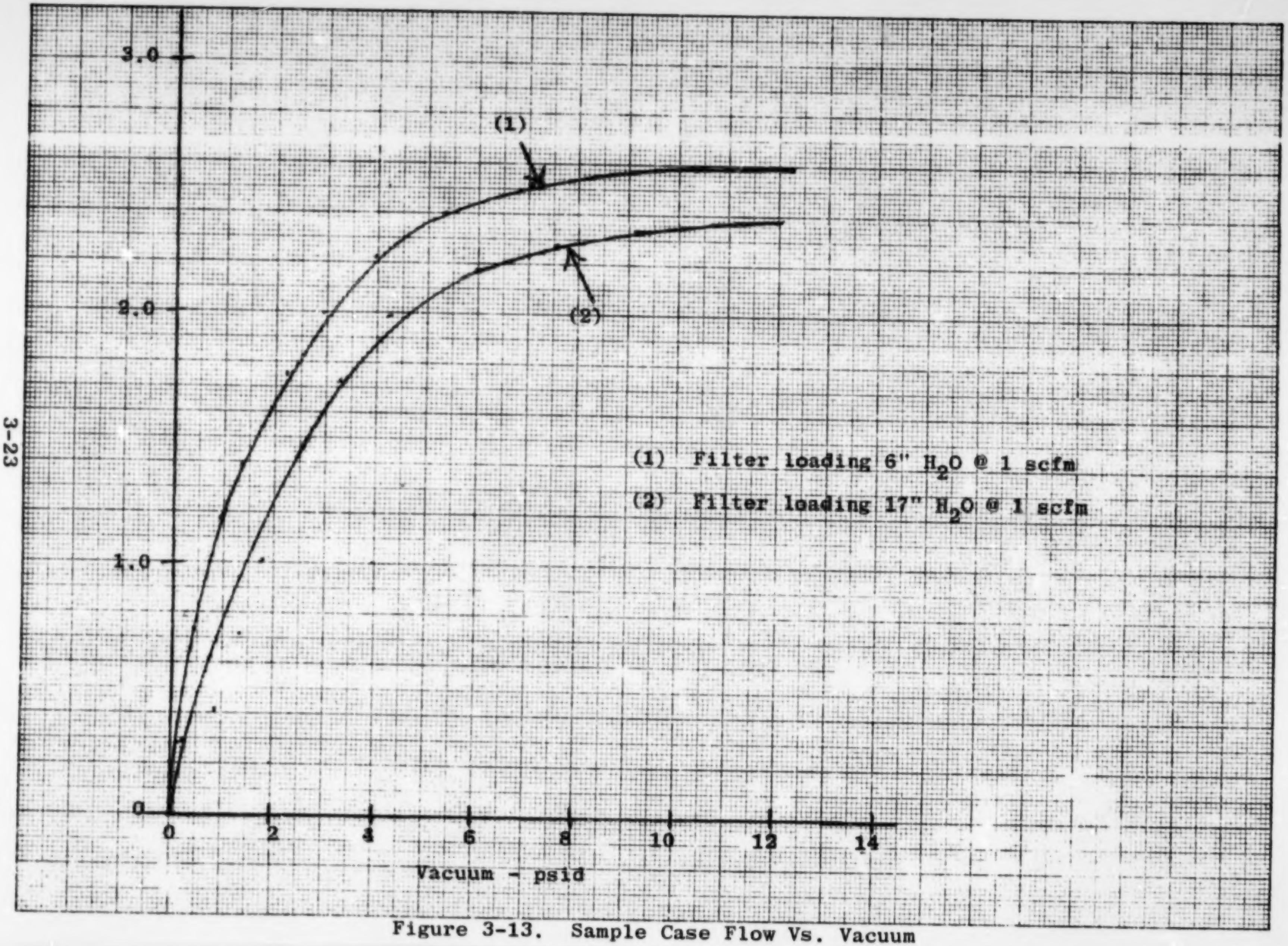

Figure 3-13. Sample Case Flow Vs. Vacuum

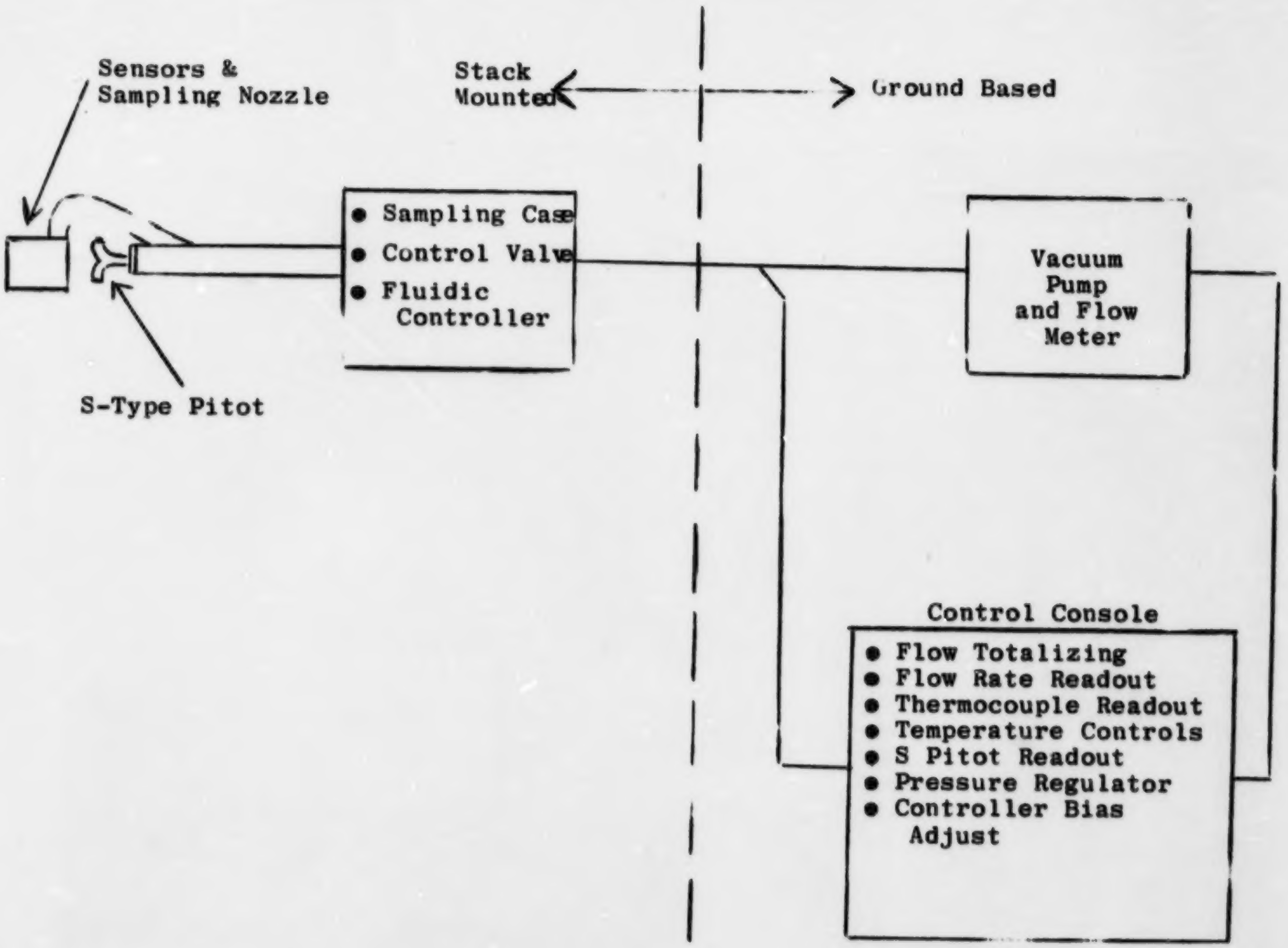

Figure 3.14. Functional Block Location

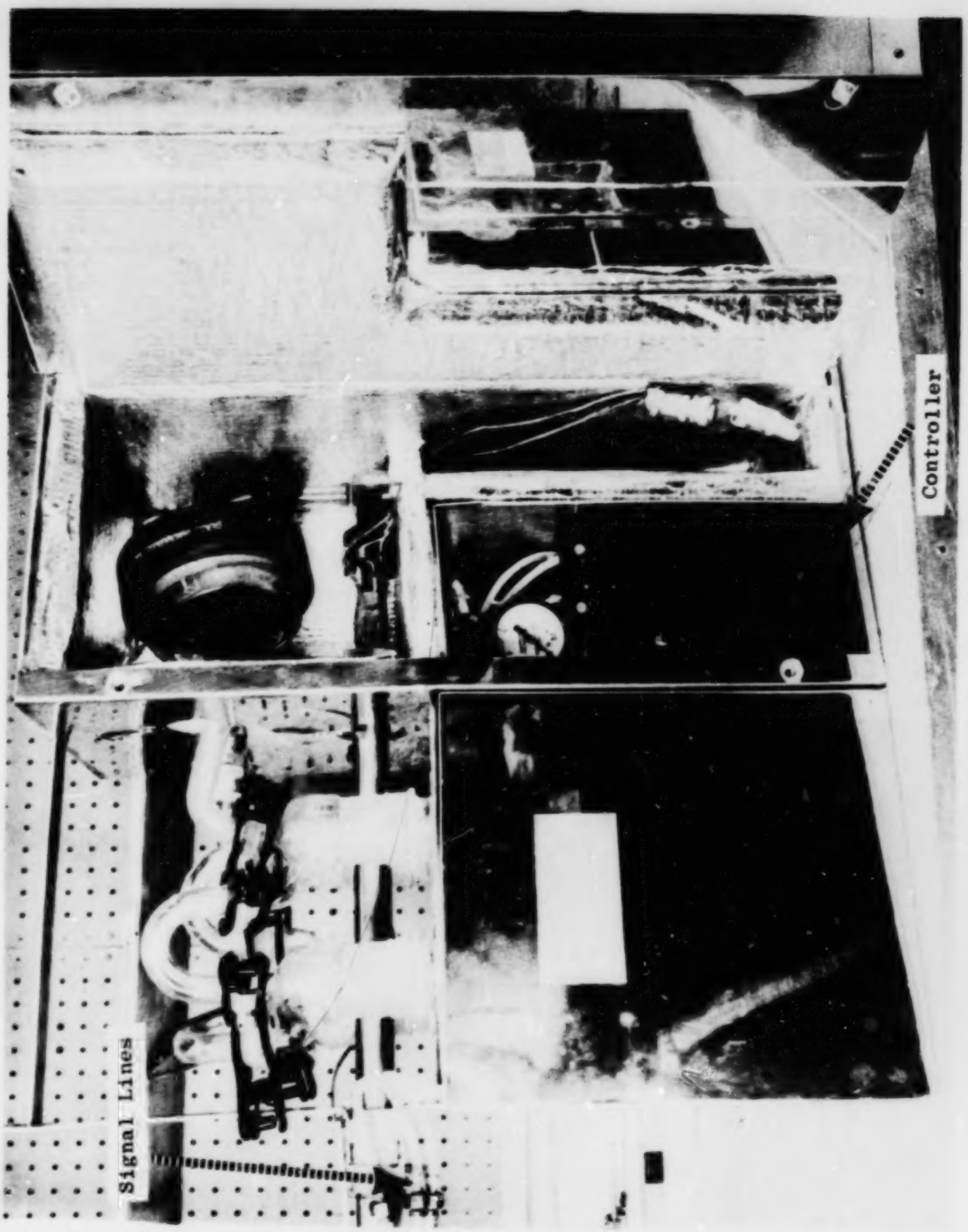

Figure 3.15 Fluidic Controller and Sampling Case

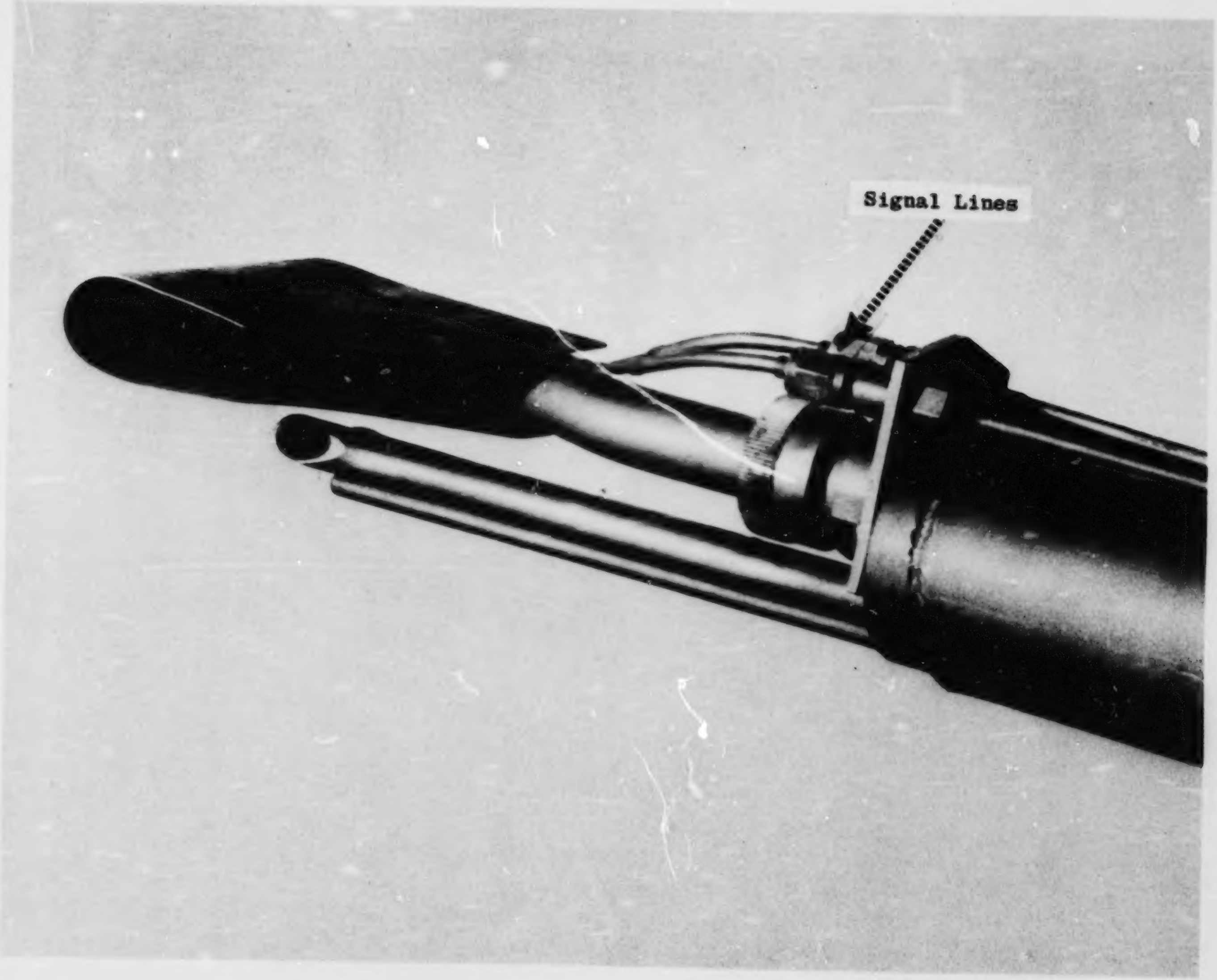

Figure 3.16 1/4 Inch Sampling Nozzle and Sensor

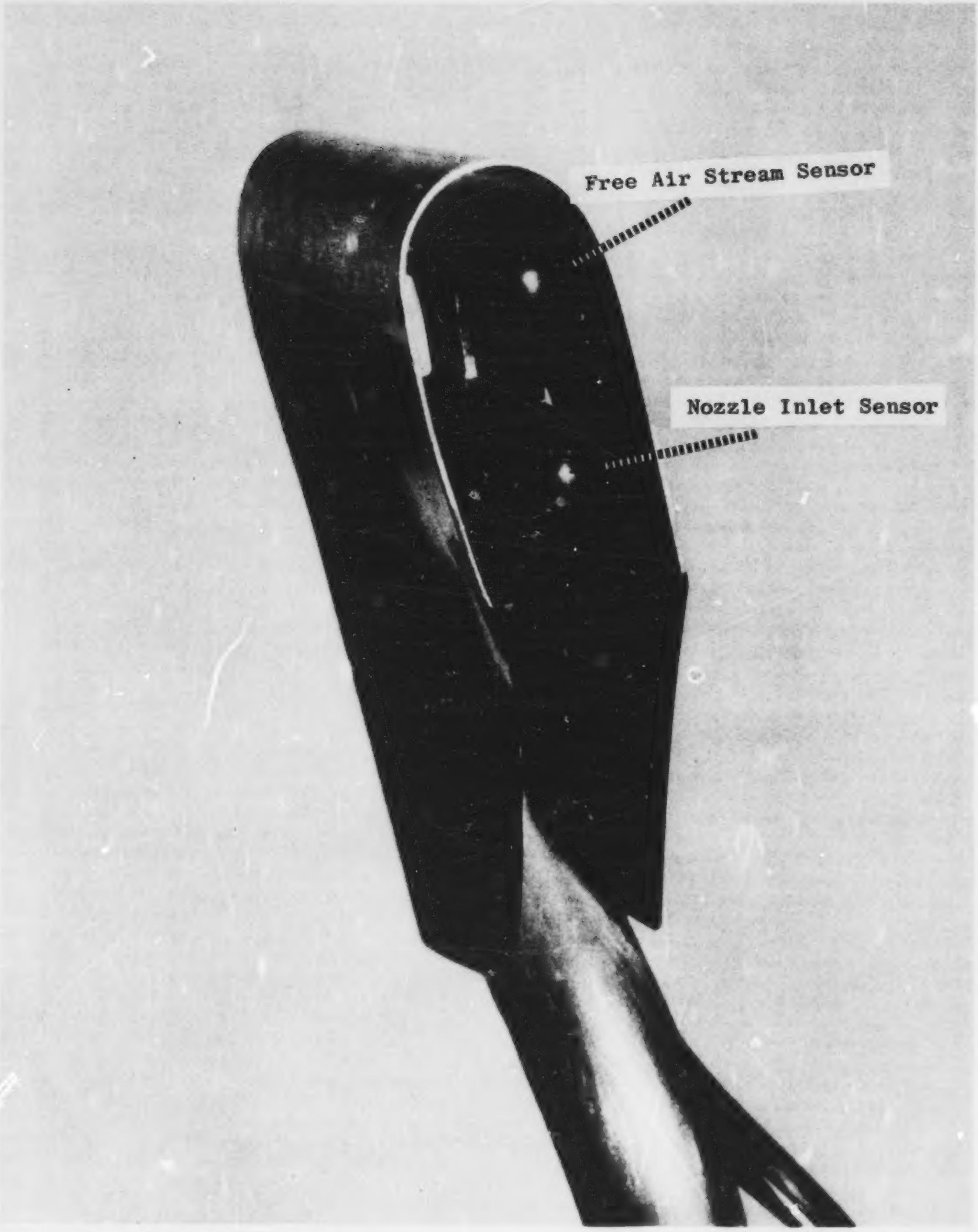

Figure 3.17 3/8 Inch Sampling Nozzle and Sensor

the wall of the tube protruding axially from the sampling nozzle. Four ports, 0.02 inch diameter, are used and they are located in the plane of the nozzle inlet. The free air stream static pressure ports are in an identical tube positioned outboard of the sampling nozzle. A protective shroud is used to prevent damage when inserting or withdrawing the probe from a sampling port.

Figure 3-18 is a photograph of the fluidic controller. The knob at the upper right hand side of the controller is a variable resistor. The steady-state gain of the controller is a function of the resistor setting. The resistor setting required to achieve a stable control mode is a function of the dynamic pressure as measured by the S-type pitot tube attached to the sampling probe and the area of the sampling nozzle. The required settings are tabulated in Table 1 under System Setup and Operation. The left hand knob is used as a two position switch. When the zero is in the vertical position, a bypass resistor is connected to the downstream side of the variable resistor giving approximately a three-to-one gain reduction. This low gain setting is used with the ¼ inch diameter sampling nozzle and high gas velocities.

The control console is shown in Figure 3-19. The lower left hand section contains the mass flow meter indicator and the flow totalizer. The mass flow meter also has an electrical output which is brought out to two jacks on a rear panel of the console for recording.

The inclined manometer is used in conjunction with the S type pitot tube on the sampling case probe to measure the velocity head of the sampled gas.

Directly above the manometer are two pressure regulators and a pressure gauge. The upper regulator sets the supply pressure to the automatic controller, the pressure gauge indicating the supply pressure. The lower regulator is used to apply a bias to the controller to offset any residual bias.

The right hand section of the console contains the sampling oven and probe jacket temperature controls as well as a transfer switch and temperature readout for the various thermocouples.

The system vacuum pump and flow meter are shown in Figure 3-20. The pump has a capacity of 7 scfm at 14.7 psia on the inlet. The flow meter is permanently attached to the pump inlet. A quick disconnect vacuum line connection is on the right hand side of the flow meter.

3.5 System Setup and Operation

Setup of the basic sampling case follows the standard procedures established for manual control. After the sampling probe has been inserted in the sampling case, the three flexible lines from the controller are connected to the mating stainless tubing on the probe by an AN connector. These connections must be tight as any leakage will cause a system error.

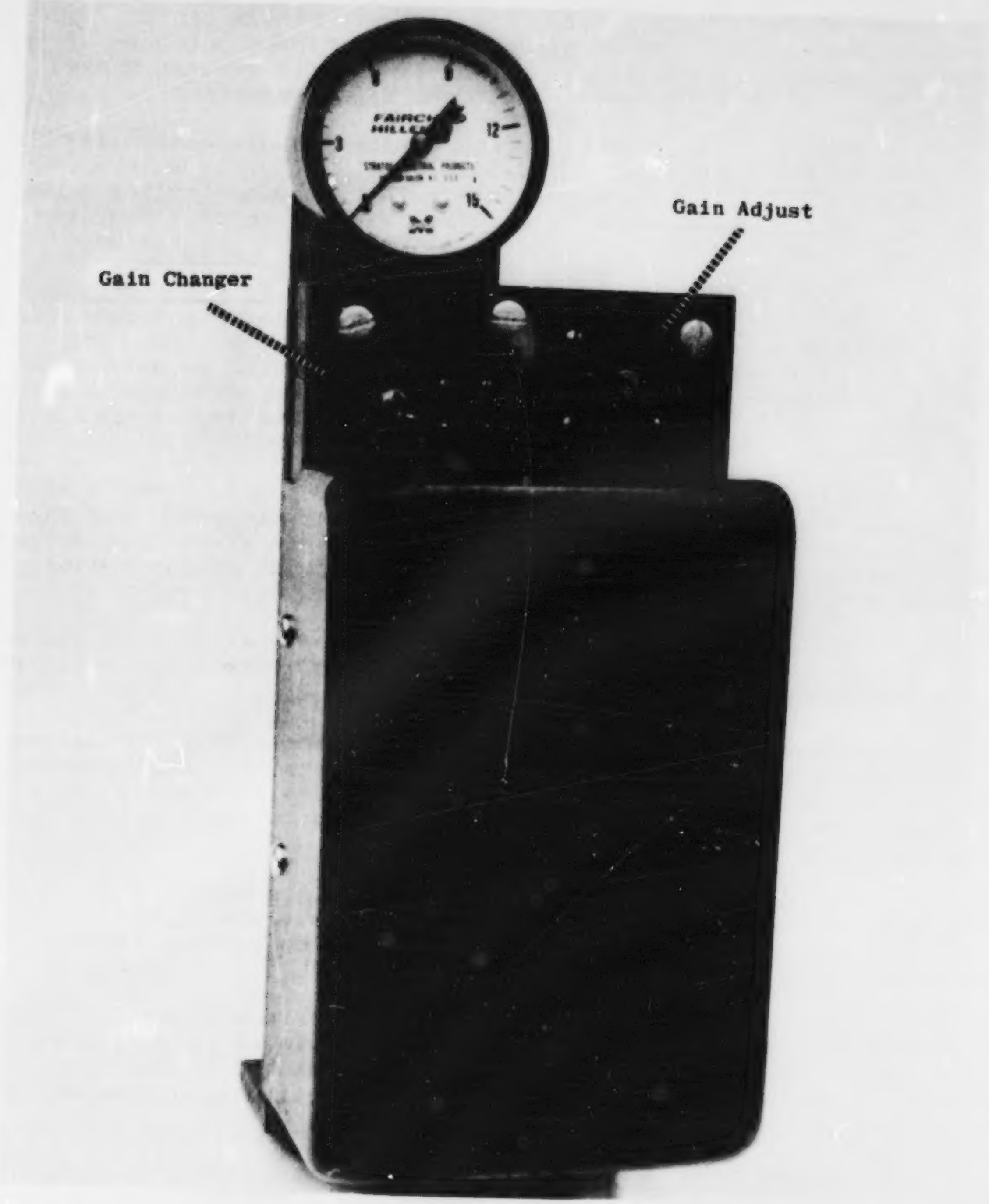

Figure 3.18 Fluidic Controller

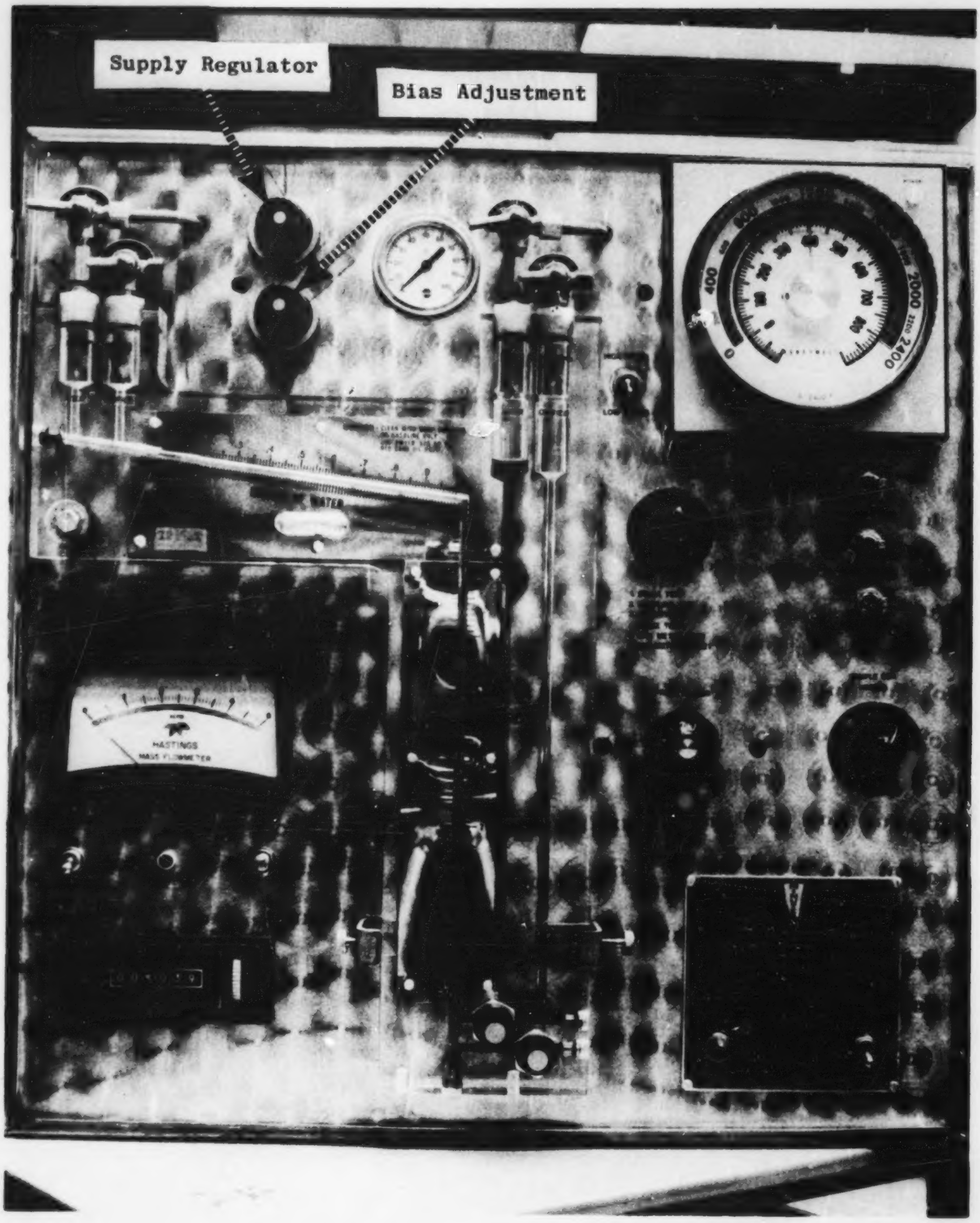

Figure 3.19 Control Console

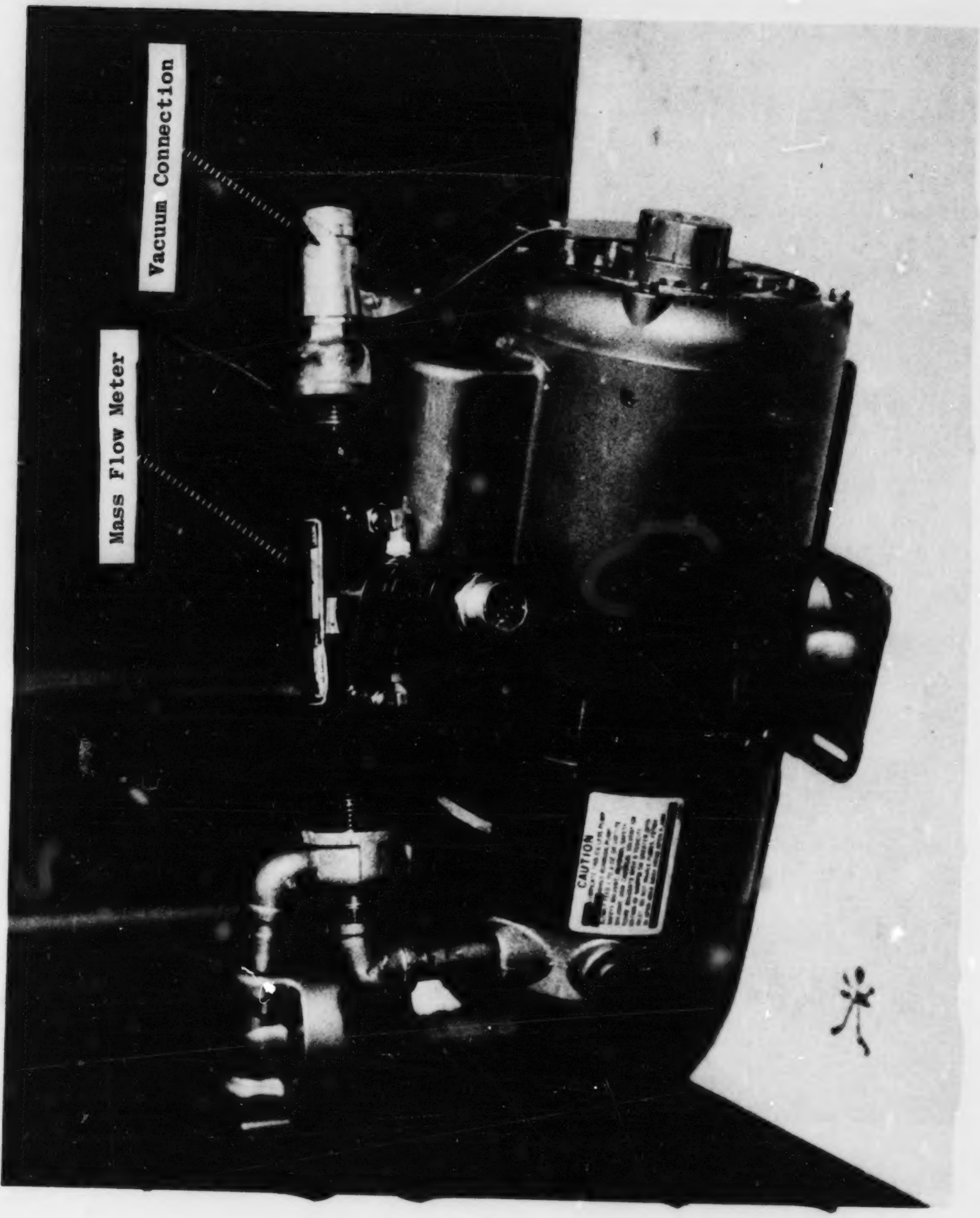

Figure 3.20 Pump and Flow Meter

The sampling nozzle and sensor assembly is inserted in the outer end of the probe. Two sensing tubes on the nozzle are connected to the mating lines on the probe through AN connectors. These two connections must also be tight to prevent any leakage.

Assuming the approximate velocity head of the gas to be sampled is known, the next step is to set the knobs on the automatic controller. Table 1 tabulates the knob setting for the particular sampling nozzle used and the velocity head. If the velocity head is a complete unknown, set the knobs to correspond to the particular sampling nozzle inserted in the probe. For the ¼ inch nozzle turn the zero on the left hand knob towards the top of the sampling case. The left hand knob should be set to a mid-range position so that the numeral four is on the index mark. These adjustments are made by turning the screw in the center of the knob CCW to loosen the knob. The knob is then set to the required position and locked by tightening the screw.

The umbilical cord, with the exception of the two pneumatic lines, can now be connected to the sampling case. The pneumatic lines are left disconnected so they can be purged to remove any debris that they may have collected in transport or storage.

The other end of the umbilical cord is connected to the control console. All connections with the exception of the vacuum line are made to a rear panel of the console. The vacuum line connection is made directly to the pump mounted flow meter.

Supply air at a pressure of 35 to 100 psig is brought into the console through a quick disconnect fitting on the rear panel. After supplying air to the console the supply regulator on the front of the console is set to give a 5 psi reading on the gauge. The second regulator knob (lower knob) is turn CW as far as it goes. This procedure purges the pneumatic lines to the sampling case. After a few seconds both regulators are turned all the way CCW. The pneumatic lines are now connected to the sampling case. The supply line is connected to the supply quick disconnect and the second line to one of two disconnects by which the bias is applied to the controller.

The supply regulator on the control console is now set for a gauge reading of 25 psig which is the system operating pressure. The second regulator is set so that the needle on the gauge on the automatic controller is in a range from just leaving the stop to two divisions above the stop. If this setting cannot be achieved, the pneumatic line must be switched to the second connection on the sampling case.

The probe is now ready for insertion into the sampling port. Supply air must be maintained to the controller continuously during a sampling run to insure backflushing of the sensor when it is exposed to a contaminated environment.

Table 1

	Controller Gain Setting		
Sampling Nozzle	Pitot Reading Inches H_2O	Variable Gain (Rt.Hd. Knob)	Fixed Gain (Lf.Hd. Knob)
3/8" Diam.	0.1	1	Zero Right ↓
	0.2	1	
	0.3	1	
	0.4	2	
	0.5	2	
	0.6	2	
	0.7	2	
	0.8	3	
	0.9	3	
	1.0	3	
¼" Diam.	0.5	3	Zero Vertical ↓
	1.0	3	
	1.5	4	
	2.0	4	
	2.5	5	
	3.0	5	
	3.5	6	
	4.0	6	
	4.5	7	
	5.0	7	

If there was no prior knowledge of the gas velocity head, the controller may not be set for the proper system gain. Too high a gain will cause the system to oscillate at a frequency of about 2 Hz. This can be observed on the pressure gauge on the automatic controller. If an oscillation is observed, the gain is lowered by turning the left hand knob on the controller to a higher number setting until the oscillation stops.

The optimum control range is 0.5 to 1.5 scfm. If the flow as indicated by the mass flow meter is out of this range, the sampling nozzle should be changed to a size which will satisfy this range.

4. TEST PROGRAM

The test program was directed at an evaluation of the overall controller. Test results obtained on specific components or sensors are presented in Appendix I and the sections discussing the particular component.

Tests were performed in the laboratory, with wind tunnels and signal generators, to establish steady-state error derivatives and dynamic response capabilities of the controller. At the completion of the laboratory tests the controller was tested at a power plant installation to evaluate the controller's capability of functioning under representative field conditions. One field test was performed early in the program, after selection of the final sensor configuration. This test, performed at an oil-fired power plant, was primarily designed to test the ability of the sensor to function in a contaminated environment. The complete engineering prototype was tested in the second test. This test was made at a coal-fired power plant.

4.1 Dynamic Laboratory Tests

The dynamic tests are designed to measure the controller's response to changes in air stream velocity. This response is a function of the system gain which in turn is dependent on the nominal dynamic pressure produced by the gas velocity and on the sampling nozzle area. The controller has a presettable gain to accommodate these variables. When properly set the overall system gain and thus response will be constant. The prime objective of the dynamic tests is to relate the variable resistor setting on the controller to the dynamic pressure head of the sampled gas. This is the basis for Table 1 under setup and operating procedure. These settings are referenced to the dynamic head read on the S-type pitot tube on the sampling probe. The test setup is illustrated in Figure 4-1. A means of modulating the free air stream with a rapid and controllable characteristic is required for the dynamic tests. The frequency range of interest (0-2 Hz) is beyond the capabilities of available wind tunnels hence special fixturing was required. The modulated air source is generated by a relatively small plenum fed from a constant flow source (choked upstream orifice). The plenum feeds two nozzles -- one nozzle approximately two diameters larger than the sampling probe produces a free jet which is directed at the probe. The second nozzle functions as a variable bleed from the plenum, where the discharge coefficient is varied in a sinusoidal fashion by a rotating cam at the nozzle exit. Step changes in air flow are produced with the same fixture by replacing the rotating cam with a spring loaded shutter.

Dynamic closed loop performance is determined by measuring the free jet velocity and comparing to probe inlet velocity as measured by a pitot tube at the probe inlet. These two velocity measurements yield the closed loop output/input ratio of the controller.

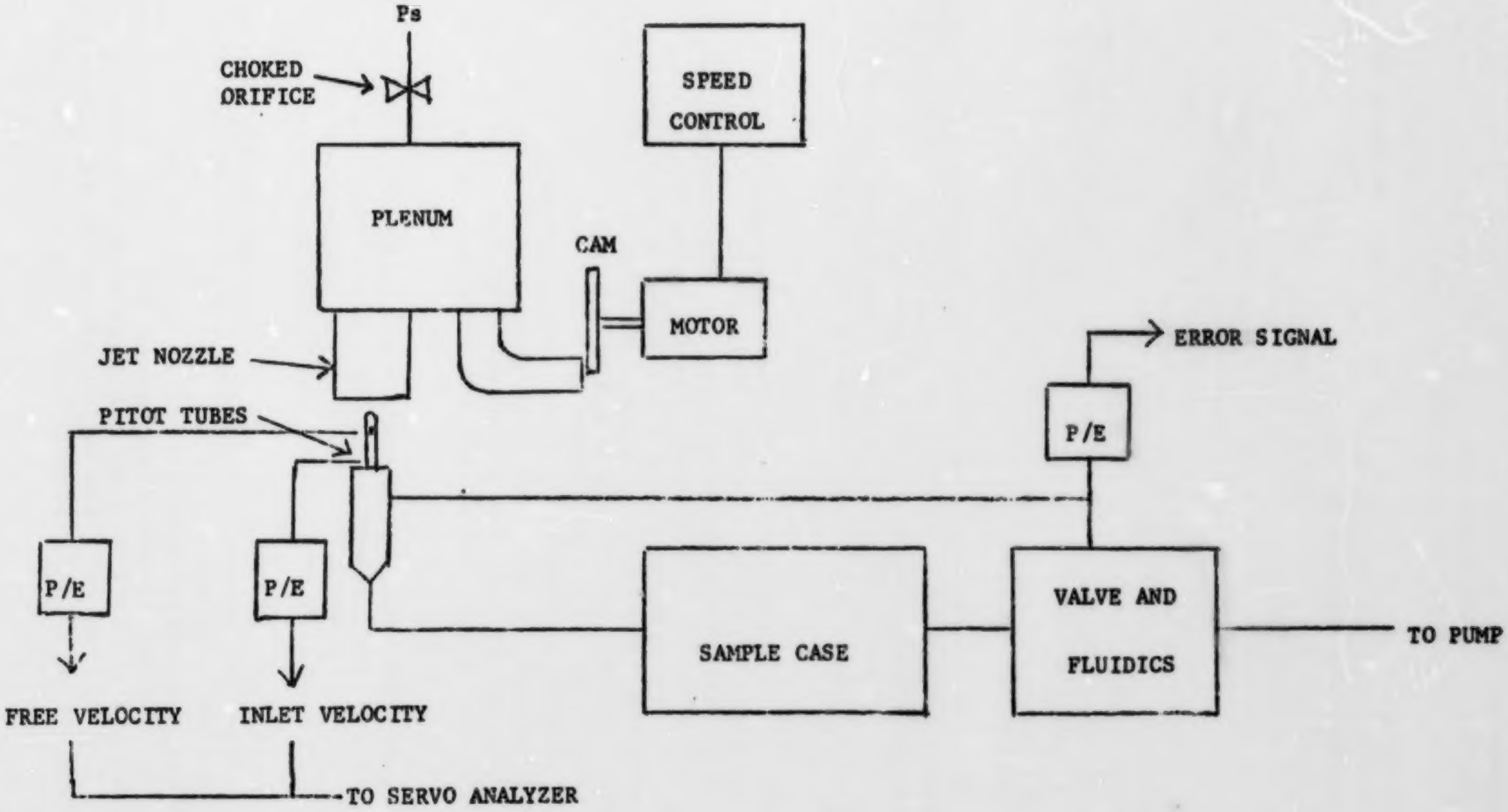

Figure 4-1. Dynamic Test Setup

The average velocity for these tests was measured by both flow measurements and by the pitot static tube at the inlet of the sampling nozzle. These were then correlated to the S-type pitot tube by steady-state tests in a wind tunnel.

Figures 4-2 through 4-4 show typical performance curves of the controller. In Figure 4-2 the velocity was held constant and the system gain varied by changing the variable resistors. A gain reduction of 2:1 from nominal results in a decrease in bandwidth to approximately 70% of the nominal with degraded damping. An increase of gain by a factor of 2:1 results in approximately a 2:1 increase in bandwidth and the control loop is on the verge of instability. The measured relationship between bandwidth, damping and gain tend to follow the predicted characteristics. The signal shaping networks were selected to give maximum phase margin at a bandwidth of 2.5 Hz and system damping will degrade as the bandwidth deviates from the nominal in either a high or low direction.

4.2 Steady-State Tests

The prime objectives of the steady-state tests were to obtain a quantitative measure of steady-state error derivatives in sampling rate as a function of nominal sampling velocity, pneumatic power supply, filter loading and component drift. The controller gain settings established in the dynamic tests were used in all steady-state testing.

The first series of tests were designed to identify those errors associated with the fluidic controller. These tests were conducted with the sampling nozzle in the wind tunnel and the controller gain set to correspond to the nominal air velocity. The output of the velocity sensor was monitored independently with an inclined manometer. The automatic controller was turned on with the bias adjust set to zero and the sampling rate recorded. The wind tunnel was then shut down and the bias control adjusted so that the needle on the controller pressure gauge moved off the stop. The wind tunnel was then turned on and the sampling rate recorded. This procedure was repeated with the bias adjusted so that the pressure gauge indicated one mark and two marks from the stop.

A base reference flow rate was established by removing the automatic controller and manually controlling the flow valve to null the velocity sensor. The fluidic controller error is the deviation from the flow rate obtained with the sensor nulled.

Results of these tests are summarized in Figures 4-5 and 4-6. The curves are normalized to the flow rate obtained with the sensor nulled. Referring to Figure 4-5, it is apparent that the controller can contribute errors as large as 15% at a gas velocity of 20 ft/sec if not compensated with the bias adjust. The uncompensated error tends to decrease with increasing gas velocities, indicating that the major source of the inherent bias in the controller is in the preamplifier stages or the gain

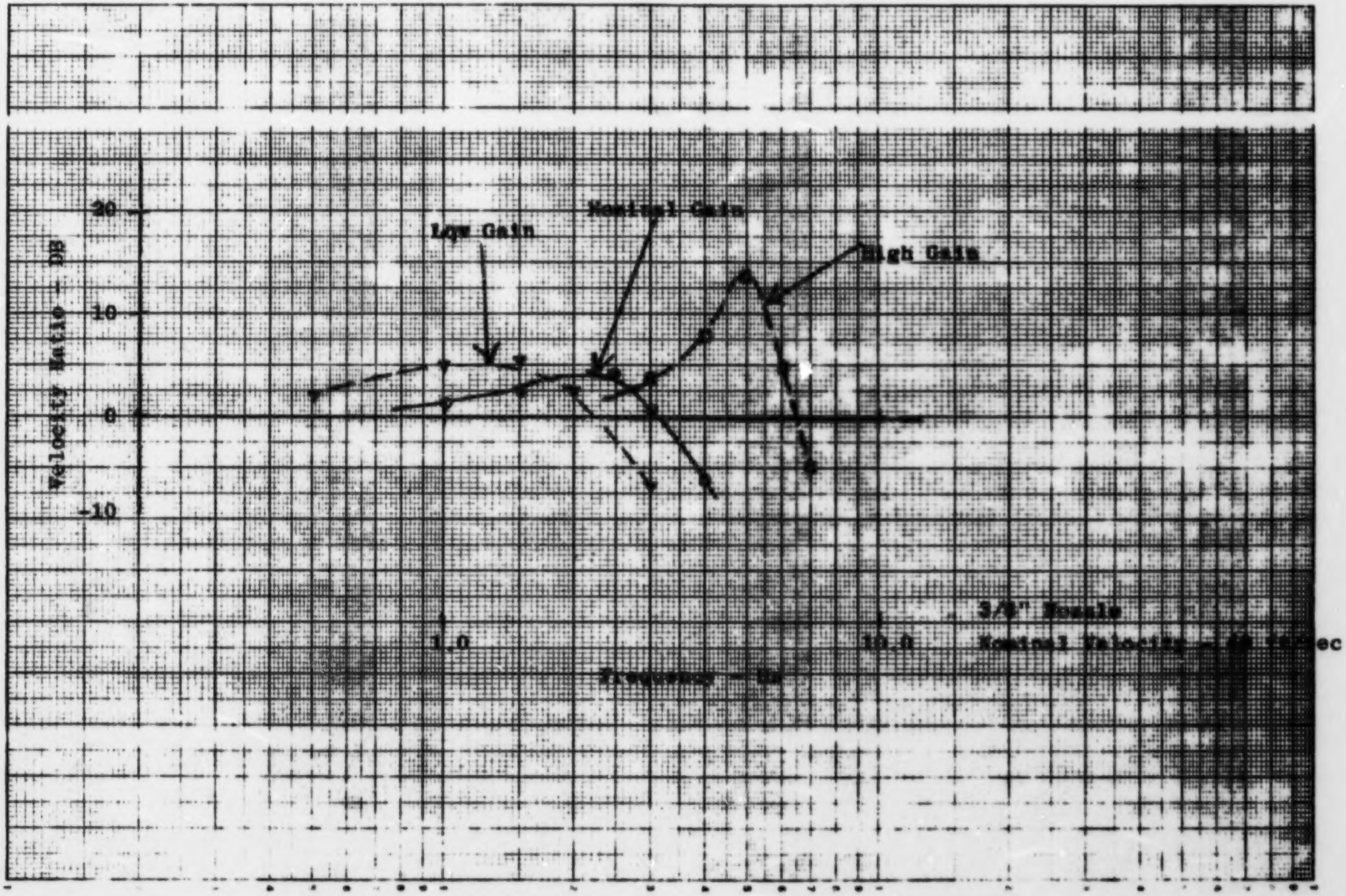

Figure 4-2. Dynamic Response at Various Gain Settings

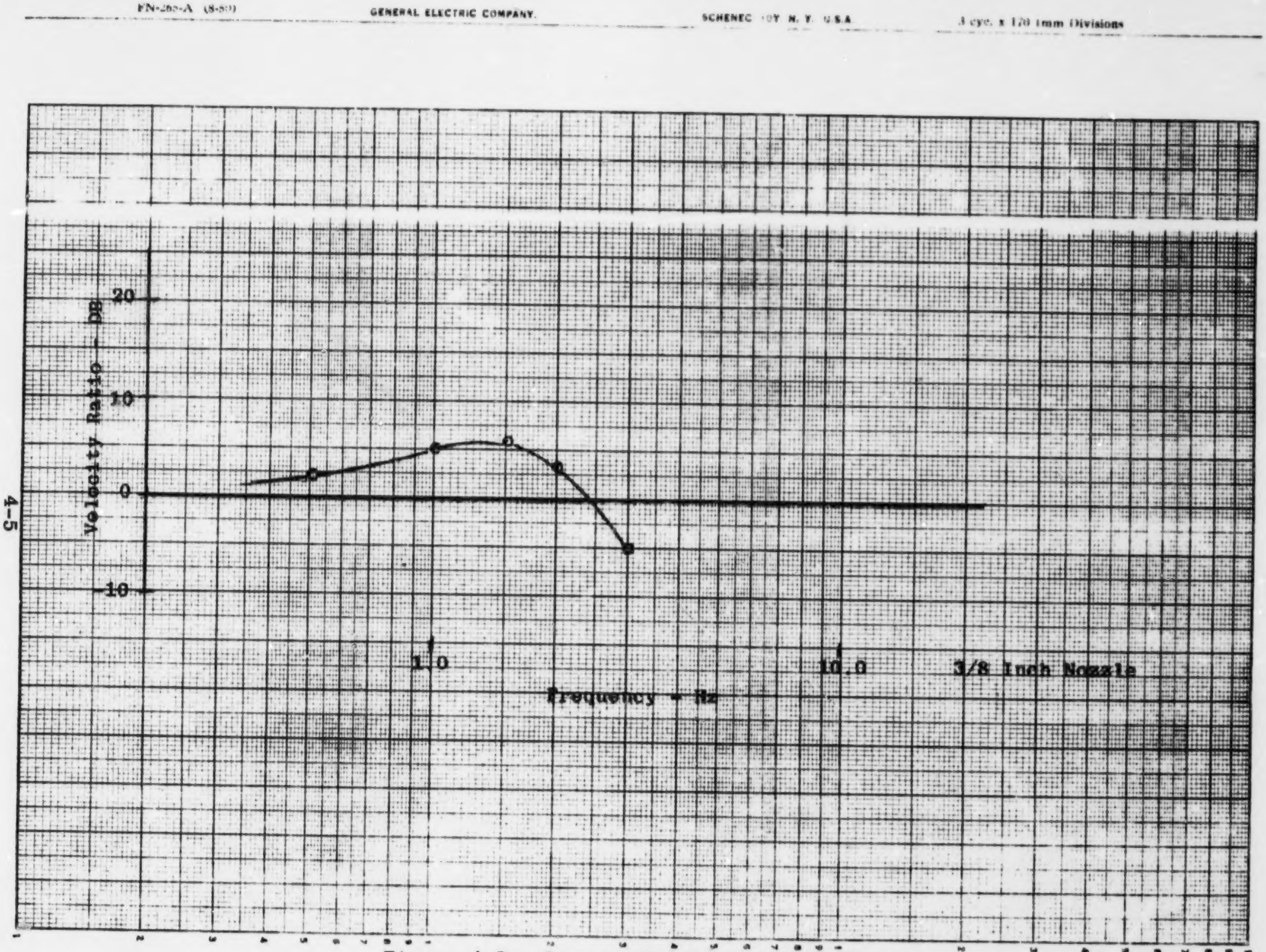

Figure 4-3. Dynamic Response - 20 Ft/Sec

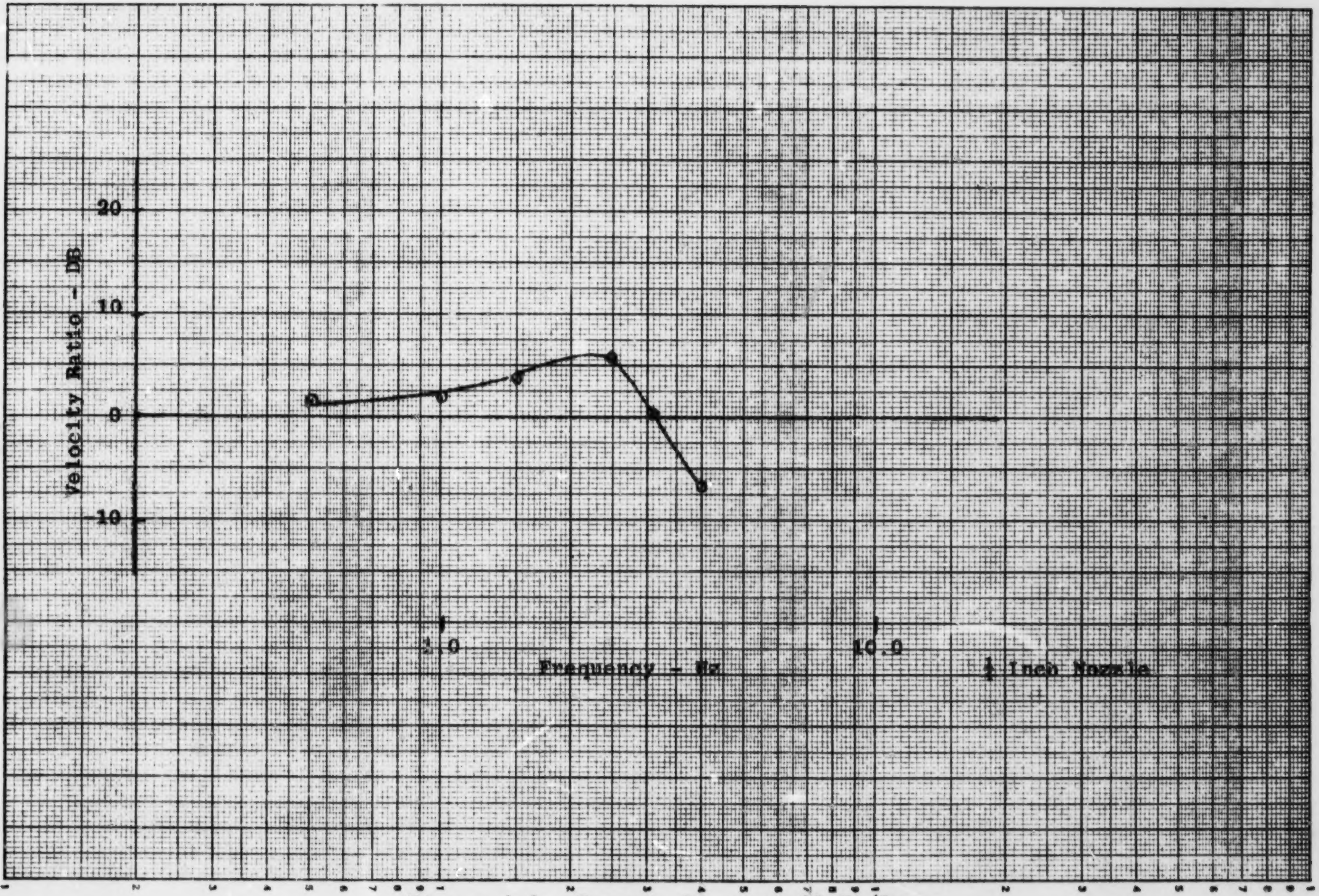

Figure 4-4. Dynamic Response-80 Ft/Sec

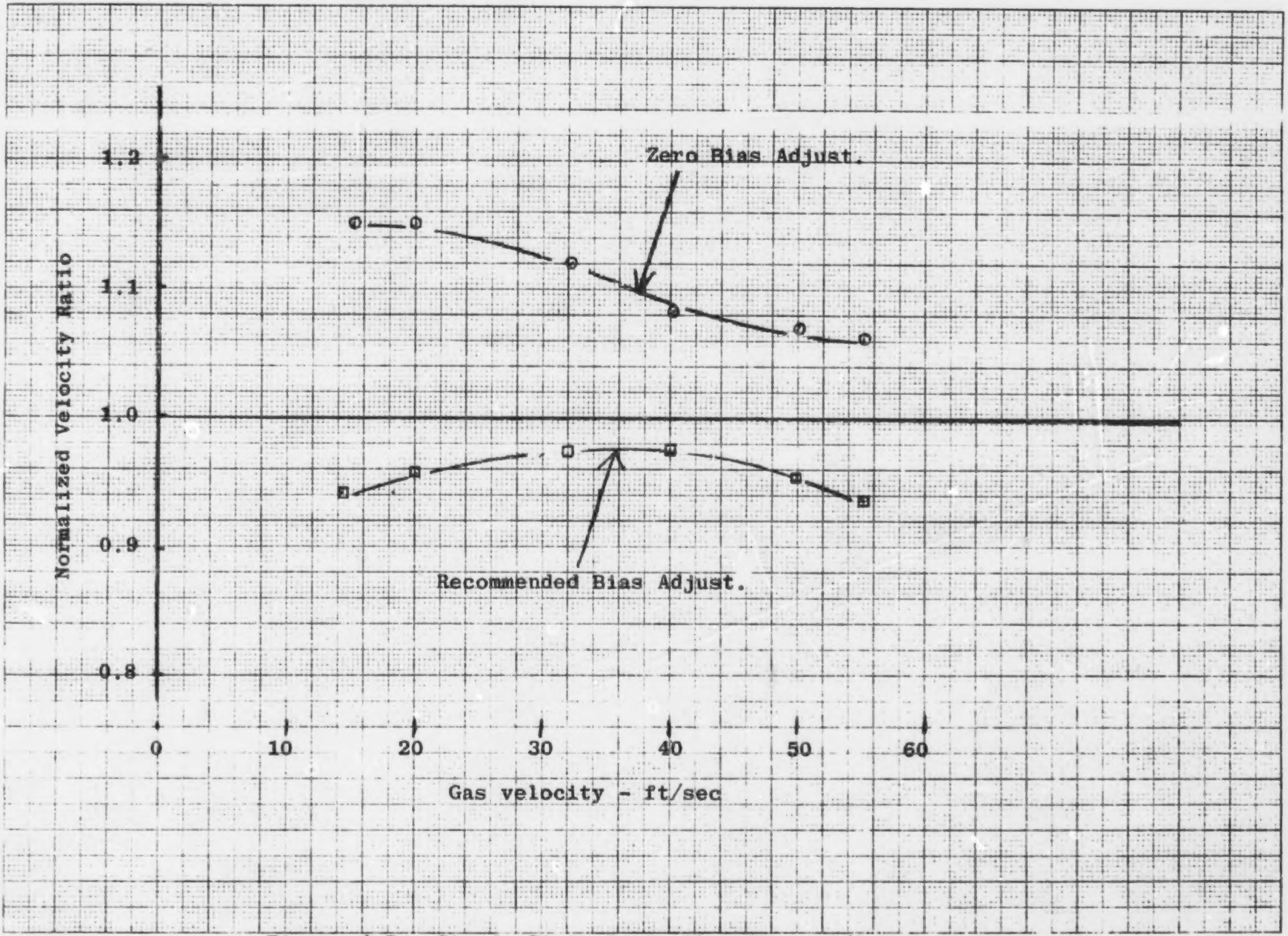

Figure 4-5. Steady-State Controller Error-3/8 Inch Nozzle

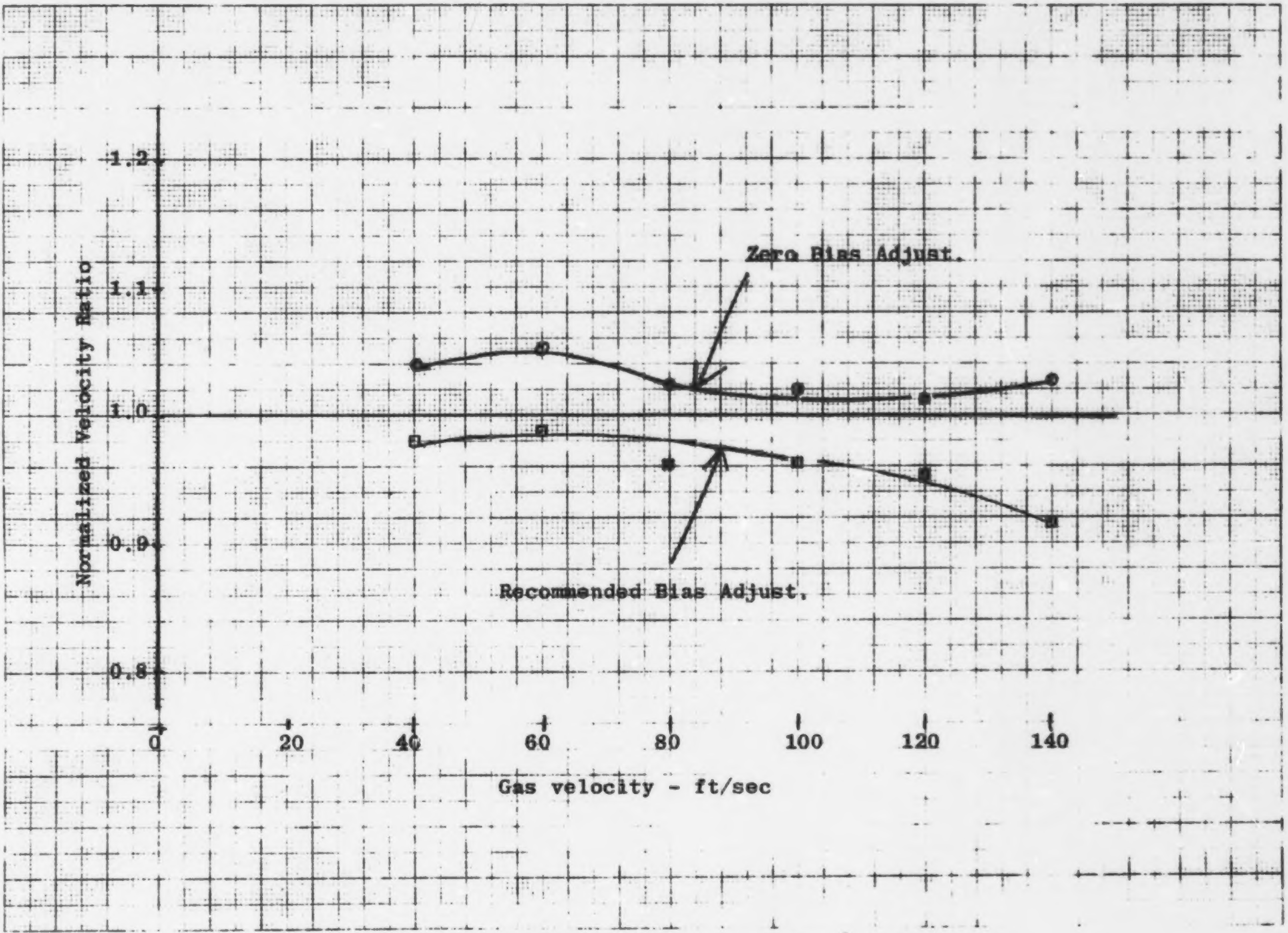

Figure 4-6. Steady-State Controller Error-¼ Inch Nozzle

changing resistors. If the inherent bias were introduced by a component following the gain changing resistors, the error would be independent of the nominal gas velocity. The error contributed by the controller will be less than 5% if the bias control is properly adjusted.

The influence of pneumatic supply pressure on the controller accuracy is summarized in Figures 4-7 and 4-8. The controller bias was adjusted with a nominal supply pressure of 25 psig. Deviations in flow were recorded as the supply was varied from the nominal. Flows are normalized to the flow at the nominal supply. Figure 4-7 is a plot of two specific tests at 20 and 40 ft/sec while Figure 4-8 is a summary of all the tests. The controller has more than adequate insensitivity to supply pressure. The primary concern would be undetected supply pressure changes during a sampling run. These changes would be minimal in that the control console supplies the automatic controller through a regulated supply.

Sampling rate error as a function of filter loading was measured by placing calibrated orifices in the outlet of the filter holder. Results of several representative tests are shown in Figure 4-9. The effects of filter loading are minimal providing the system is not near the mass flow limit at the start of a sampling run. This is illustrated by the nominal 1.7 scfm test. This is almost at the 2.0 scfm limit imposed by a clean filter and the sampling case impingers, and additional pressure drops cannot be readily accommodated by the controller. A range of pressure drops representative of field conditions is 4 inches of H_2O to 20 inches of H_2O. This range encompasses effects of filter loading and sampling flow rates of 0.5 to 1.5 scfm.

Results of calibration tests of the automatic controller prior to the final field test are shown in Figures 4-10 and 4-11. In each instance the automatic controller was set up with the predetermined gain setting and the bias adjust varied to bring the pressure gauge needle to the second mark above the stop.

As indicated in Figure 4-10, the controller is maintaining isokinetic conditions to better than 10% over a velocity range of 15 to 40 ft/sec and that the major source of error is in the sensor. The sensor characteristic which was obtained independently by nulling with an inclined manometer is shown as the dashed curve. At the maximum velocity of 54 ft/sec the controller is contributing significant error because of system flow limiting (1.8 scfm flow rate). The upper curve defines the maximum flow rate control range that can be established with the bias control. Within this range the sensor error can be compensated for by calculating isokinetic flow from measured gas temperature and the S-type pitot pressure differential. The bias control can then be adjusted until the system flow meter indicates the correct flow.

The $\frac{1}{4}$ inch diameter sampling nozzle has a constant error with velocity as shown in Figure 4-11. The error is approximately 15% and of a polarity to cause the sampled velocity to be lower than the free air stream velocity.

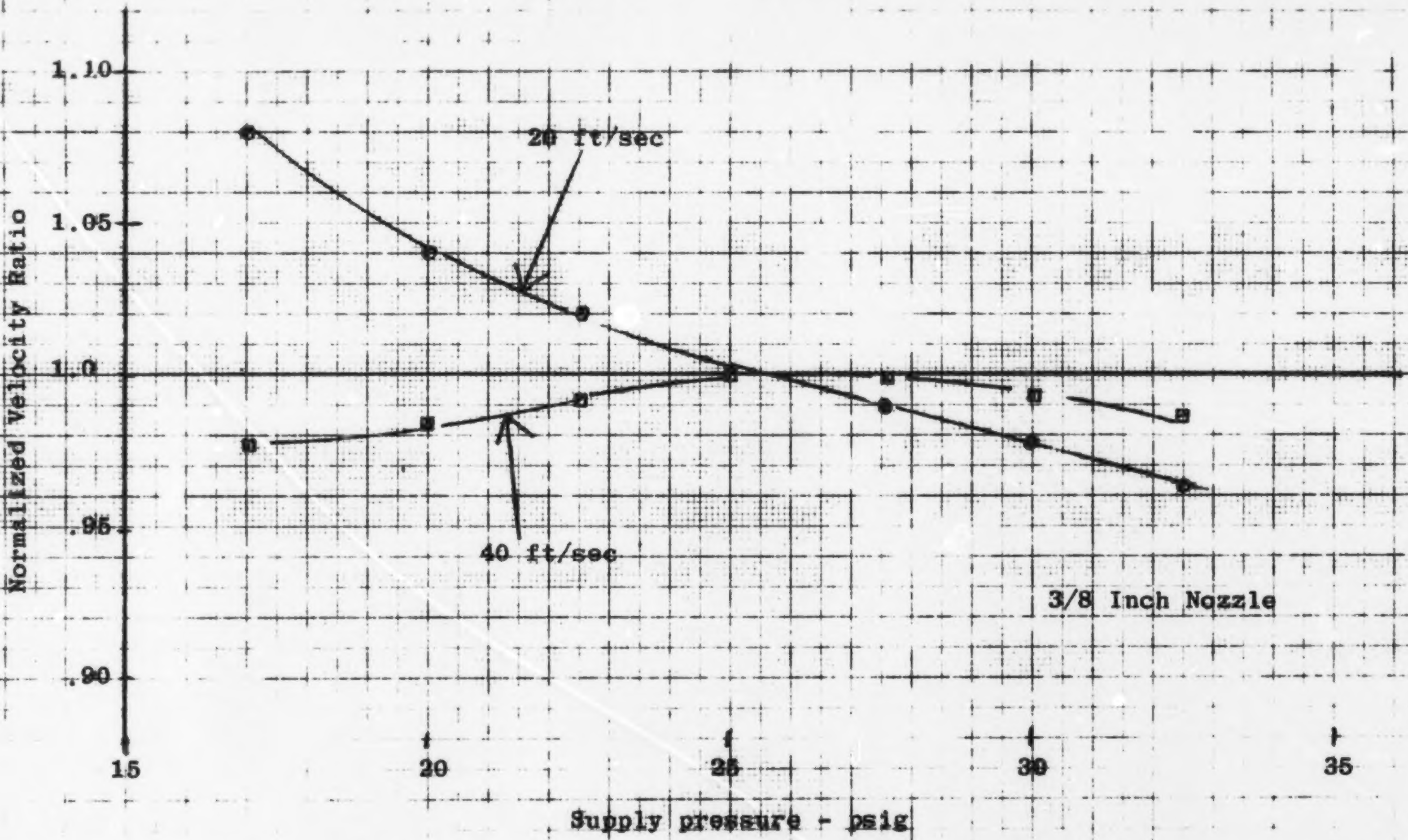

Figure 4-7. Controller Error Vs. Supply Pressure

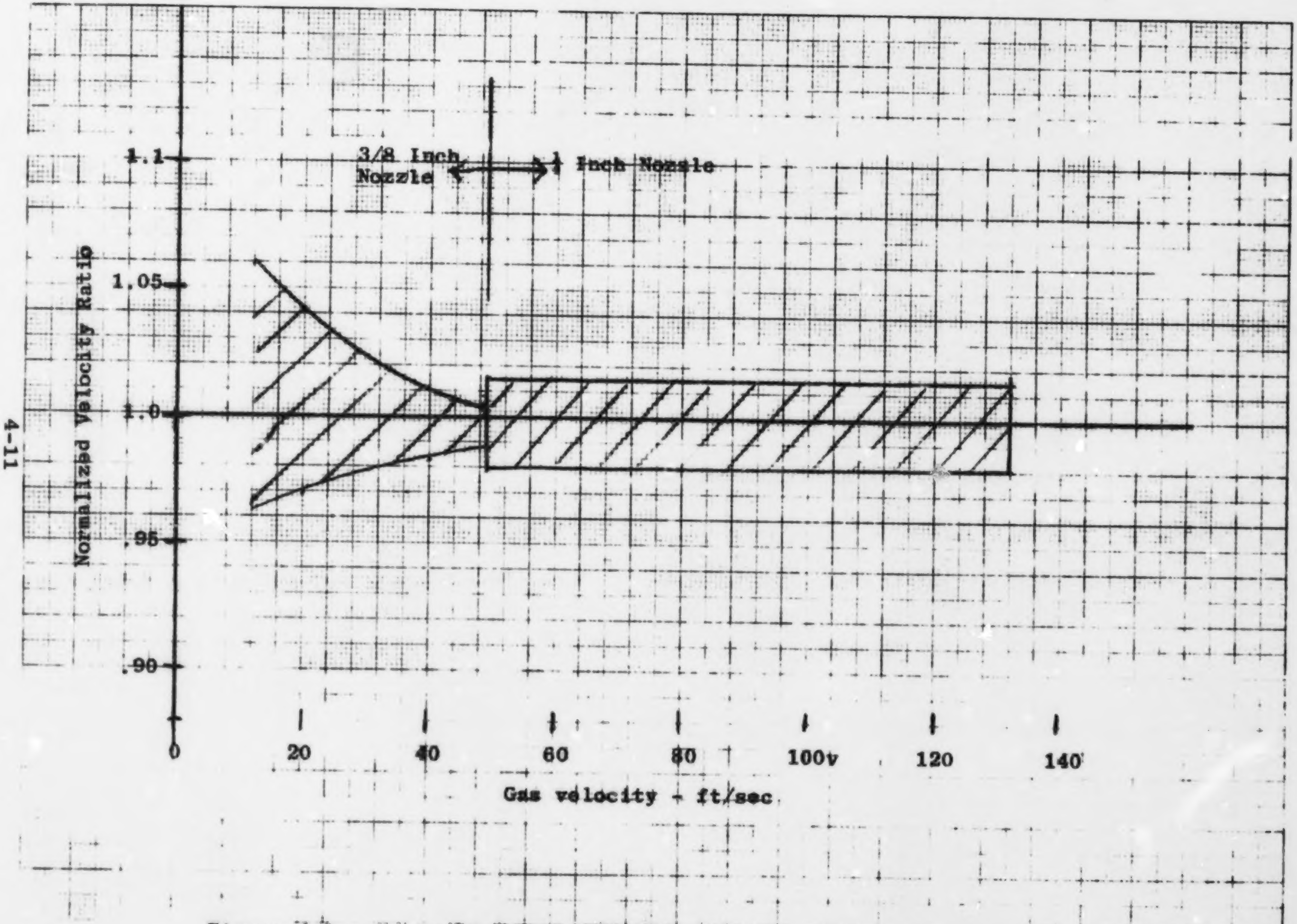

Figure 4-8. Controller Error Vs. Velocity for ±20% Supply Variation

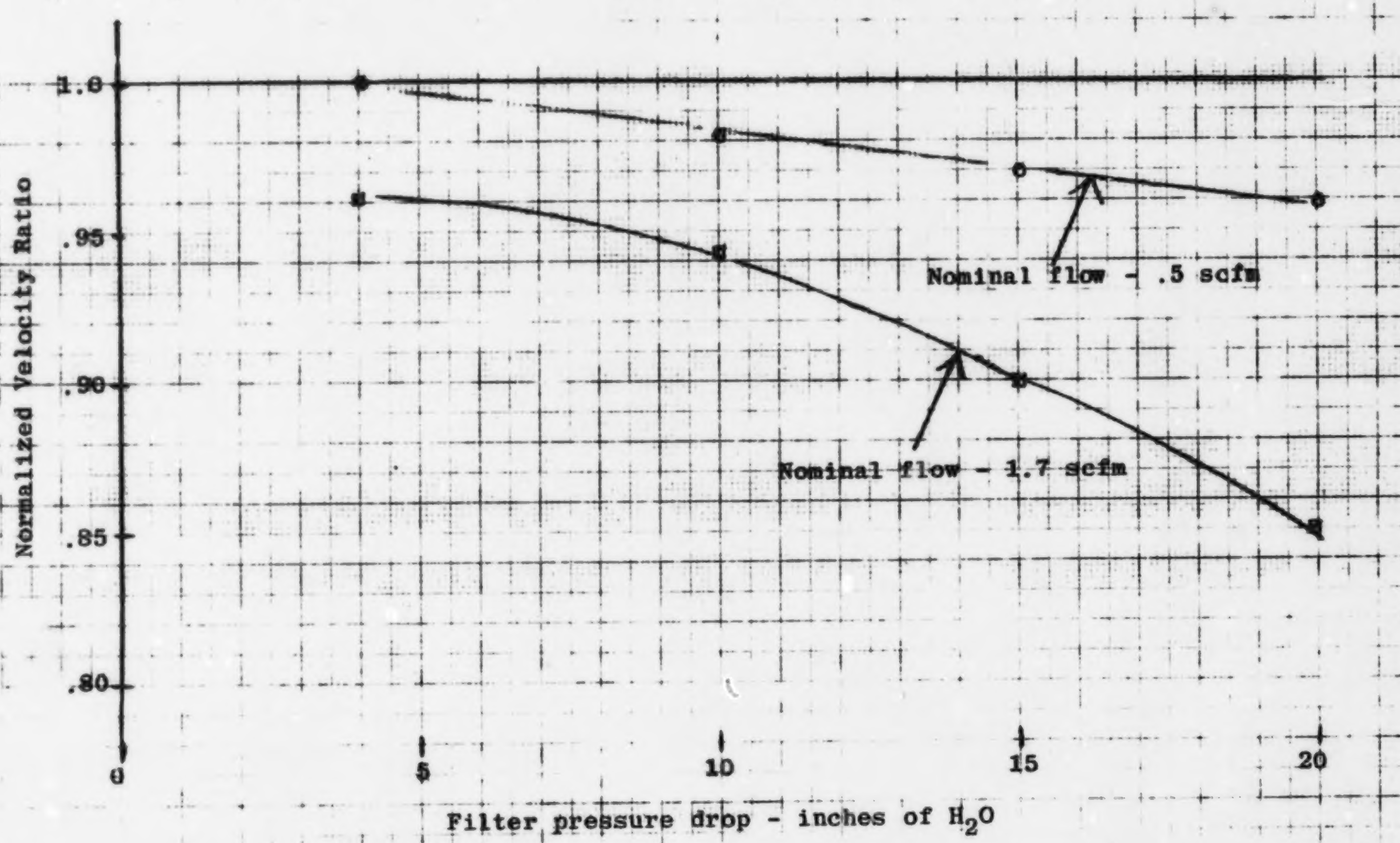

Figure 4-9. Sampling Error Vs. Filter Pressure Drop-3/8 Inch Nozzle

180x250 1mm Divisions

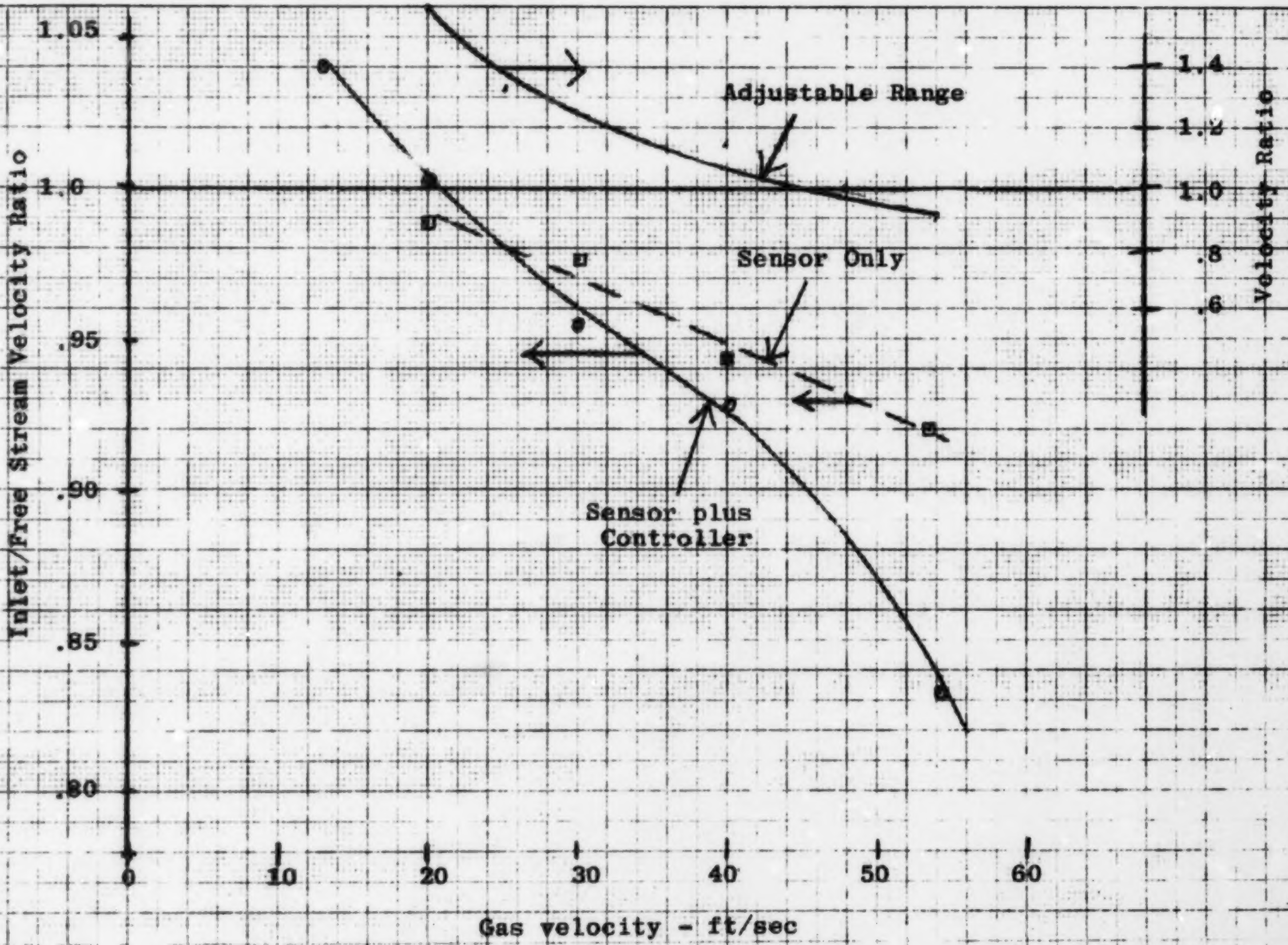

Figure 4-10. Steady-State Calibration-3/8 Inch Nozzle

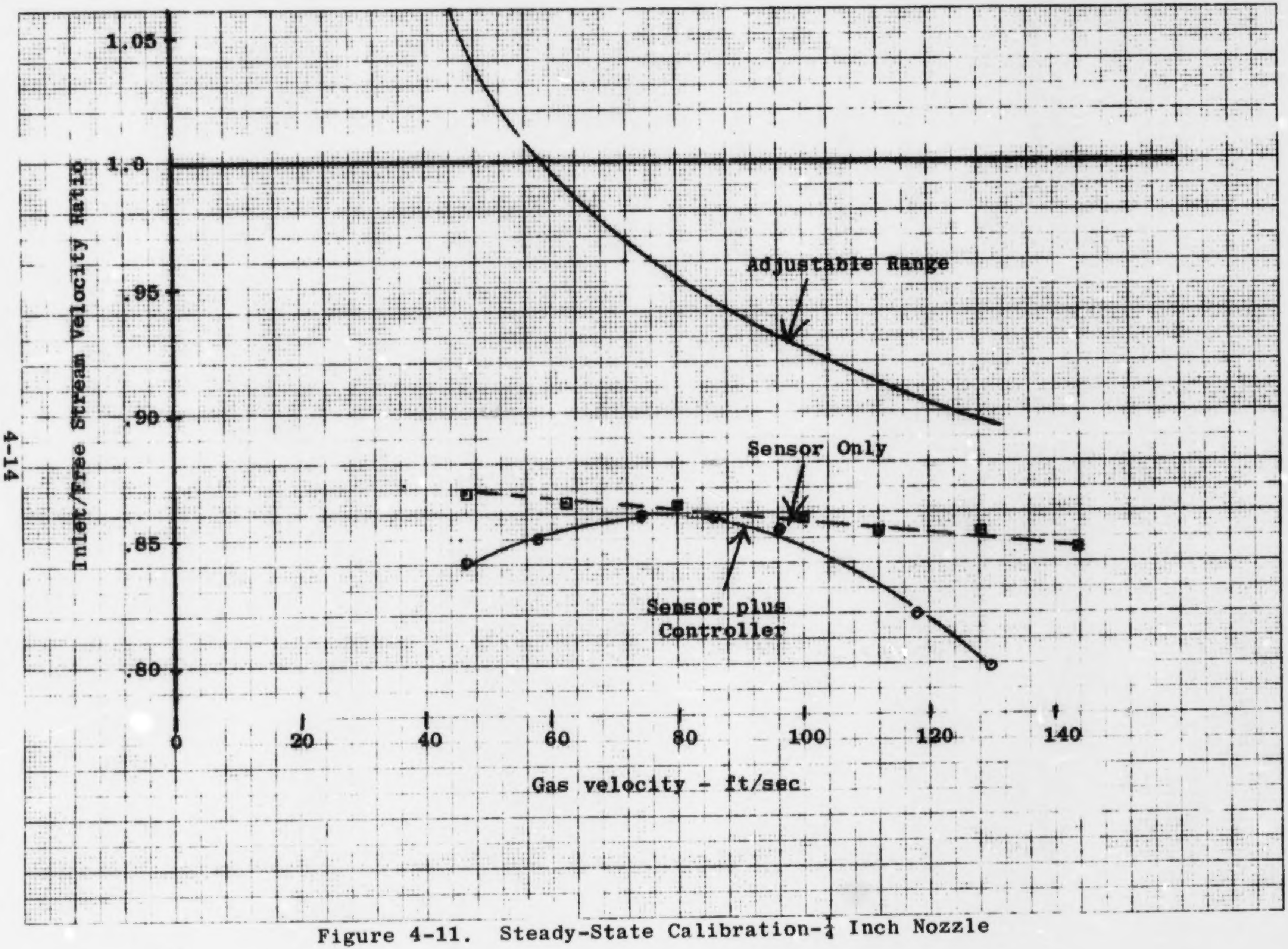

Figure 4-11. Steady-State Calibration-¼ Inch Nozzle

4.3 Field Tests

Two field tests were conducted on the equipment. A preliminary field test was directed at evaluating the basic sensor concept. Isokinetic flow was maintained manually for this test. Several required design changes in the sensor were identified in the preliminary test.

These changes were subsequently incorporated in the prototype sensor which was evaluated in the second field test. Sampling rates were controlled by the automatic controller during the second test.

4.3.1 Preliminary Field Test

Test Location - Number three stack of the General Electric Power Station at Schenectady, New York. This plant is an oil-fired installation. Tests were conducted on January 19, 1973.

Test Procedure - The test procedure and sampling train configuration of Method 5 (Determination of Particulate Emissions from Stationary Sources) as specified in EPA Standards of Performance for New Stationary Sources in the Federal Register dated December 23, 1971, was used in conducting the tests. The tests were conducted by Mr. David Wilson of the General Electric Technical Services Laboratory.

The test nozzles were standard nozzles modified to incorporate free air stream and nozzle inlet static pressure ports. After insertion of the sampling nozzle into the stack, the sensor was maintained at null by manually controlling the vacuum pump suction. The null was monitored with an inclined water manometer with a reading accuracy of better than 0.01 inches of water.

With the sensor nulled the pressure differential across the calibrated orifice was recorded and compared to the calculated pressure differential corresponding to isokinetic nozzle flow. The calculation was performed with a standard nomograph and dry and wet molecular weights as determined by a prior test on the stack.

Two sample nozzle sizes were tested. A 3/8 inch diameter nozzle was considered the primary test nozzle--isokinetic flow on this nozzle corresponds to about 0.85 scfm, which is an optimum range for the control unit instrumentation. The second sensor had a ¼ inch diameter nozzle with an isokinetic flow of approximately 0.33 scfm. This is a low range for accurate quantitative measurements. This sensor nozzle was operated with the nozzle axis misaligned 30 degrees relative to the free air stream velocity. This orientation yields a component of particulate velocity normal to the surface of the sensing tube and the inlet of the sensing ports and represents a "worse case" operating mode.

The output of a fluid amplifier used to establish a backflushing flow into the sensor and to amplify the sensor differential pressure was monitored throughout the test. A positive pressure of 0.5 inches of water relative to stack static (averaged approximately 0.5 inches of water) was maintained by this amplifier.

Test Results - Figure 4-12 is a plot of the ratio of nozzle inlet velocity with the sensor nulled to the computed inlet velocity on the 3/8 inch diameter sampling nozzle. The nominal value of 0.9 agrees quite well with the results of a pretest calibration run made in a laboratory environment. On the basis of dynamic head the gas velocities encountered in the stack correspond to a velocity range of 26 to 34 ft/sec on the calibration curve. Total variation of the nozzle inlet velocity was compared to the computed value was 5% over the two-hour run. After 80 minutes of test time the four-inch diameter filter used in the sample case became so heavily loaded that the pump could no longer maintain the sensor at null. During the subsequent removal and replacement of the filter, the sensor was left in the stack and was exposed to a severe anisokinetic operating condition for 15 minutes. During the remainder of the test the sensor was operated at null. The volume of dry gas collected during the run was 102 cubic feet, referenced to standard conditions.

Figure 4-13 shows the results obtained on the ¼ inch nozzle. The change in ratio as a function of test time remains within 5%; however, because of nozzle misalignment, the nominal ratio departs considerably from the laboratory calibration. The volume of dry gas collected during this run was 27 cubic feet referenced to standard conditions.

The output of the fluid amplifier was monitored throughout the run. It had an initial offset before the sensor was inserted in the stack equivalent to 0.02 inches of water on the input. This offset remained virtually unchanged as the probe was inserted into the stack and nulled.

After the field test was completed the sensors were rechecked in an "as is" condition in the calibration setup. Figures 4-14 and 4-15 show the comparison of before and after the field test. The change in characteristics is considered acceptable. The maximum change of 6% occurred on the ¼ inch nozzle in the range of 33 ft/sec.

Figures 4-16 and 4-17 are photographs of the two sensors taken after the stack tests. The 3/8 inch diameter nozzle is shown in Figure 4-16. The sensors are made of 1/8 inch OD stainless steel tubing. The free air stream sensor is located above and slightly to the right of the nozzle inlet. The straight, upright tube is used to establish a positive backflushing pressure relative to the stack static pressure. The contamination deposition pattern is clearly evidenced in the photographs with the major deposition occurring on the leading surfaces of the tubes. Buildups of as much as 0.03 inches occurred on the stack static reference tube. The surface of the sensing tubes containing the static pressure ports are parallel to the gas flow and exhibit virtually

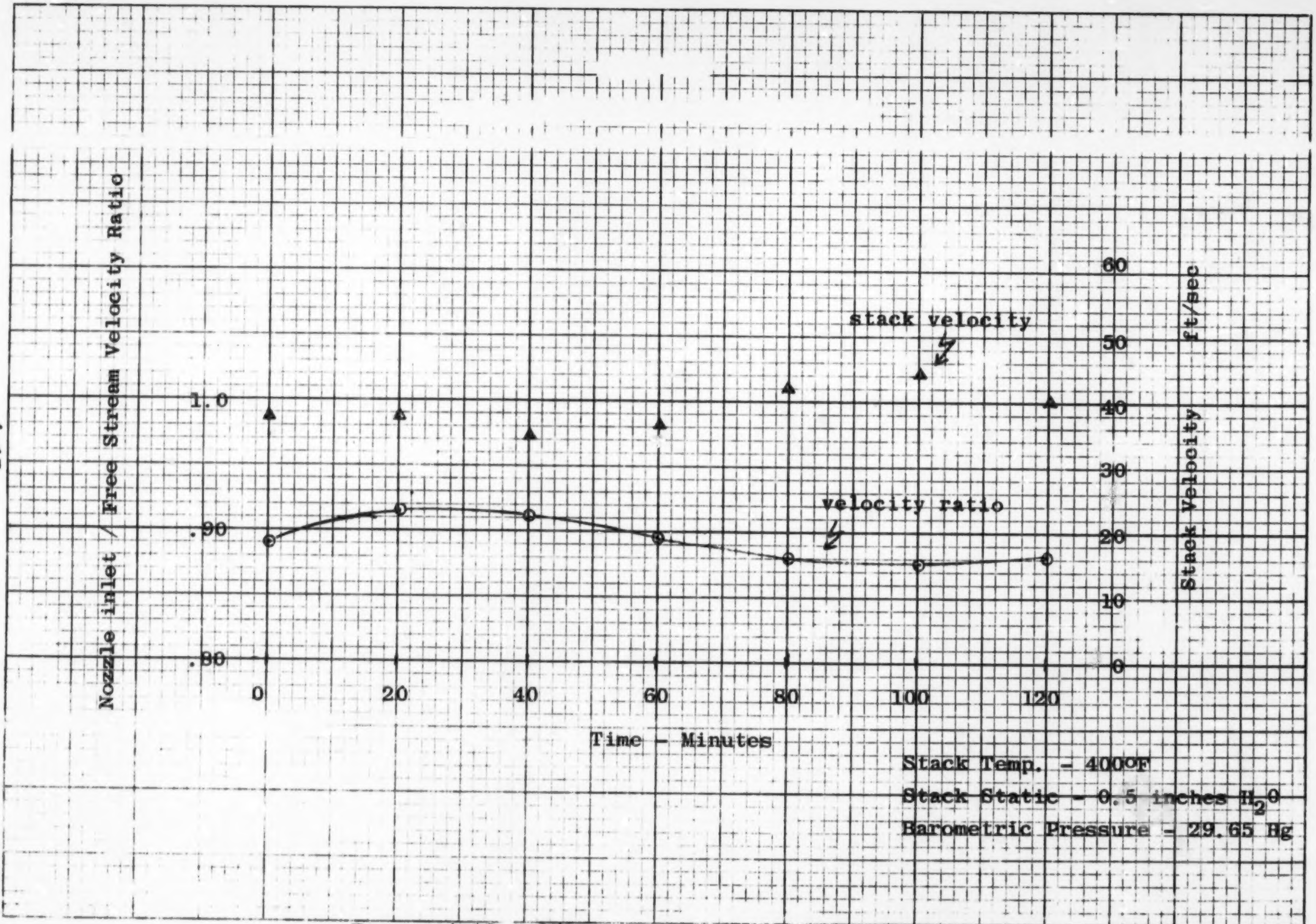

Stack Temp. - 400°F

Stack Static - 0.5 inches H_2O

Barometric Pressure - 29.65 Hg

Figure 4-12. 3/8 Inch Diameter Sampling Nozzle

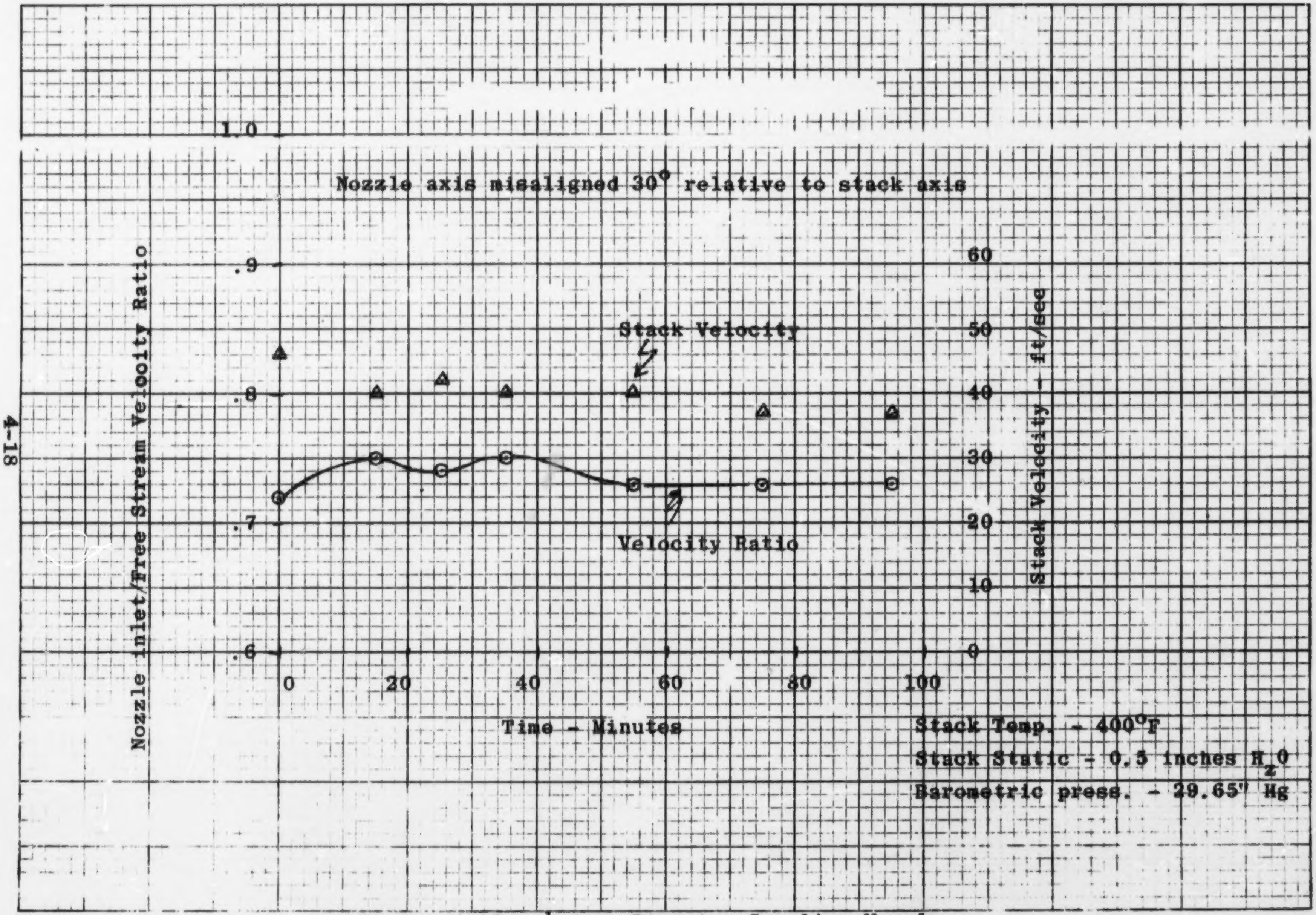

Figure 4-13 $\frac{1}{4}$ Inch Diameter Sampling Nozzle

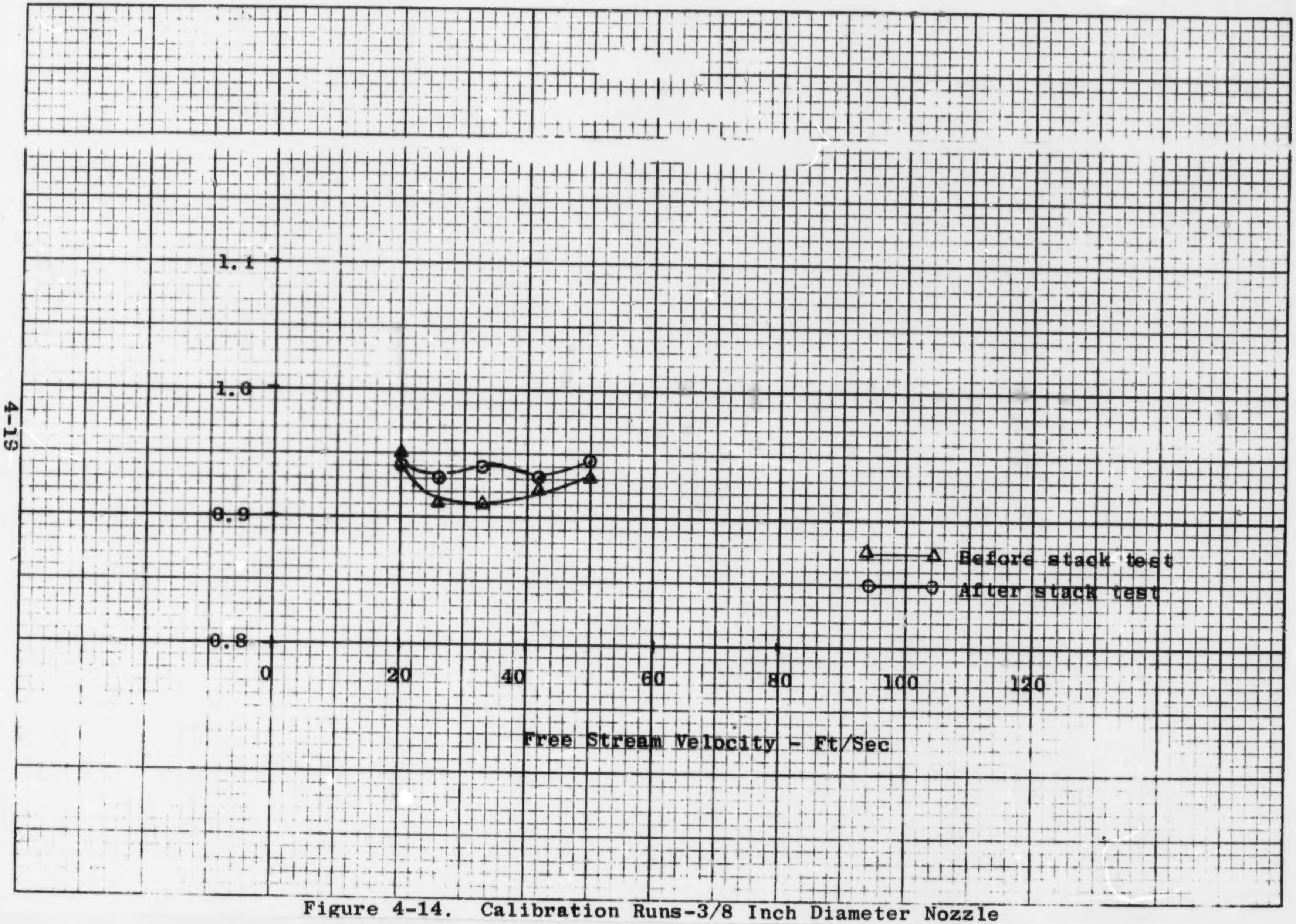

Figure 4-14. Calibration Runs-3/8 Inch Diameter Nozzle

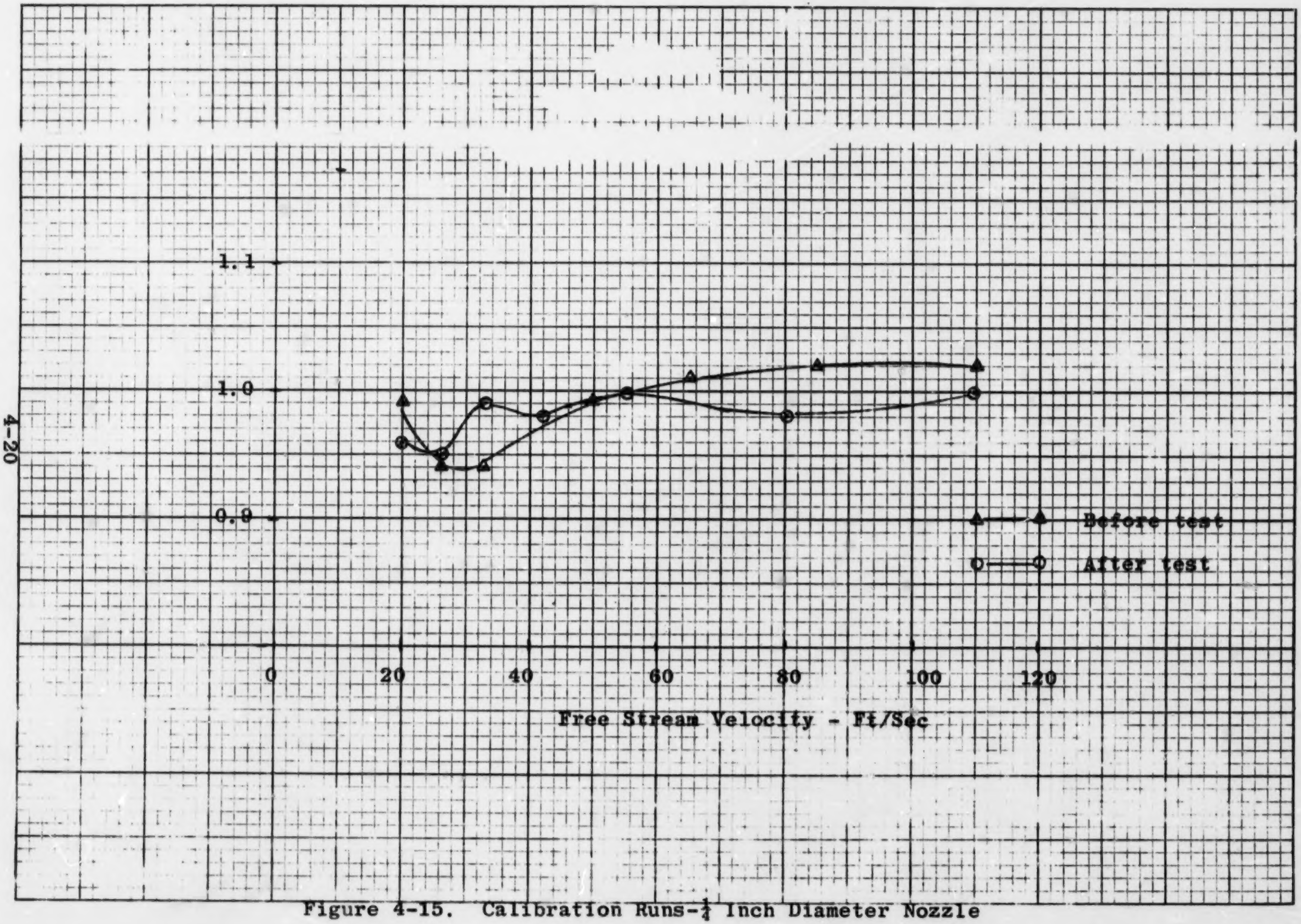

Figure 4-15. Calibration Runs-$\frac{1}{4}$ Inch Diameter Nozzle

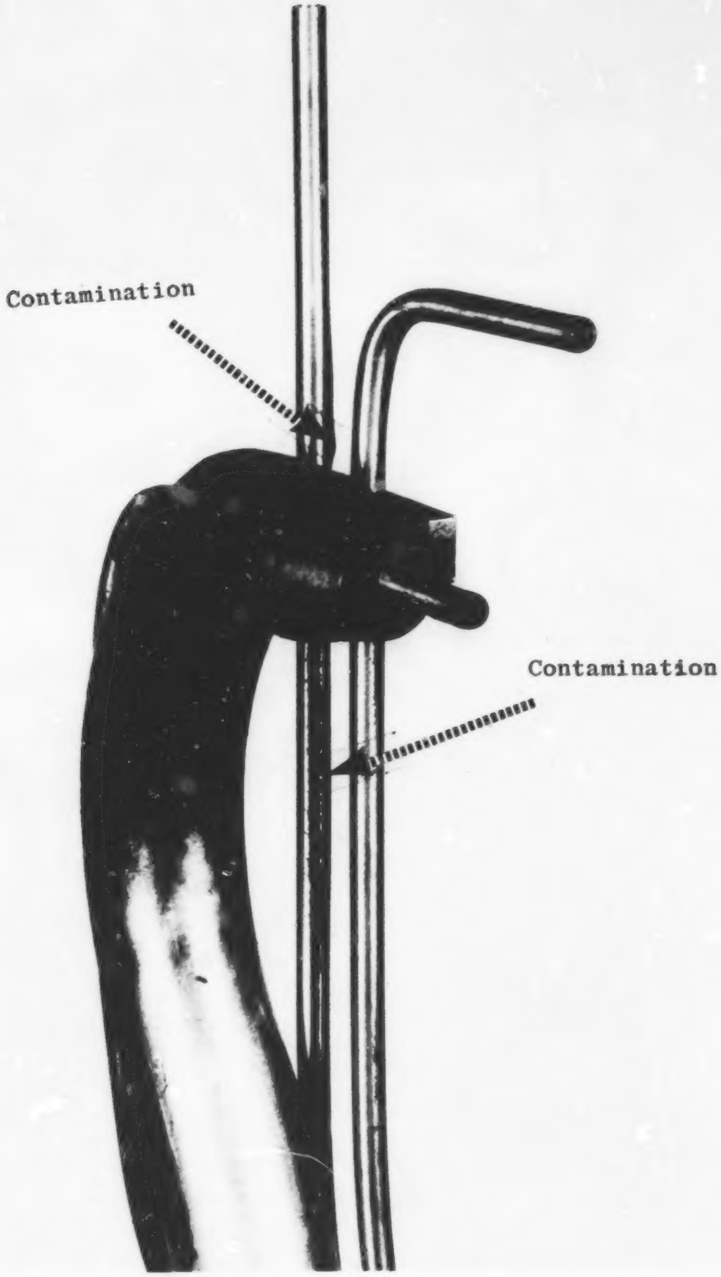

Figure 4.16 3/8 Inch Nozzle

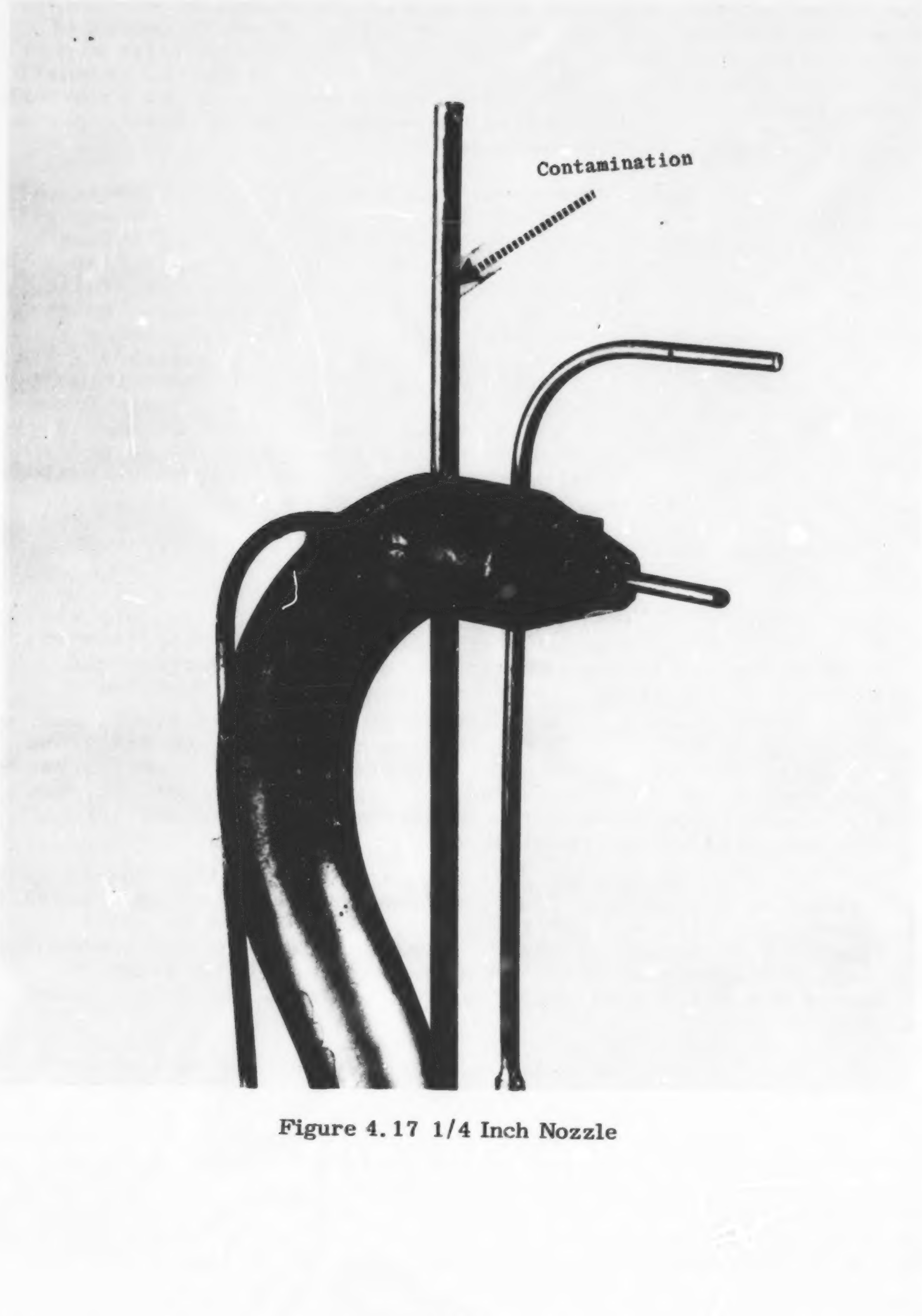

Figure 4.17 1/4 Inch Nozzle

no buildup of contaminates. Although not evident in the photograph, some buildup did occur on the blunt nose of the nozzle inlet sensor. Examination of the sensor under a microscope showed no contamination in or near the free air stream sensor ports. A small amount of contamination occurred on that portion of the nozzle inlet sensor tube inside the nozzle. The contamination was deposited in small clumps, rather than the homogeneous layer which occurred on external tube surfaces and is believed to be caused by the 15-minute period required to change the sample case filter.

Figure 4-17 shows the ¼ inch diameter nozzle. Its configuration is the same as the 3/8 inch nozzle with the exception that the sensors are fabricated out of 0.085 inch OD stainless tubing, as compared to the 1/8 inch tubing used on the larger nozzle. The band of contamination on the 1/8 inch stack static pressure tube is indicative of the degree of misalignment between the free air stream and the nozzle axis; the free air stream velocity being almost normal to the plane of the photograph. The free air stream sensors remained clean even though there is a component of velocity normal to the tube surface and the sensing port. The surface of the inlet sensor tube upstream of the nozzle inlet and on the side exposed to a normal component of velocity did have a small amount of contamination and contamination buildup was starting on the edges of the sensing port.

4.3.2 Field Test on Engineering Prototype

Test Location - This test was conducted on the number two boiler of the General Electric Power Station at Erie, Pennsylvania. This is a coal-fired installation. The probe was inserted in the horizontal ducting between the boiler and the precipitator. The tests were conducted on January 9, 1974.

Test Procedure - A sampling train configuration, as specified under Method 5 (Determination of Particulate Emissions from Station Sources) as specified in EPA Standards of Performance for New Stationary Sources in Federal Register #247, Pt. II, was used in these tests. The full complement of cyclone and porous filters was used in the sampling case.

The initial gain settings and sampling nozzle size were based on logged data from previous tests made at this location. The controller gain was set to correspond to an S-type pitot reading of 0.85 inches of water. Available data on gas temperature and velocity indicated that the optimum flow control range of between 0.5 and 1.5 scfm would be obtained with the ¼ inch sampling nozzle.

The controller bias adjustment was made and with the controller on, the sampling probe was inserted in the duct and the test started. Isokinetic sampling flow rate was calculated from the observed pitot readings and gas temperature and compared to the flow rate established by the controller. The sampling nozzle flow rate was 15% lower than the calculated isokinetic flow but corresponded almost exactly to the room temperature calibration tests presented in Figure 4-11. The controller was operating stably and no further adjustment of the gain setting resistors was required.

These initial settings were retained for the first test. On subsequent tests the controller bias was adjusted to establish isokinetic sampling flow.

On all the tests the following data was recorded:

- Stack Temperature
- Stack Velocity
- Sampling Flow Rate
- Control Valve Pressure Differential

Test Results - The test probe was operated in the duct for a total elapsed time of 3 hours and 15 minutes. Operation was continuous with the exception of three short interruptions to change filter membranes.

Figure 4-18 is a plot of the velocity ratio maintained during the test. The first portion of the test was run with no adjustment of the controller bias other than the initial adjustment prior to inserting the probe in the duct. The controller maintained sampling flow rate to within a band of better than ±5% of the value determined by laboratory calibration.

At the end of 1 hour and 8 minutes of test time, the controller was shut down and the filter replaced. After replacing the filter the controller bias was adjusted to make the sampling rate equal to the calculated flow for isokinetic sampling. The bias control was left at this setting for the duration of the test.

The sampling case filter was replaced once during the test. As apparent from the plot of velocity ratio, there is a trend towards a decrease of sampling nozzle gas velocity with time. This is indicative of increased pressure drop in the sampling case due to the filter becoming loaded. In the latter portion of the test the controller was operated continuously for 1½ hours without replacing the filter. Isokinetic sampling was maintained to an accuracy of better than 6%.

Figure 4-19 shows the flow control valve input pressure as recorded during the test. This parameter is significant in that it is a direct indication of filter loading and can be used as a criteria for judging when the sampling case filter should be changed. The maximum change, between filter replacements, is 0.30 psi. Referring to Figure 3-9, it is apparent that this is less than 20% of the linear control range of the valve and indicates that the control valve has adequate range capability.

The total gas sample collected during the test was 118 standard cubic feet. Of this total, 80 cubic feet were collected while maintaining isokinetic velocities to an accuracy of 5% or better. The remainder was collected with sampling velocity approximately 15% lower than the stock velocity. The weights of solid particulates collected during the test were 9.45 grams by the cyclone filter and 1.78 grams by the porous

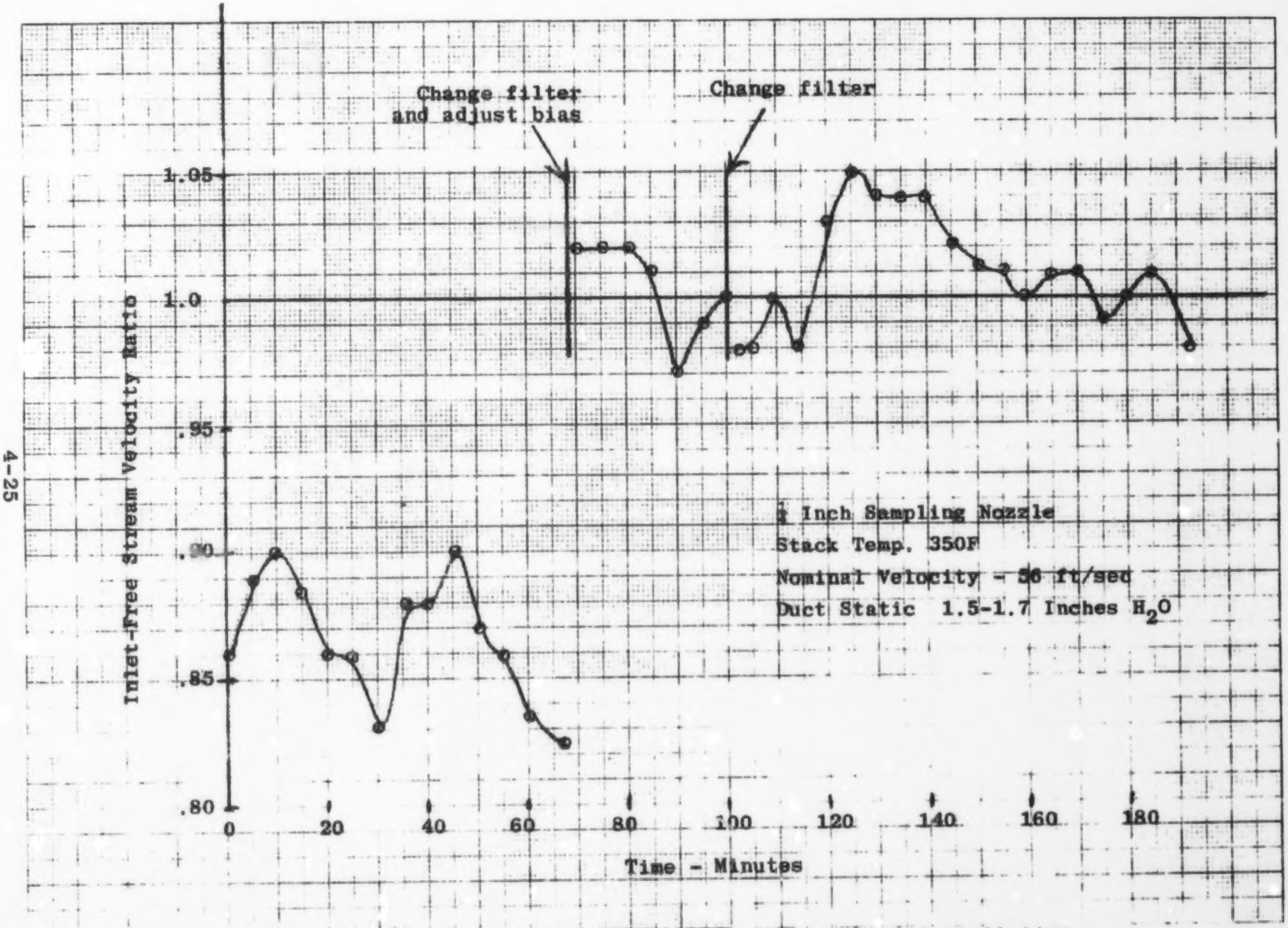

¼ Inch Sampling Nozzle
Stack Temp. 350F
Nominal Velocity - 56 ft/sec
Duct Static 1.5-1.7 Inches H_2O

Figure 4-18. Velocity Ratio Vs. Time on Coal-Fired Installation

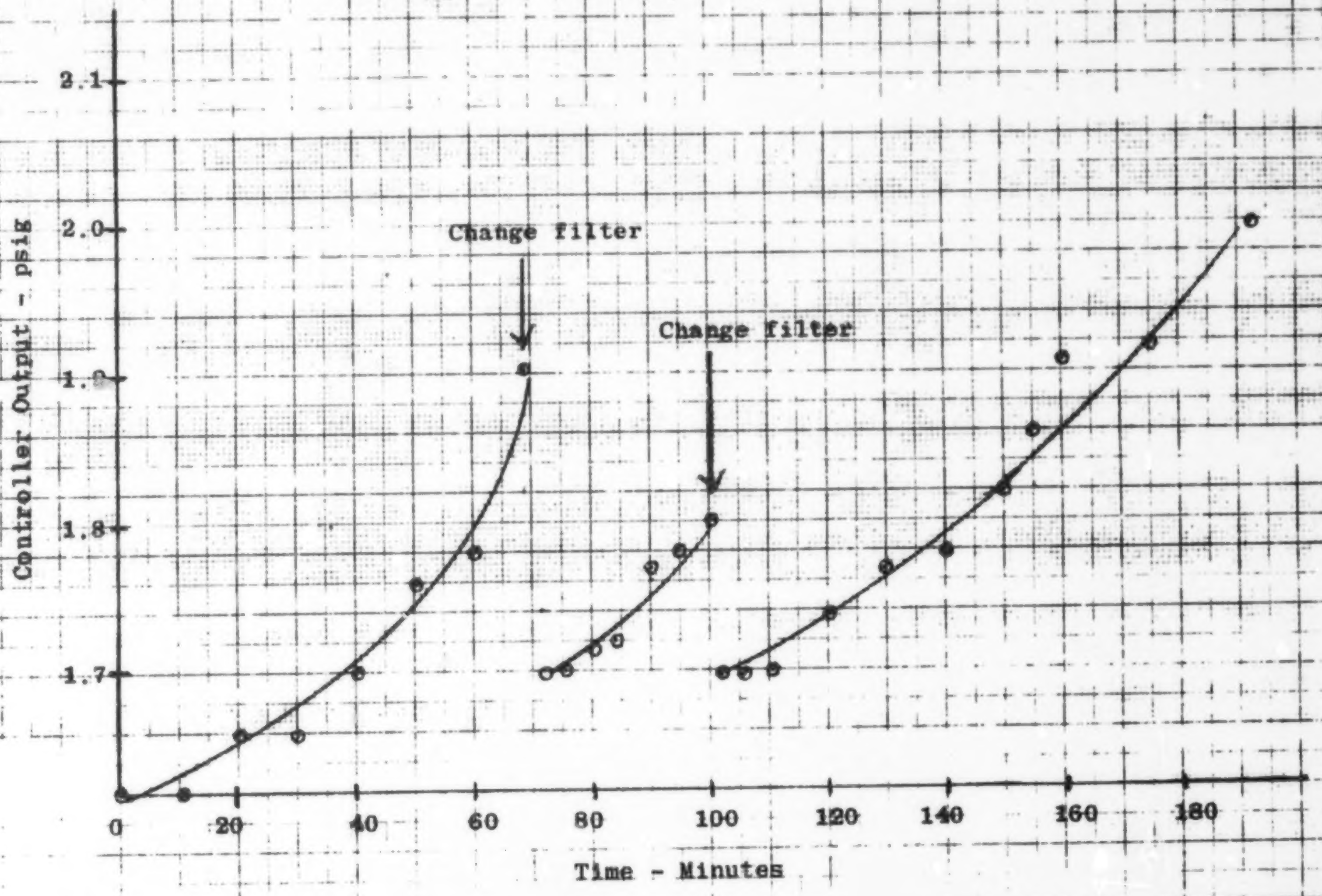

Figure 4-19. Fluidic Controller Output Pressure Vs. Time

filter. Considering only the particulates collected while maintaining accurate isokinetic sampling, the particulate concentration is 0.094 grams per standard cubic foot.

After completion of the test the controller was returned to the laboratory and disassembled. All of the fluidic amplifier modules were removed and each lamination given a microscopic examination for evidence of contamination. No evidence of contamination was found, indicating that backflushing and referencing the input amplifier to the duct static pressure effectively prevents particulates from entering the sensor ports and signal lines.

Visual inspection of the sampling nozzle and the sensor showed virtually no adherence of particulates on any part of the sensor or nozzle. This is in contrast to experience on the oil-fired installation where particulates adhered and caused a significant buildup of contaminates on all leading edges of the nozzle and sensor tubes.

APPENDIX I

ISOKINETIC SENSOR TESTS

APPENDIX I

Sensor Test Results

The major development effort on the program was devoted to the test and evaluation of the gas velocity sensors. The sensor is a critical component in that it must function in a heavily contaminated environment, at elevated gas temperatures, and over a broad range of stack velocities. Three basic sensor configurations were fabricated, tested and evaluated. These configurations were the cross-flow sensor, the co-flow sensor, and the differential static probe.

The sensor characteristics of primary concern in this application are:

- Ability to function with air flow exiting from all signal ports. This is considered a prime prerequisite in avoiding malfunction from contamination.
- Isokinetic velocities must be retained at the free air sensor. Flow disturbances introduced by the sensor result in an error in measuring free air stream velocity and in corresponding error at the inlet to the sampling nozzle.
- The signal-to-noise ratio of the sensor must be compatible with the design goals on system bandwidth.
- A sensor gain independent of velocity is highly desirable though not absolutely necessary.
- A high sensor scale factor is highly desirable.
- The diluent flow introduced into the sampling nozzle should be a minimum. This flow must be accounted for in the totalized flow on a sampling run.
- Sensor configuration must be compatible with insertion and withdrawal through existing sampling ports of three inches in diameter.

Differential Static Sensor

This sensor went through three design evolutions as illustrated in Figure A-1. The original concept placed the free air stream sensor several inches in front of the sampling nozzle inlet. This configuration is ideal from the standpoint of flow disturbance at the free air stream sensor. This configuration was abandoned because of the physical constraints imposed by existing sampling ports. By displacing the free air stream sensor axially as shown in A-1b the overall length is reduced to under three inches and the sensor can be inserted into existing sampling ports. This configuration was field tested, and operating experience gained on that test indicated that protective shrouding was necessary, leading to the final configuration shown in A-1c.

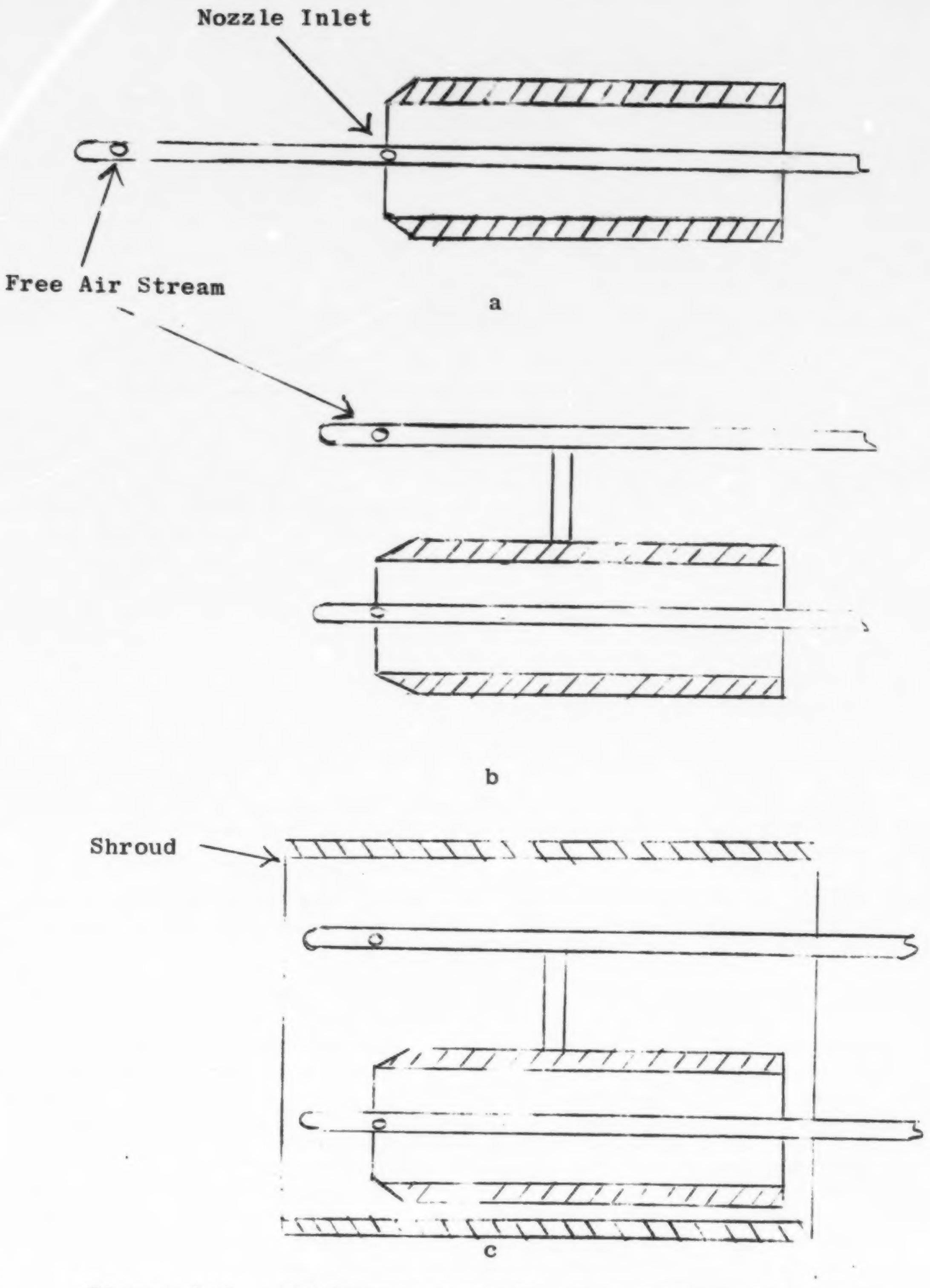

Figure A-1. Differential Static Sensor Configurations

Figure A-2 shows the performance characteristics of the three configurations. These tests were performed in a wind tunnel. The sensor was nulled and the sampling nozzle flow measured. The sampling nozzle inlet velocity was computed from the measured flow area and the effective area of the sampling nozzle. As apparent from Figure A-2 the protective shroud introduces losses which cause the sampling nozzle inlet velocity to be smaller than the free air stream velocity.

This effect becomes more pronounced at the higher velocities as evidenced by Figures A-2 and A-3.

The sensor gain was determined by varying the nozzle inlet velocity relative to the free air stream velocity and noting the differential pressure across the sensor.

Figure A-4 is a plot of the sensor gradient. The x axis represents probe velocity normalized to isokinetic velocity, while the y axis is the measured probe static differential pressure referenced to kinetic head. The measured sensitivity is approximately 70% of the theoretical sensitivity shown by the dashed line on Figure A-4. This discrepancy, attributed to the inadequate spacing between static probes, does not affect the probe's ability to sense isokinetic conditions.

The sensor noise characteristics are shown in Figure A-5. The peak-to-peak noise output is approximately six times the RMS values shown on Figure A-5. In the lower velocity range a quantitative noise measurement was not obtained because instrumentation background noise exceeded the sensor noise.

Co-Flow Sensor

The pertinent performance characteristics of the co-flow sensor are summarized in Figures A-6 through A-13. Sensor gain vs. supply pressure is shown in Figure A-6. The lower gain curve was obtained when the receiver was backpressured to a value which insured outflow at the maximum air stream velocity of 150 ft/sec. Backpressuring reduces the sensor gain to approximately 60% of a sensor operating with no back pressure. For both cases, sensor gain varies approxiamtely as the 2/3 power of supply pressure.

Figure A-7 gives the equivalent sensor noise in ft/sec. Observed peak-to-peak values of noise are five times the RMS values. Sensor noise is essentially independent of supply pressure.

The ratio of sensor gain to the DC pressure level at nulled condition is shown in Figure A-8. This curve is significant when considering the sensor's susceptibility to drift from variations in back pressure and amplifier input impedances. A high ratio is desired; hence, the co-flow sensor should be operated with the minimum acceptable nozzle supply pressure. A marked degradation in sensor gain and linearity occurs at supplies lower than 3 psig. A lower limit of 5 psig was selected to give a reasonable operating margin.

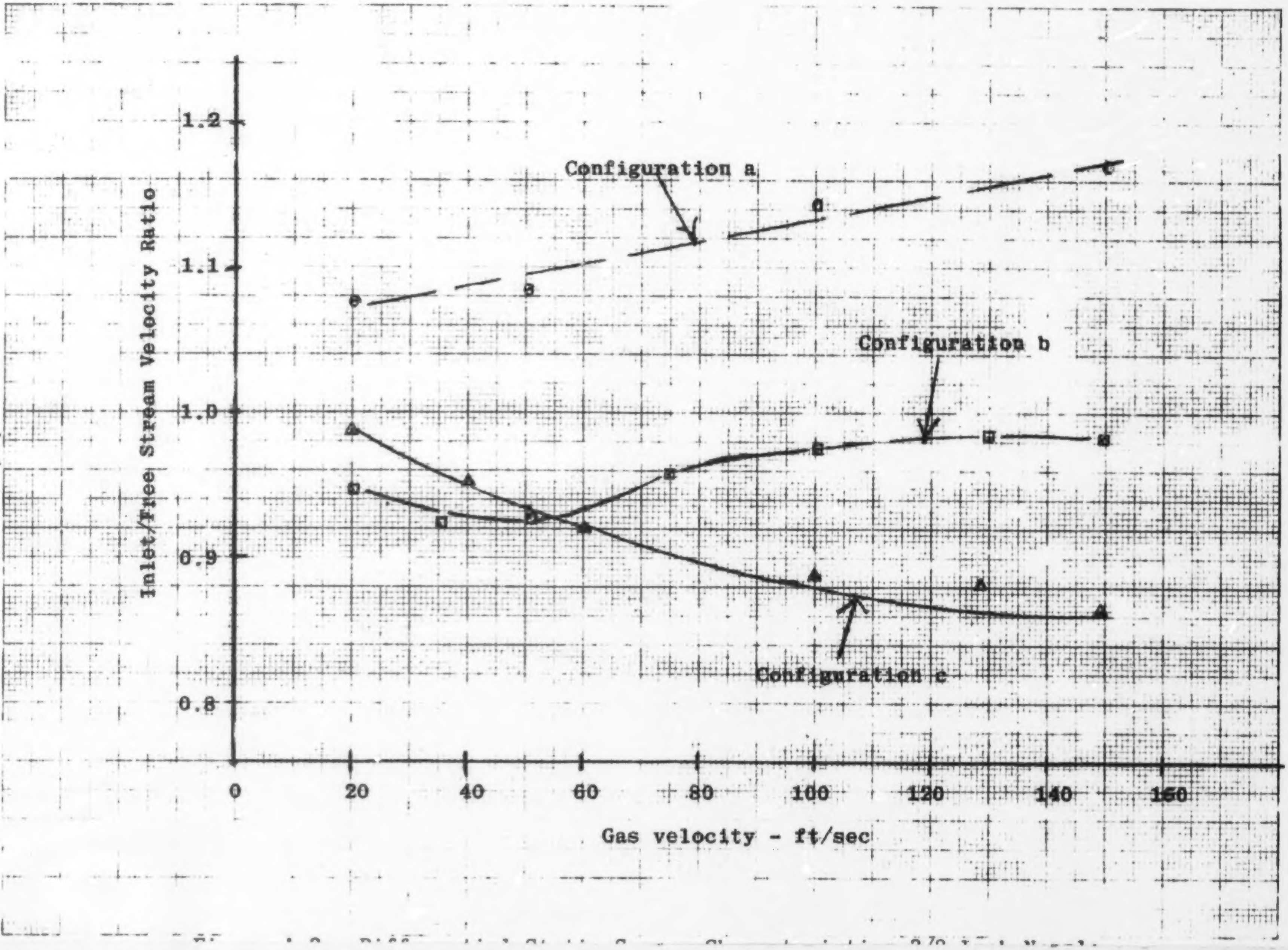
Configuration a
Configuration b
Configuration c
Inlet/Free Stream Velocity Ratio
1.2
1.1
1.0
0.9
0.8
0
20
40
60
80
100
120
140
160
Gas velocity - ft/sec

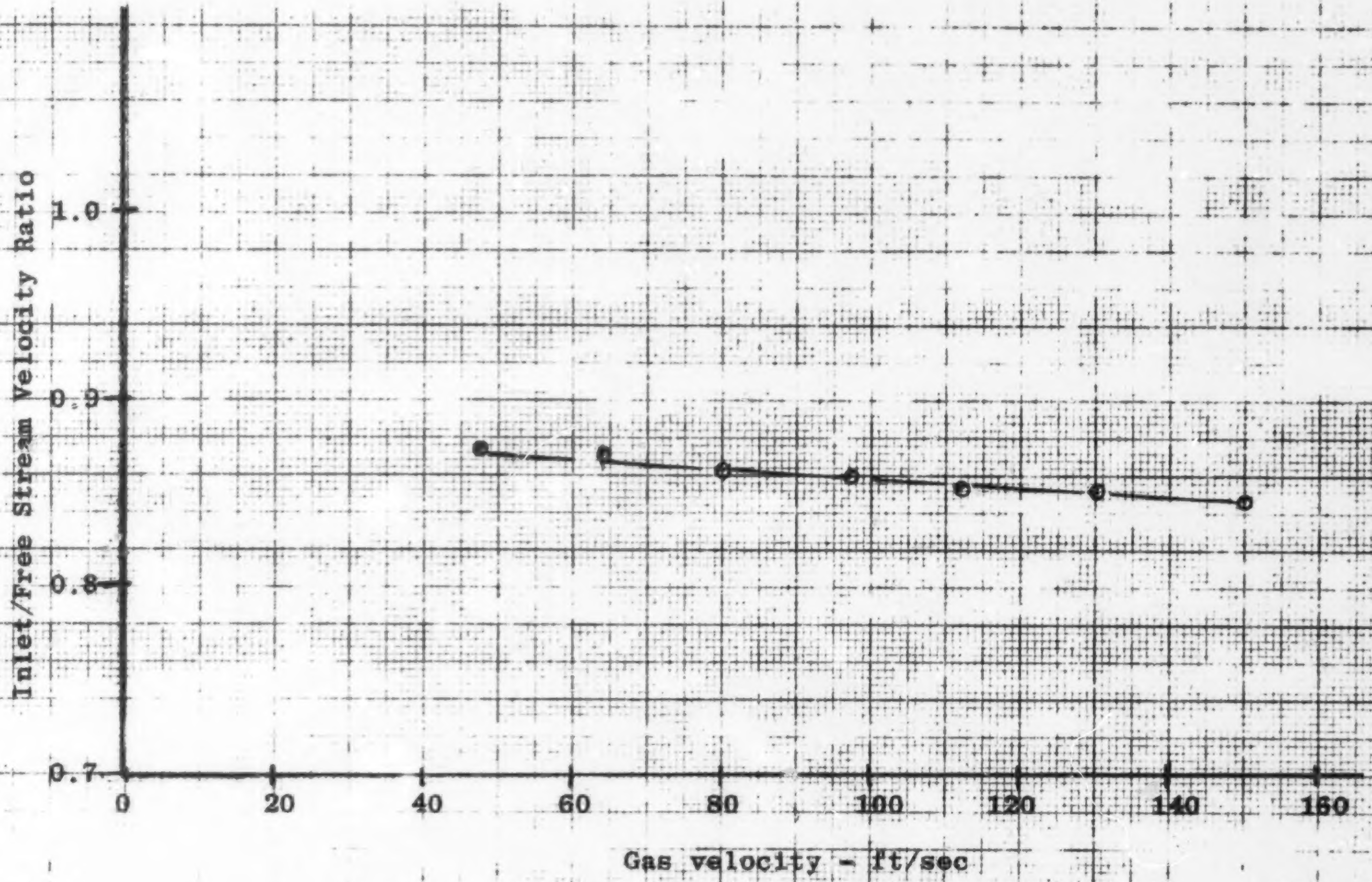

Figure A-3. Differential Static Sensor Characteristics-¼ Inch Nozzle

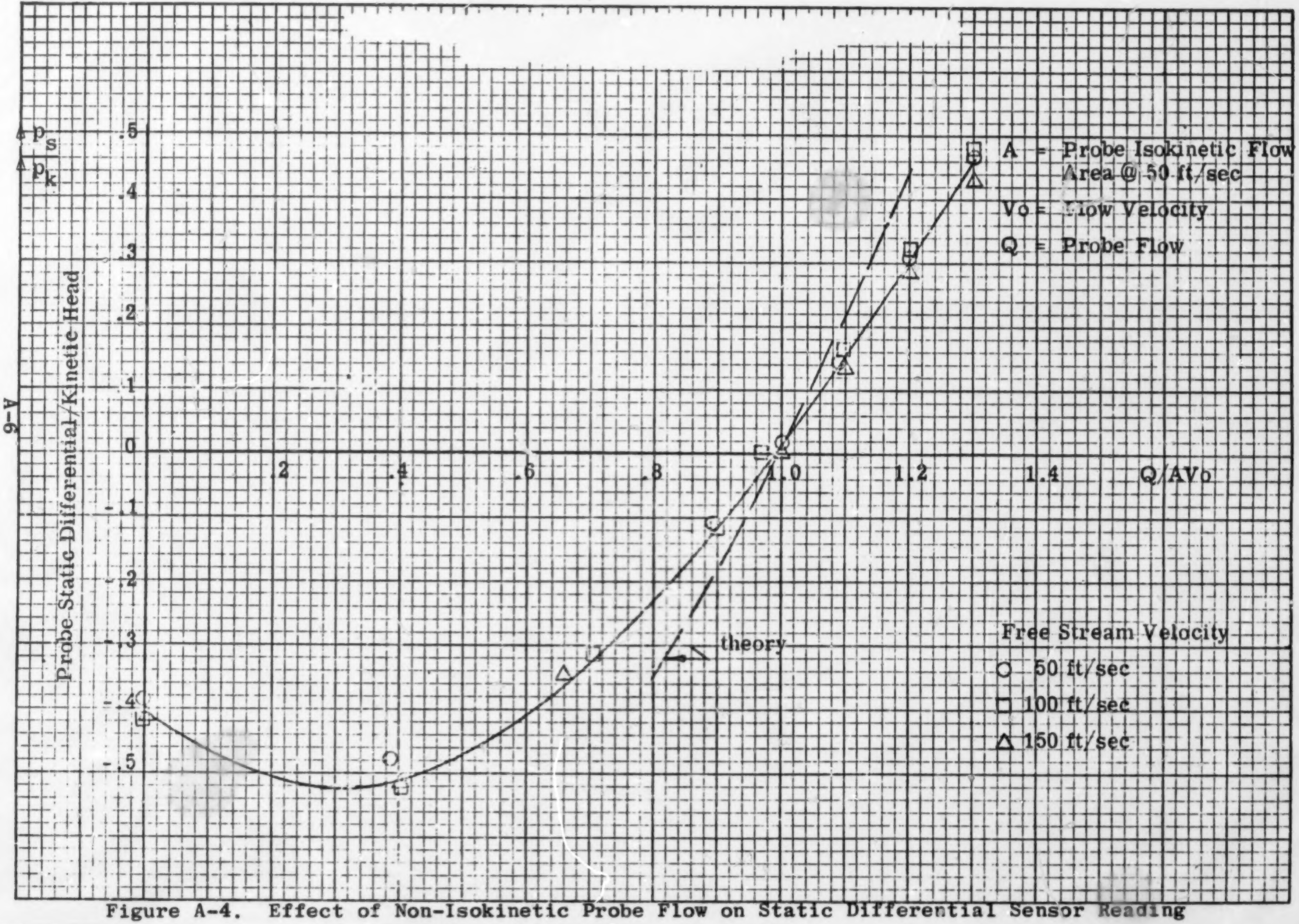

Figure A-4. Effect of Non-Isokinetic Probe Flow on Static Differential Sensor Reading

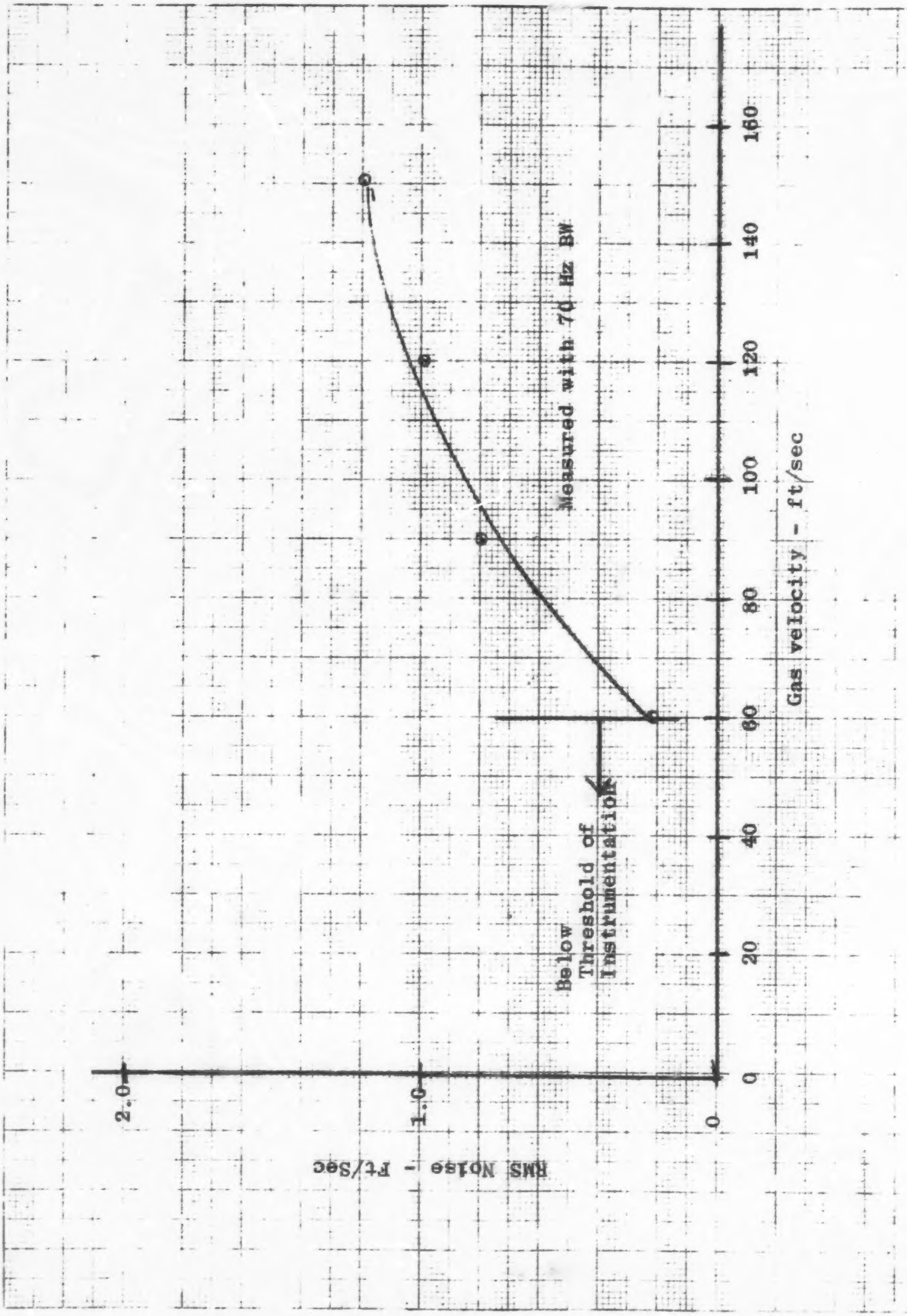

Figure A-5. Static Sensor Noise

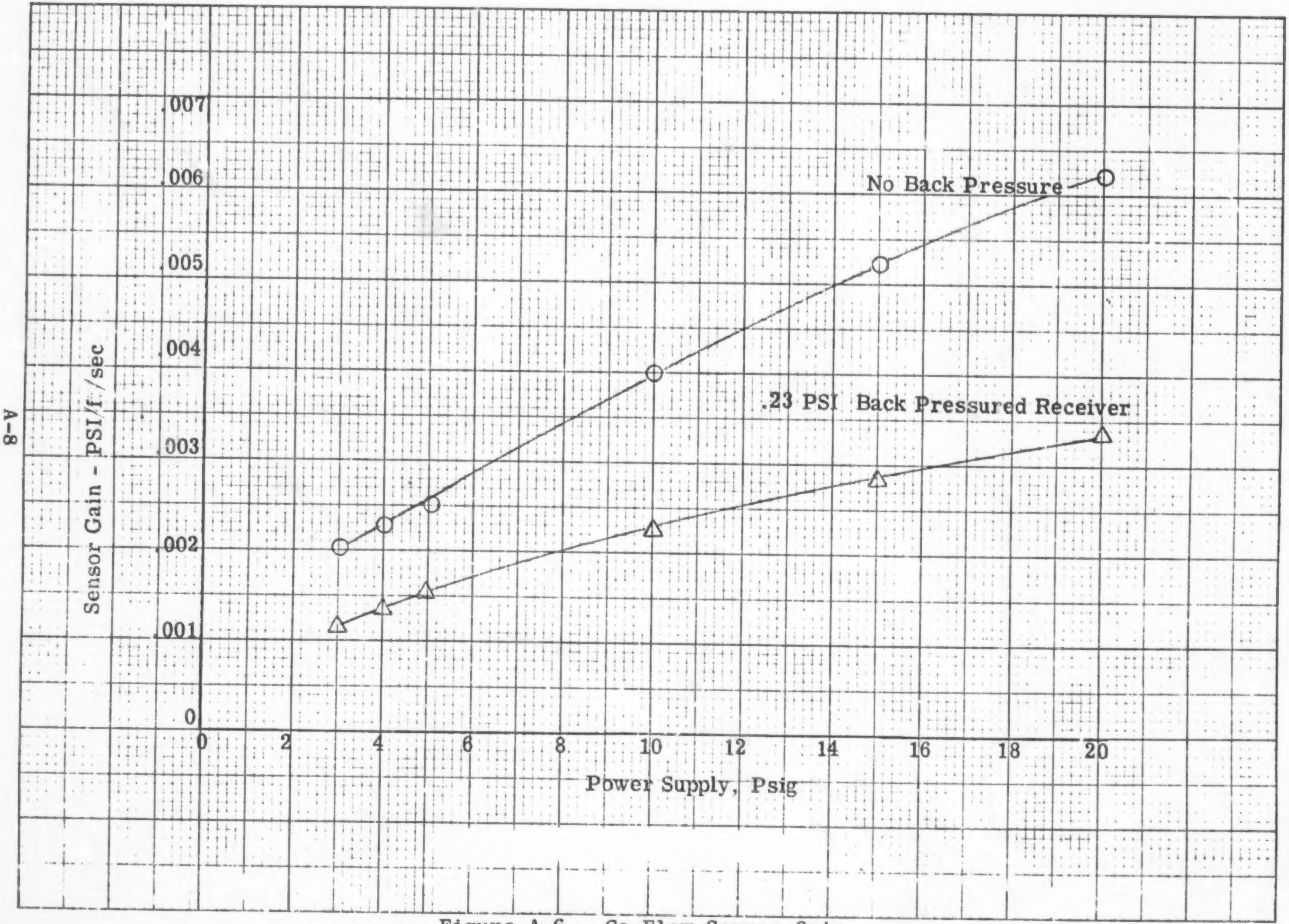

Figure A-6. Co-Flow Sensor Gain

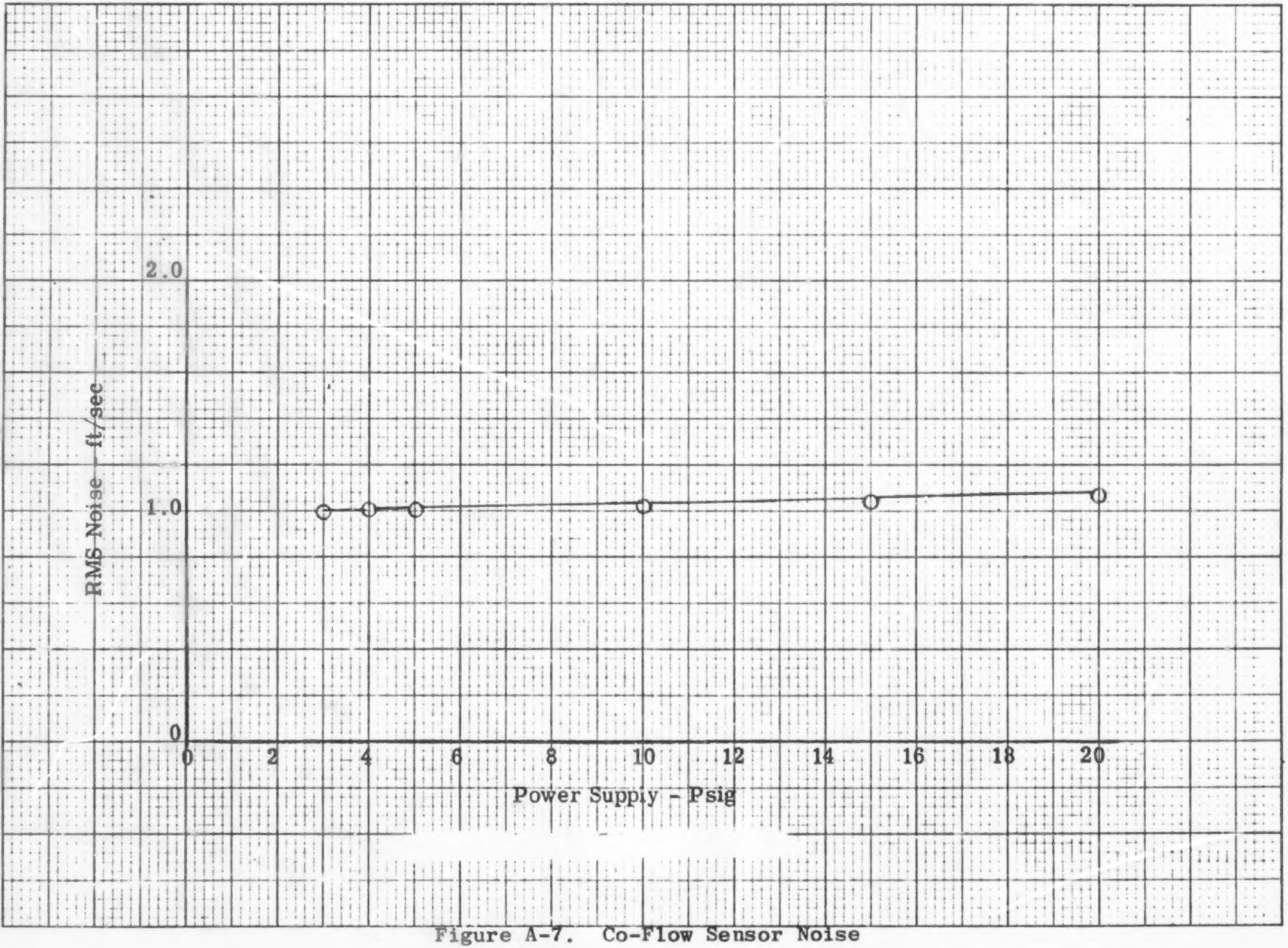

Figure A-7. Co-Flow Sensor Noise

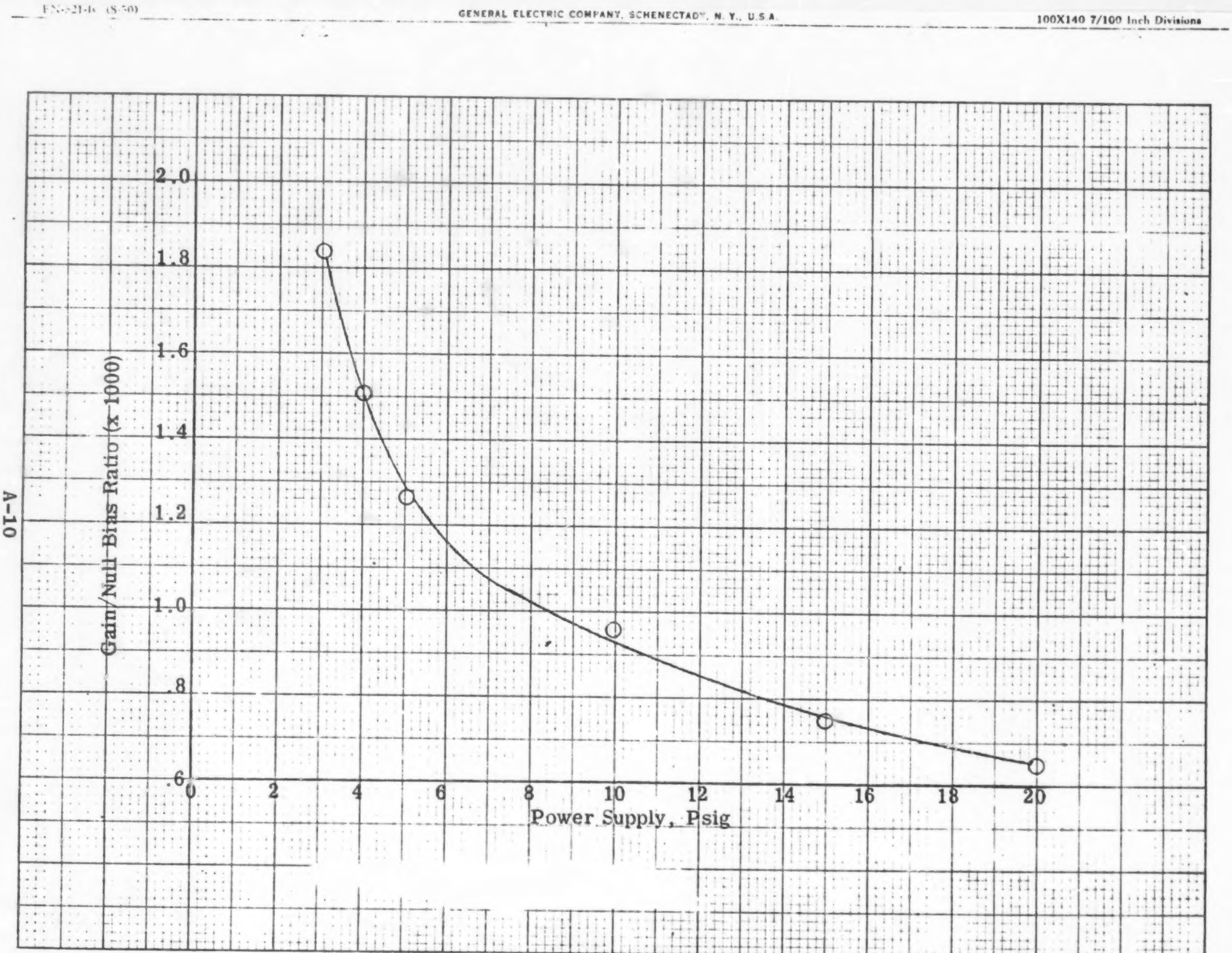

Figure A-8. Co-Flow Sensor Gain/Null Bias Ratio

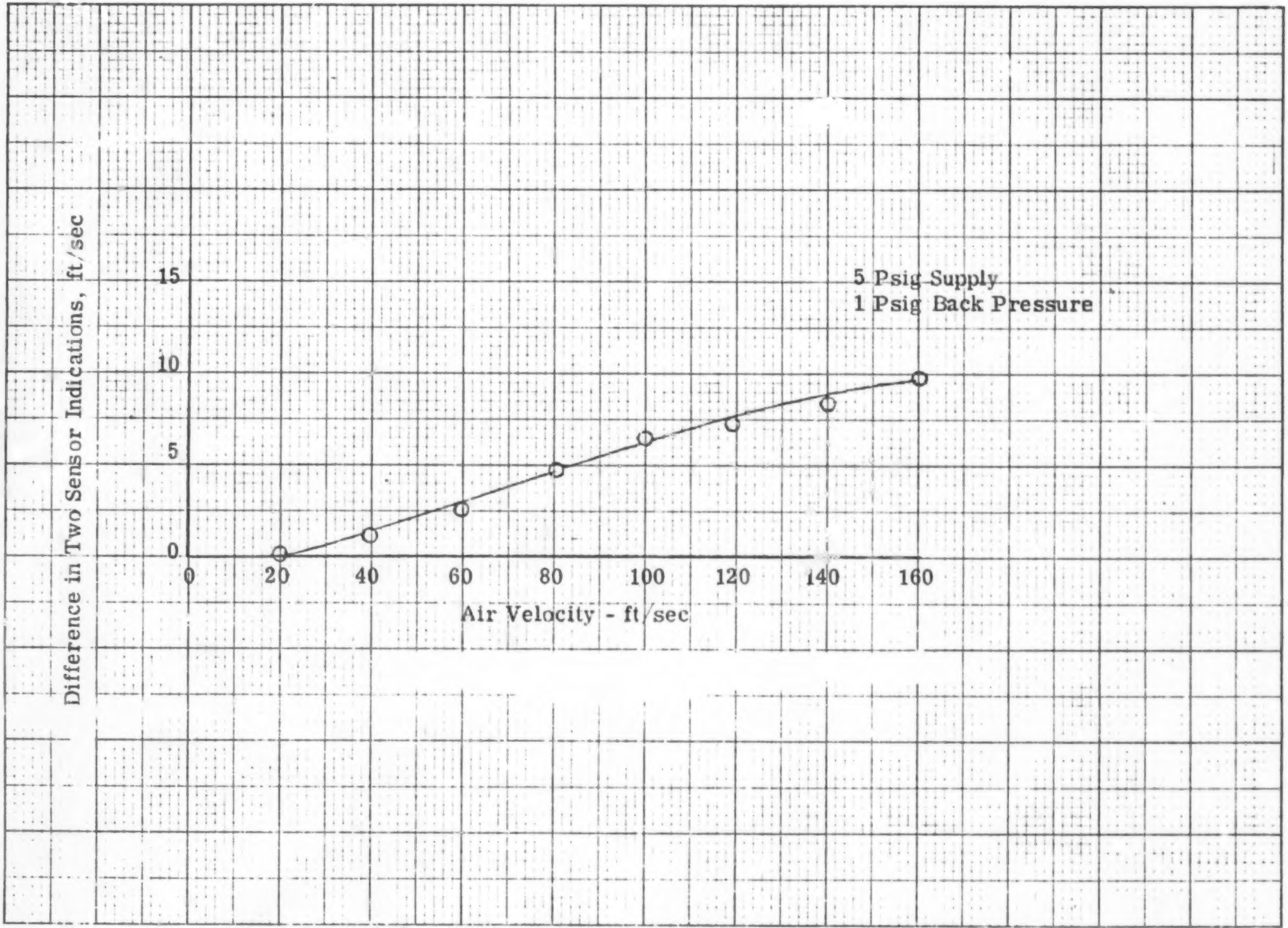

Figure A-9. Difference in Two Co-Flow Sensor Indications

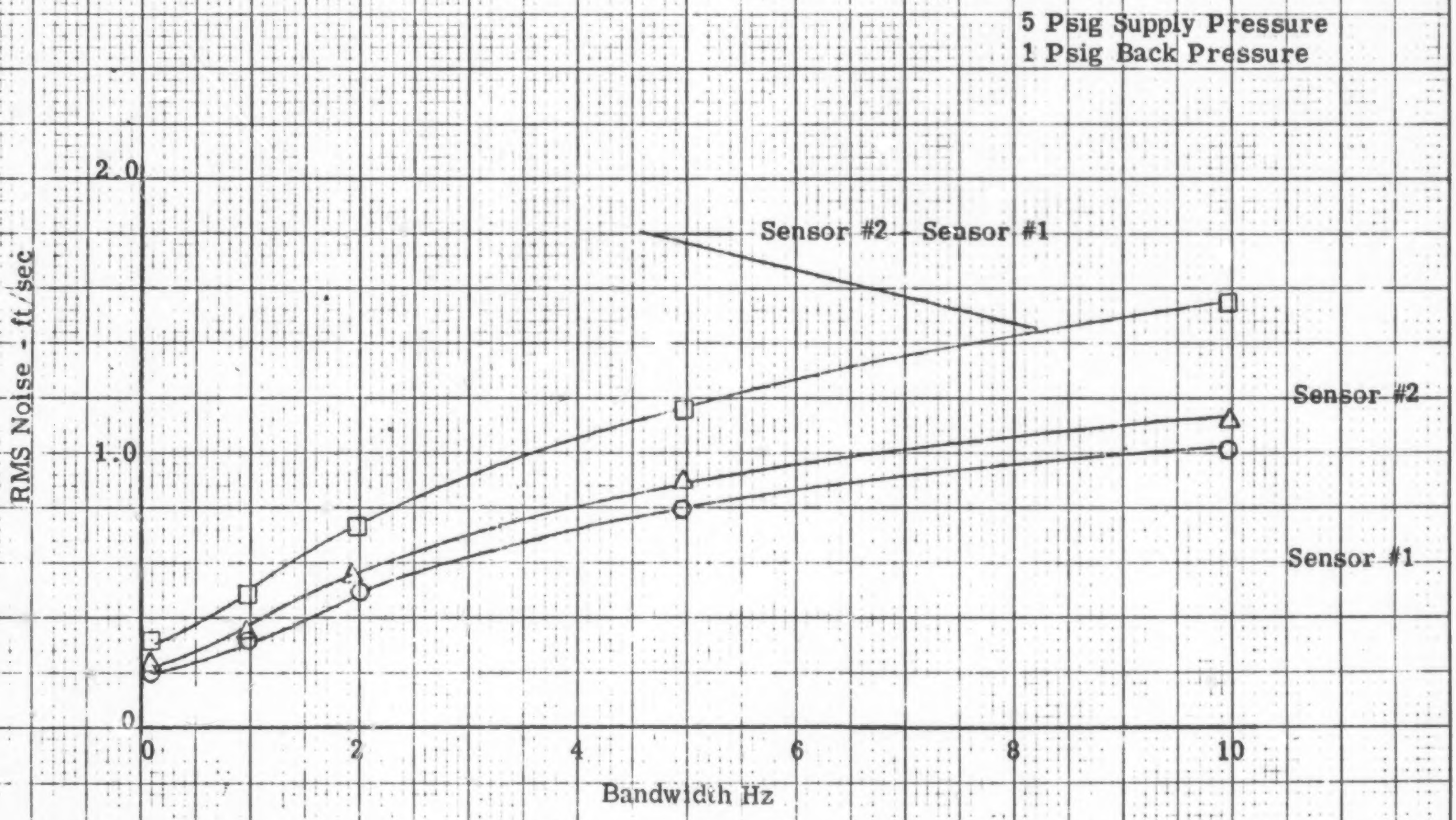

Figure A-10. Co-Flow Sensor Noise Vs. Bandwidth

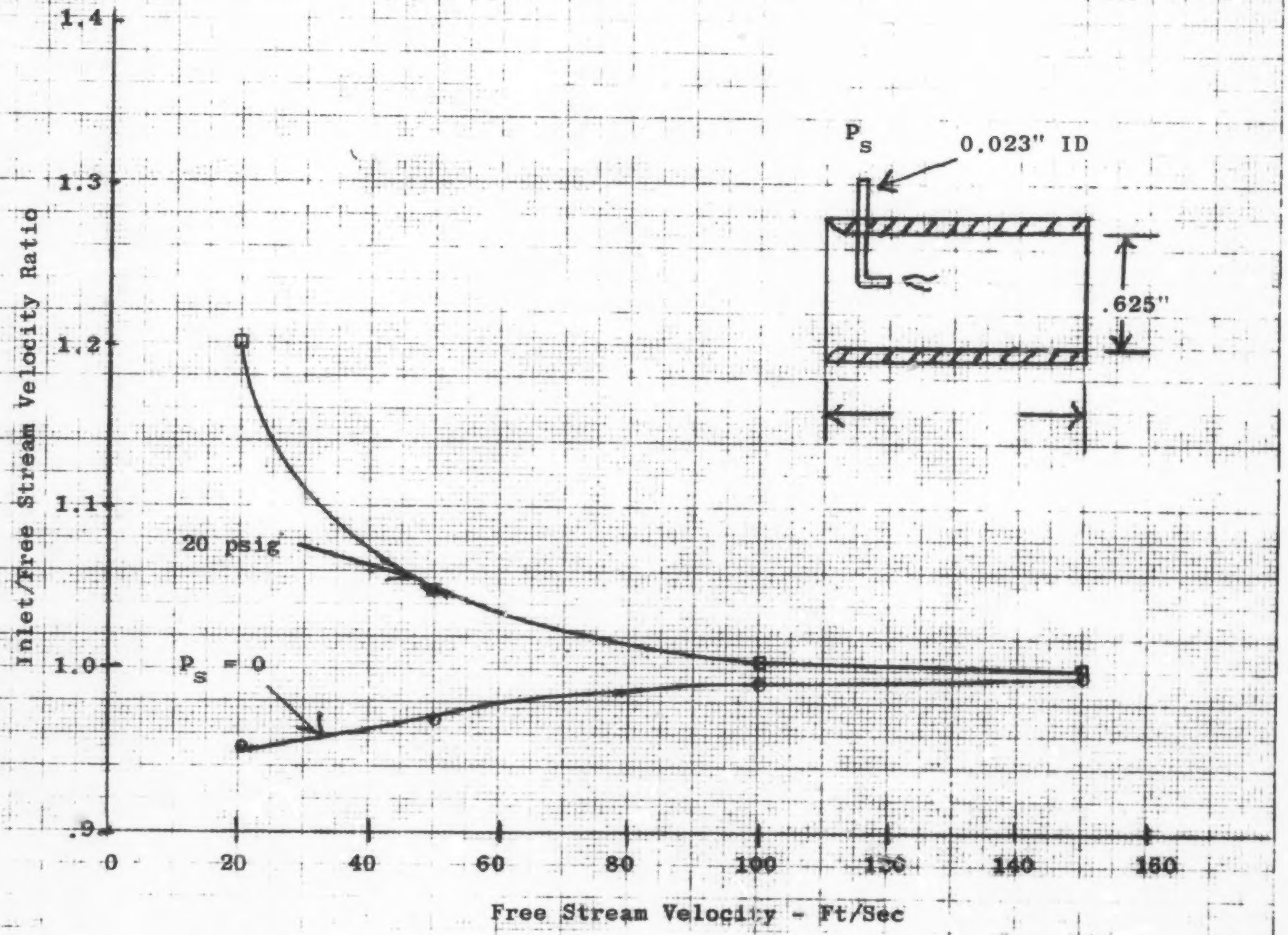

Figure A-11. Velocity Acceleration at Nozzle Inlet

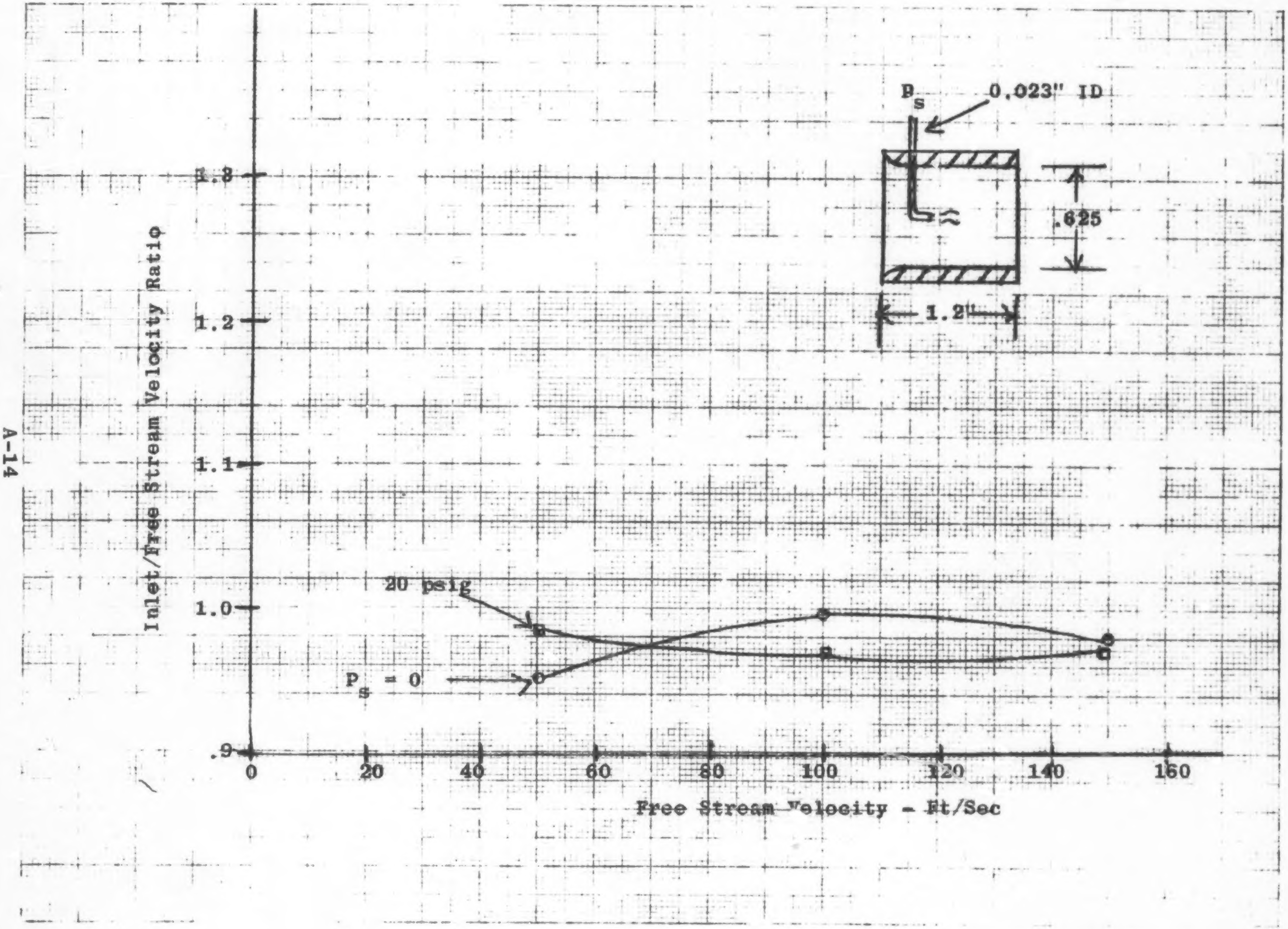
B_s
0.023" ID
.625
1.2"
Inlet/Free Stream Velocity Ratio
1.3
1.2
1.1
1.0
.9
0
20
40
60
80
100
120
140
160
Free Stream Velocity - Ft/Sec
20 psig
P_s = 0

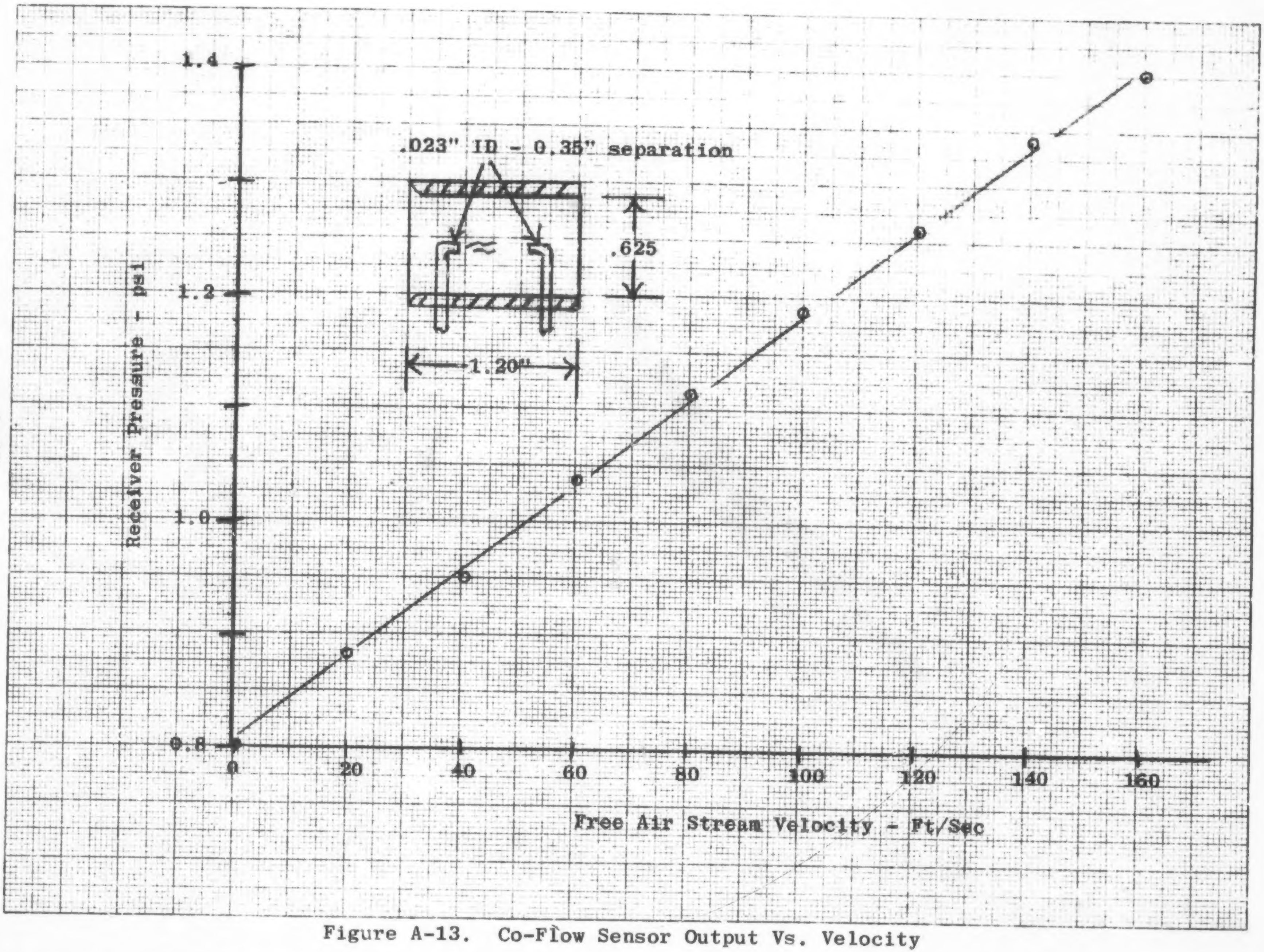

Figure A-13. Co-Flow Sensor Output Vs. Velocity

Figure A-9 shows the differential pressure between two sensors exposed to the same air velocity. The sensors were nulled at 20 ft/sec air velocity by adjusting the receiver back pressures with variable series resistors. The resistors were then left fixed and air velocity varied. At the maximum velocity of 160 ft/sec, the sensor error is 6%. The error vs. velocity is well behaved, indicating one sensor has slightly higher gain. This type of characteristic can be compensated by adding two more variable resistors, shunting the sensor receiver.

Figure A-10 shows the noise vs. bandwidth characteristics of two sensors. The differential noise between the reference sensor and the sampling probe sensor will be the effective noise applied to the amplifier following the sensor. The noise has a Gaussian distribution and absolute magnitude is proportional to the square root of bandwidth. Considering a 2 Hz closed loop bandwidth on the automatic sampling control, the RMS noise is approximately 0.7 ft/sec which on the basis of an overall assessment is very acceptable. The full impact of sensor noise does not become apparent until a specific mechanization of the control is considered. For example, to meet a steady-state accuracy of better than 5% requires a forward loop gain of at least 20 times the product of gas density and probe area. This requirement also translates into a gain of 20 from an air velocity error signal to the controlled output velocity. Noise in the frequency range between the closed loop bandwidth (2 Hz) and the lowest tolerable bandwidth on a noise filter (approximately 10 Hz) will then be amplified by approximately 20. The RMS noise in this band can be obtained from Figure A-10 and is 1.4 ft/sec with peak-to-peak values of 7 ft/sec. If no saturation or filtering occurred, peak-to-peak noise values of 140 ft/sec would occur in the output. The sampling case is an effective filter in this frequency range; hence the noise would not show up on the output. However, the flow control valve would respond and would be commanded to a level corresponding to total excursions of 140 ft/sec. The velocity range that can be achieved in the sampling probe is inherently fixed by the sampling case pressure drops and typically will be a range from 0 ft/sec (with throttling valve) to a maximum approaching two times the nominal control velocity. Assuming a nominal of 70 ft/sec, the control valve will be overdriven, by noise, by a factor of 7:1 -- going to a fully closed to fully open position. An acceptable value would be on the order of 50% of full range, indicating a required noise reduction of approximately 15:1. A filter to yield this reduction requires a bandpass of .04 Hz and would restrict the closed loop bandwidth to approximately 0.2 Hz as compared to the design objective of at least 2 Hz.

The sensor noise has the characteristic of noise from jet turbulence and has about the expected magnitude; hence, it is unlikely that any significant reduction in sensor noise can be achieved.

Figures A-11 and A-12 show the effect of sensor flow on the inlet velocity to the shroud. As shown by Figure A-11, the sensor aspirates and increases the inlet velocity relative to the free air stream velocity. For any given sensor configuration it is apparent that the sensor flow can be selected to compensate for inlet losses. The inlet velocity is strongly influenced by shroud length, as shown by Figure A-12. With a length to diameter ratio of 2:1 the inlet velocity is relatively insensitive to sensor flow, staying well within a 5% error range for sensor supply pressures up to 40 psig. The sensor output as a function of free air velocity is shown in Figure A-13. A linear output with a scale factor of .004 psi/ft/sec (10 psig sensor supply) was obtained over the test range of 0-160 ft/sec.

Cross-Flow Sensor

Characteristics of the cross-flow sensor are summarized in Figures A-14 through A-19. A sketch of the sensor configuration is shown in the upper right hand corner of Figure A-14. Both upstream and downstream receivers were tested. The data plotted in Figure A-14 was obtained on the upstream receiver. The upstream receiver has a usable range of 20 to 140 ft/sec with a gain variation of approximately 5:1 over the range. The gain is relatively constant over the range of 80 to 140 ft/sec.

The output from the downstream receiver is shown in Figure A-15. The optimum range for the sensor is [illegible] ft/sec to an upper limit determined by the supply pressure.

The specified velocity range of 20 to 150 ft/sec can be accommodated by using the upstream receiver for the high velocity range and the downstream for the low velocities.

The sensor scale factor and range are strongly influenced by the nozzle supply pressure with the optimum supply pressure being the maximum that can be utilized in the sensor. In view of the optimum trend a series of tests were performed in a wind tunnel to empirically determine the maximum sensor flow vs. diameter and length of the shroud. The probe inlet velocity was measured and compared to the free air stream velocity. Three representative test results are shown in Figures A-16, A-17 and A-18. Figure A-16 shows the results obtained with the sensor enclosed by a 0.375 inch diameter shroud. The inlet losses associated with the shroud are excessive as indicated by the inlet free stream velocity ratio with no flow injected into the shroud. Introduction of sensor flow significantly decreases the sampled velocity, as shown by the series of curves obtained at different supply pressures. Figures A-17 and A-18 were obtained with a 0.625 inch diameter shroud enclosing the sensor. This diameter is about the minimum diameter that can be used to maintain inlet losses to an acceptable value. The percent error resulting from sensor flow has been significantly reduced as compared to the 0.375 inch diameter shroud. The influence of shroud length is not particularly strong, as shown by comparison of Figures A-17 and A-18. The empirical relationship derived from this test series is given by the following:

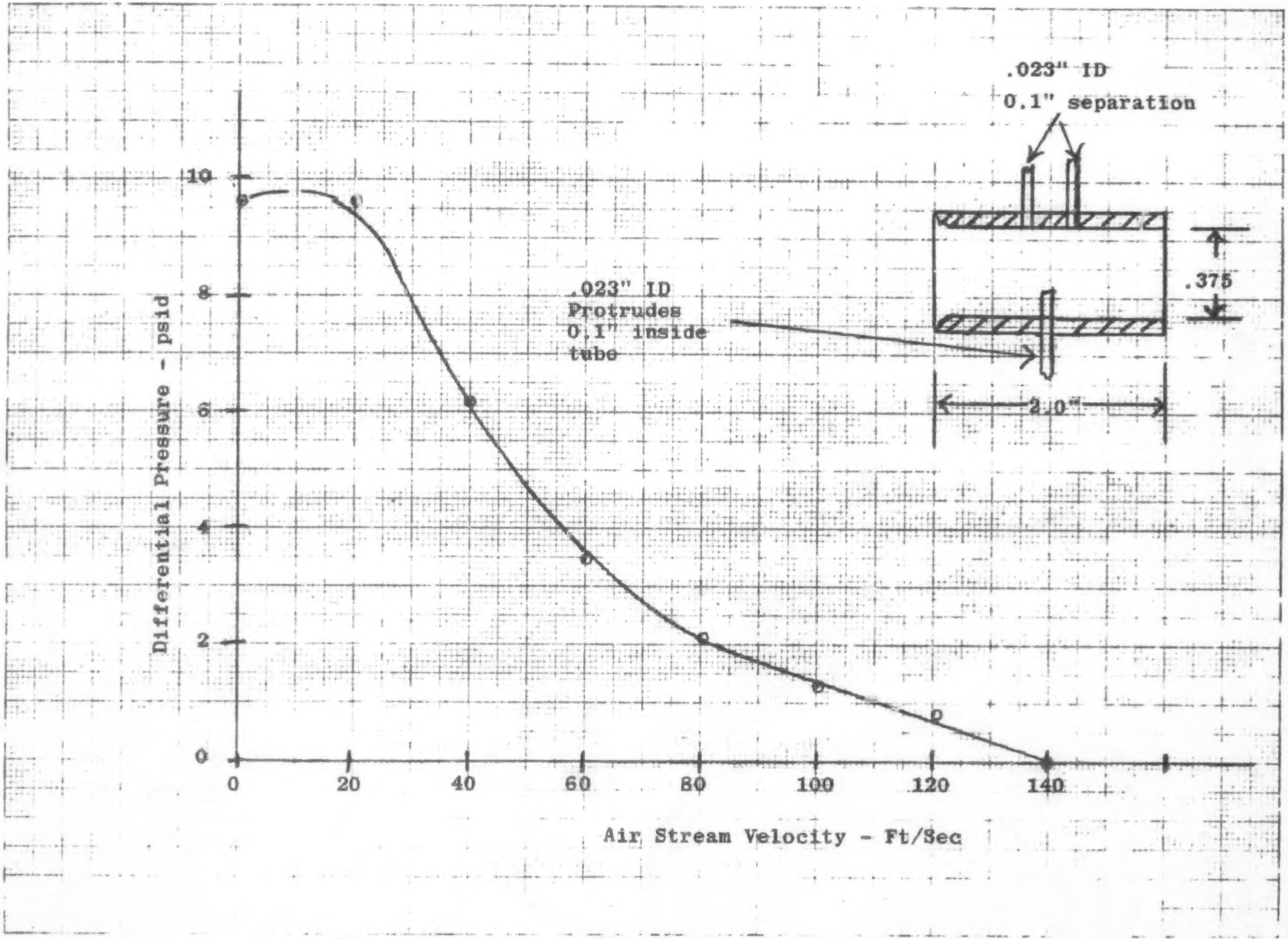

Figure A-14 Cross Flow Signal Upstream Receiver

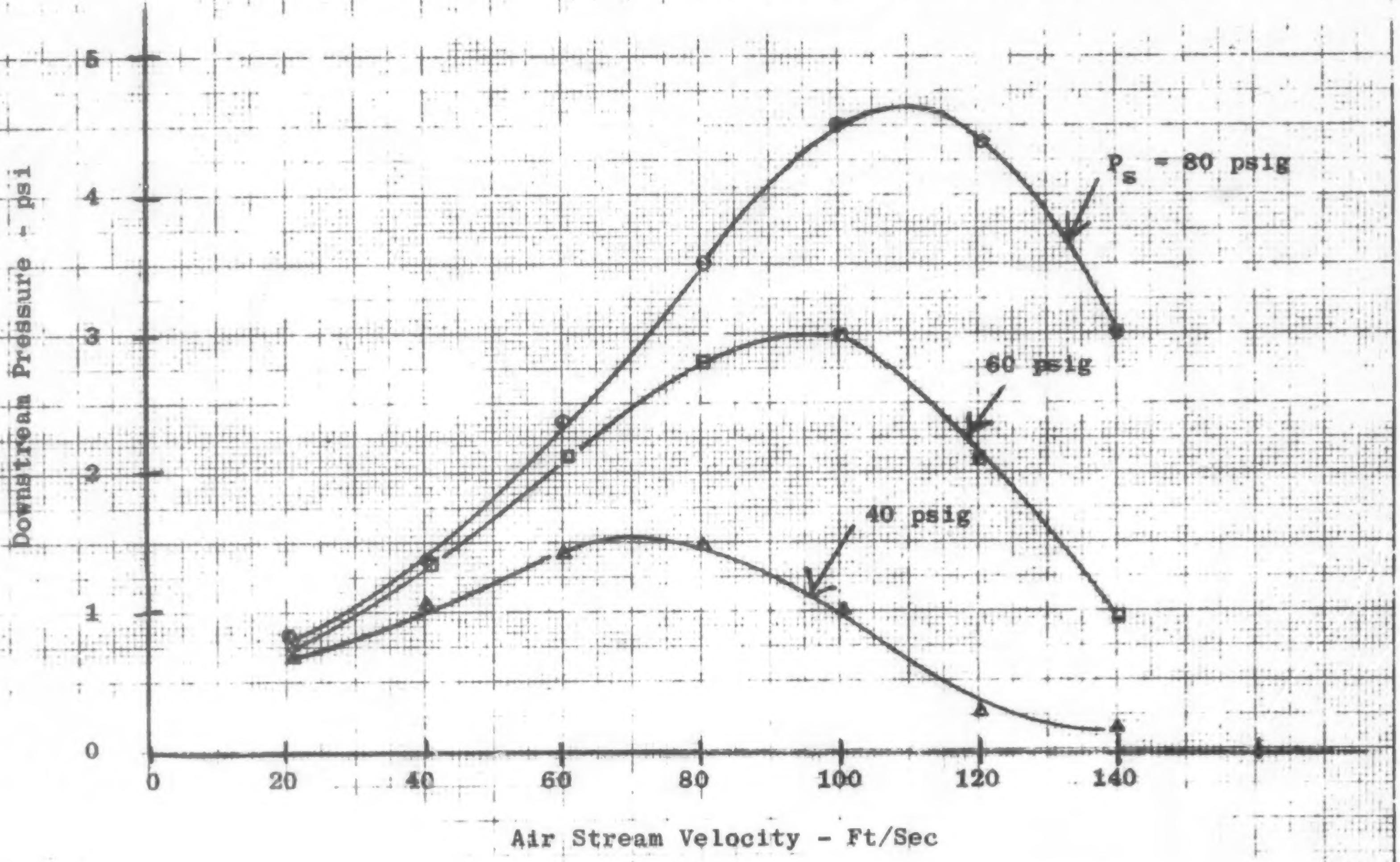

Figure A-15. Cross-Flow Signal Downstream Receiver

UN-155 (8 GENERAL ELECTRIC COMPA SCHENECTADY, N. Y. U.S.A. 160X220 29/61 5 Divisions

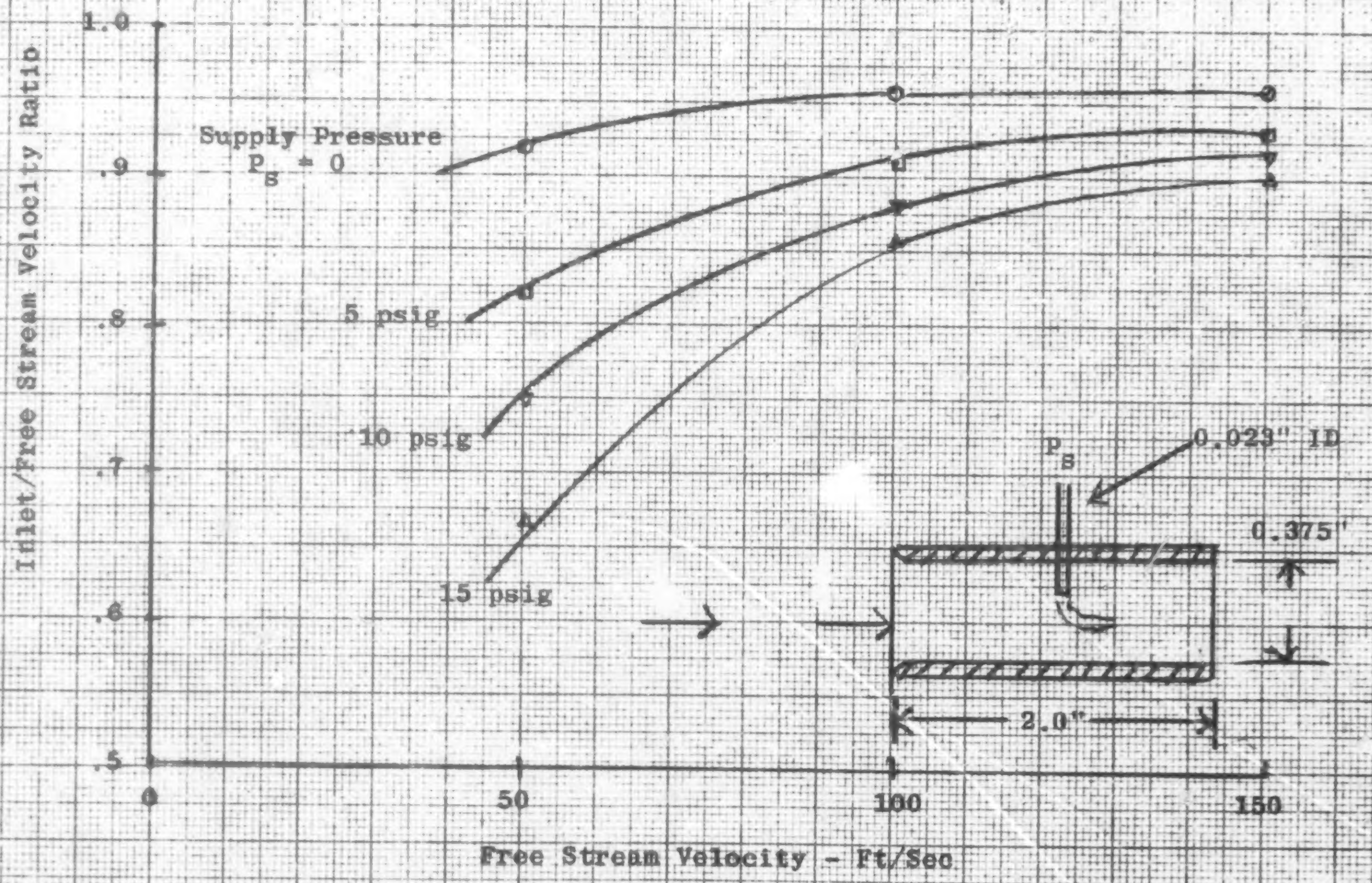

Figure A-16 Velocity Deceleration at Inlet

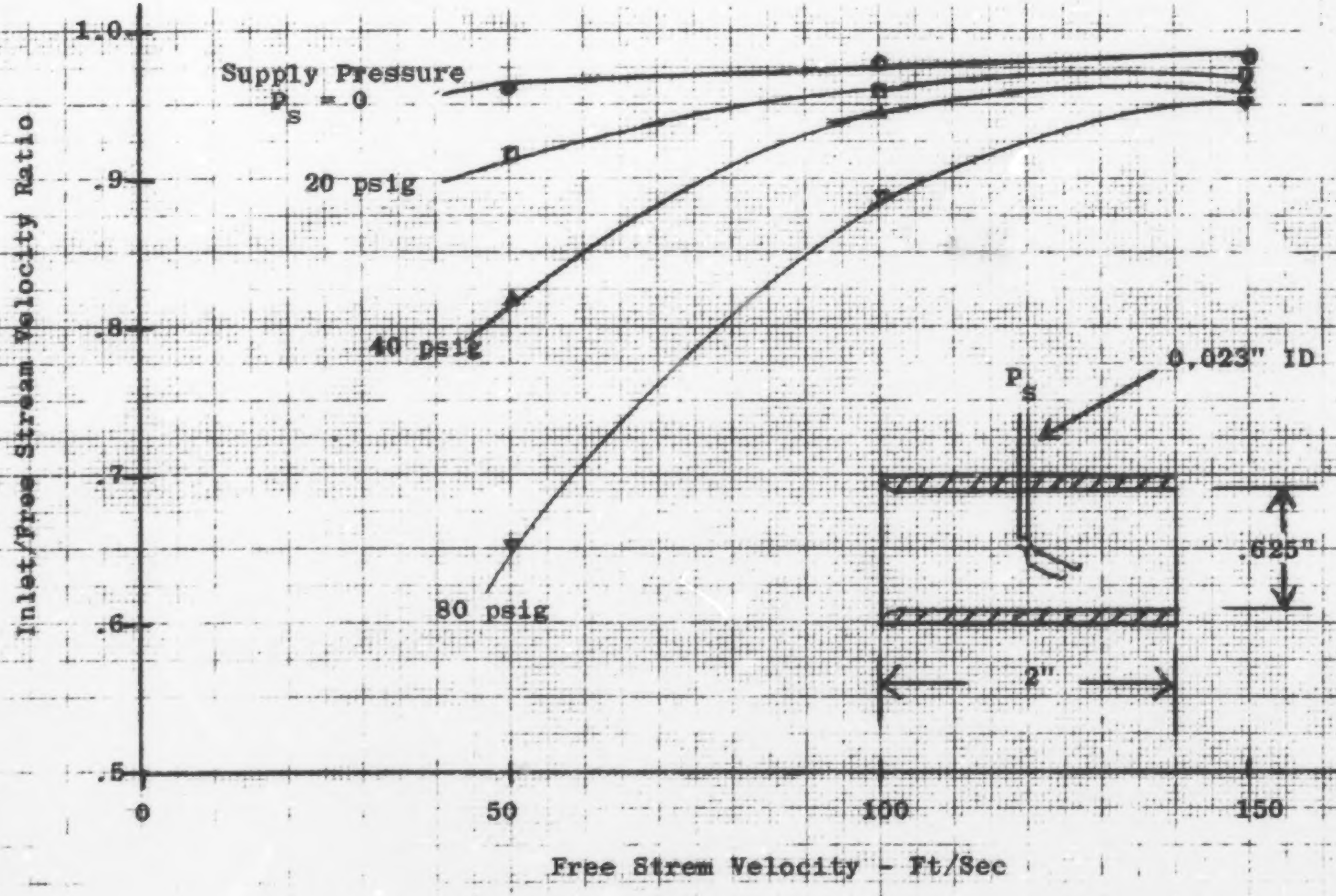

Figure A-17. Velocity Deceleration at Inlet

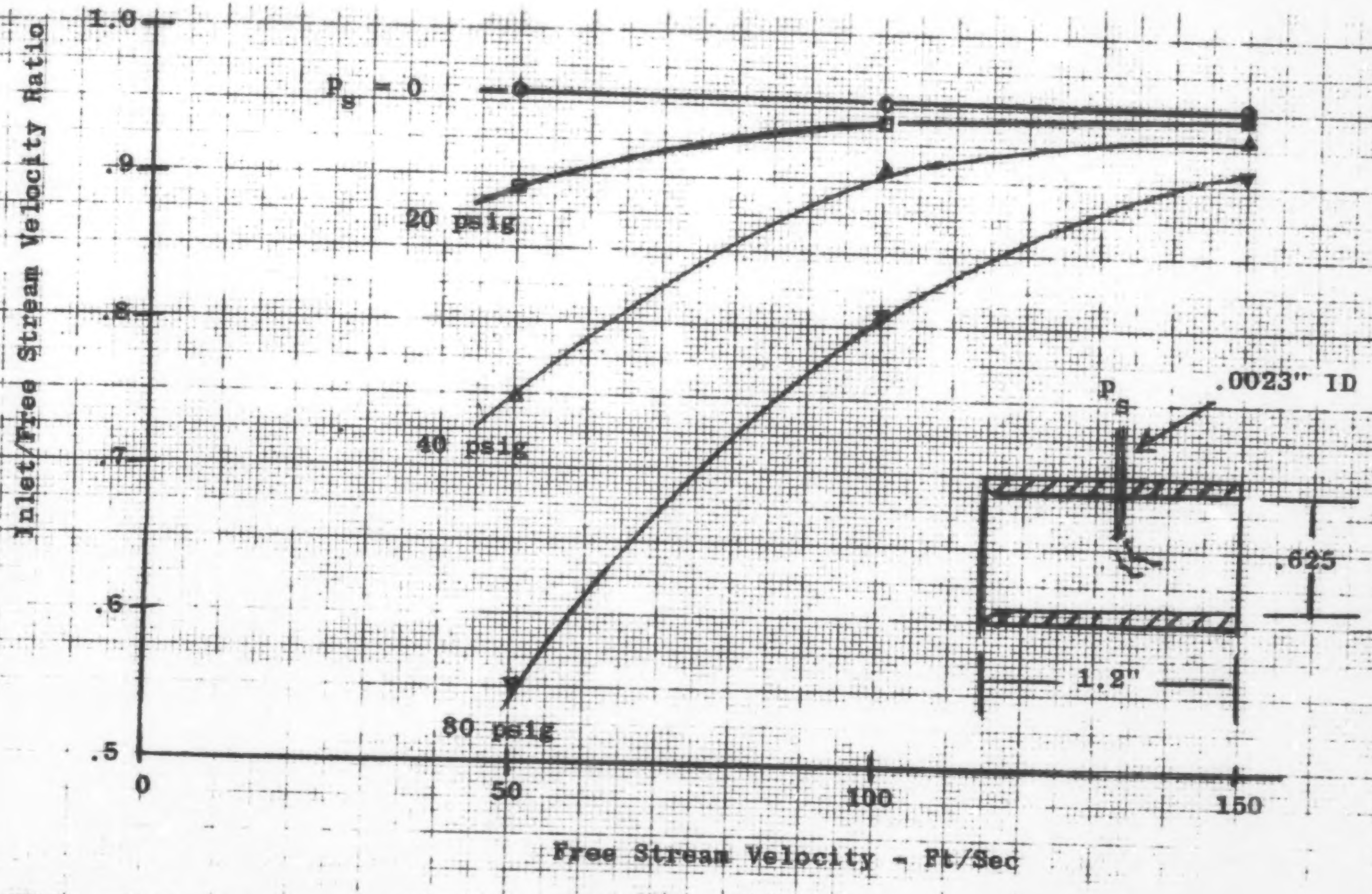
Inlet/Free Stream Velocity Ratio
1.0
.9
.8
.7
.6
.5
0
50
100
150
Free Stream Velocity - Ft/Sec
P_s = 0
20 psig
40 psig
80 psig
P_s
.0023" ID
.625
1.2"

$$\% \text{ of error} \propto \frac{w}{A^2 V_o^2} = (1 - V/V_o)\ 100$$

where w = sensor mass flow
A = shroud area
V_o = free stream velocity

Extrapolation of these results to 20 ft/sec and 1000F yields a minimum shroud diameter on the order of 3.5 inches and a length of 7 inches to maintain the error to less than 5% with a 40 psig supply. In addition to the prohibitive size, the advantage of being able to use identical geometry for the free air stream and sample probe sensor is lost.

The sensor noise characteristics are plotted in Figure A-19.

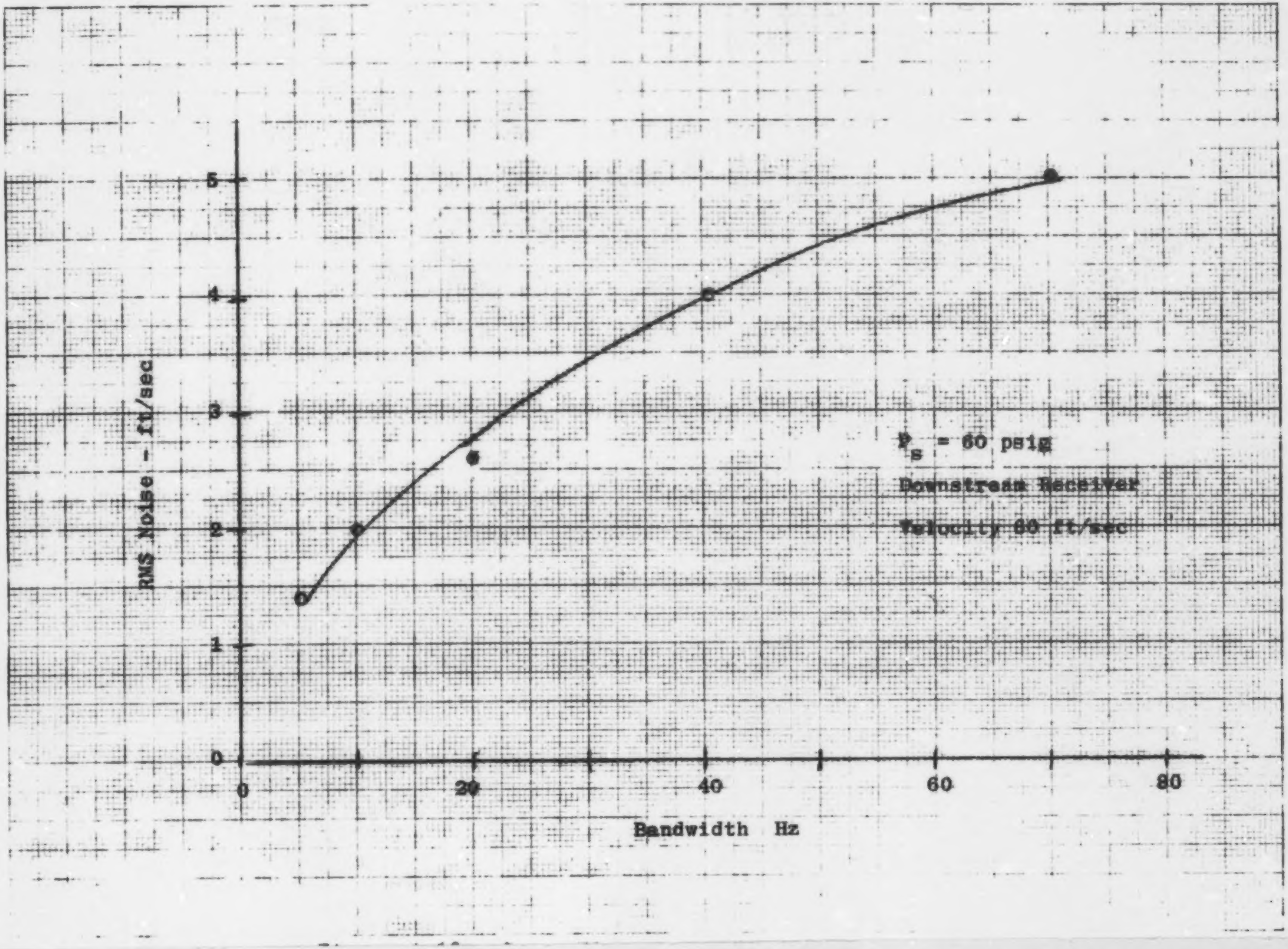
RMS Noise - ft/sec
5
4
3
2
1
0
0
20
40
60
80
Bandwidth Hz
P_s = 60 psig
Downstream Receiver
Velocity 60 ft/sec

APPENDIX II

FLUIDIC CONTROLLER PARTS IDENTIFICATION

APPENDIX II

Figures A-20 and A-21 show the location of the component parts making up the fluidic controller and the input-output connections. Figure A-22 shows the location on inlet and outlet connectors to the console.

The component parts, with the function and General Electric model number, are listed in Table #2. The input-output connectors are identified in Table #3.

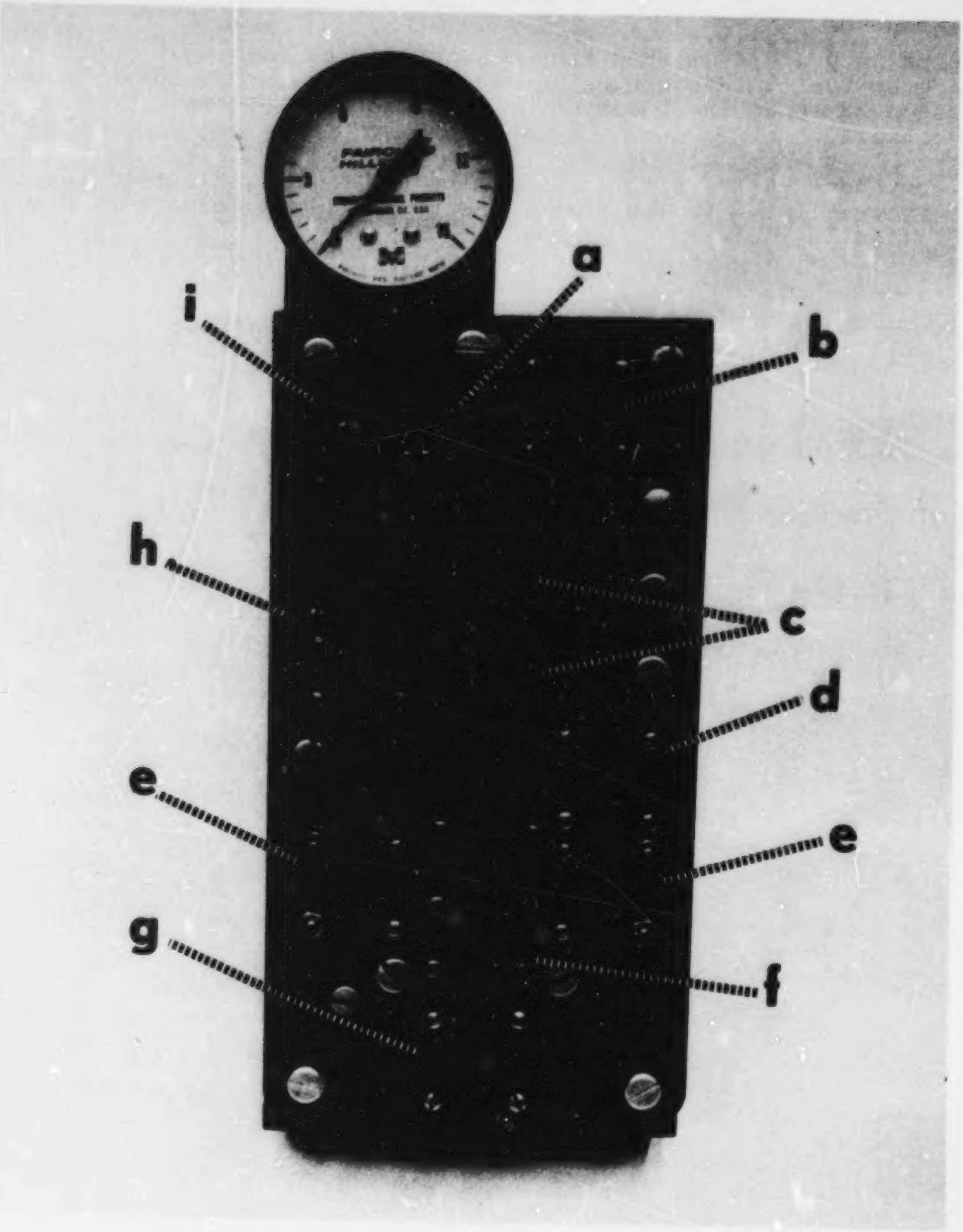

Figure A-20 Fluidic Controller - Front Face

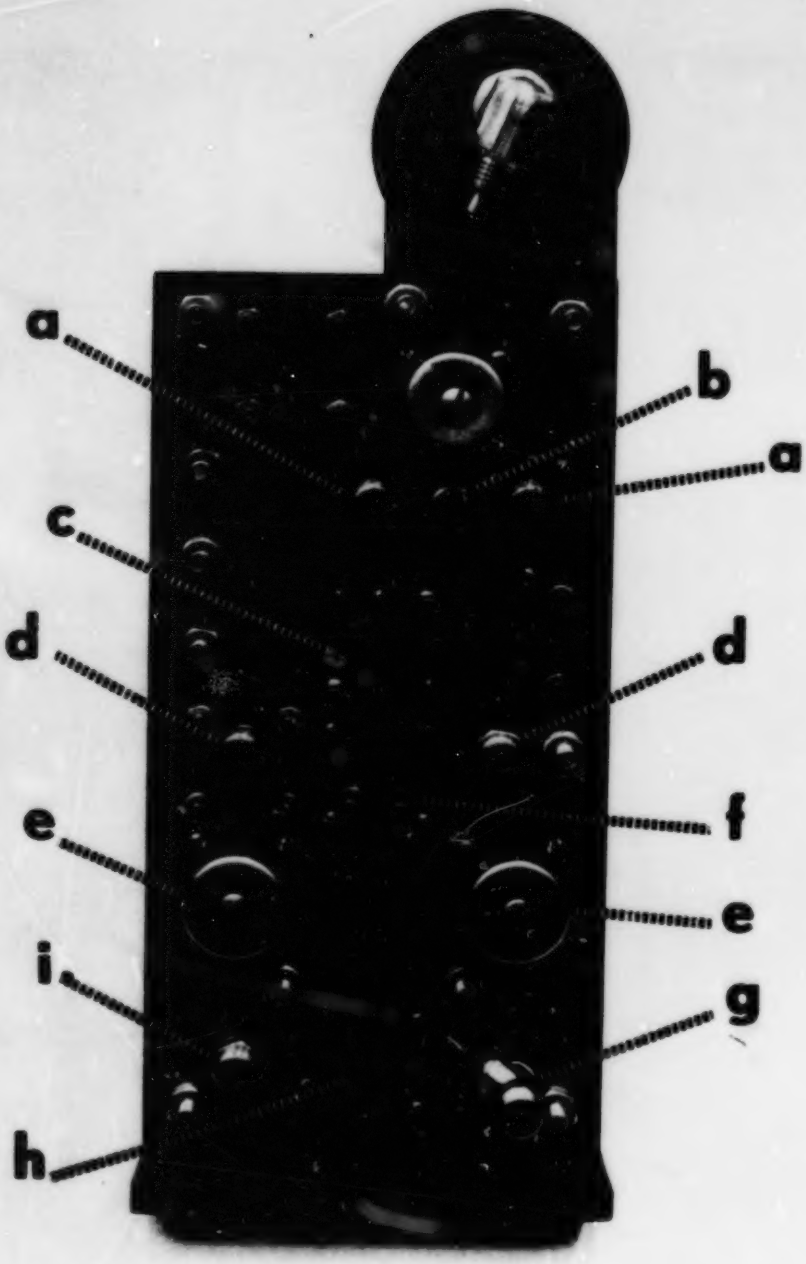

Figure A-21 Fluidic Controlkr - Back Face

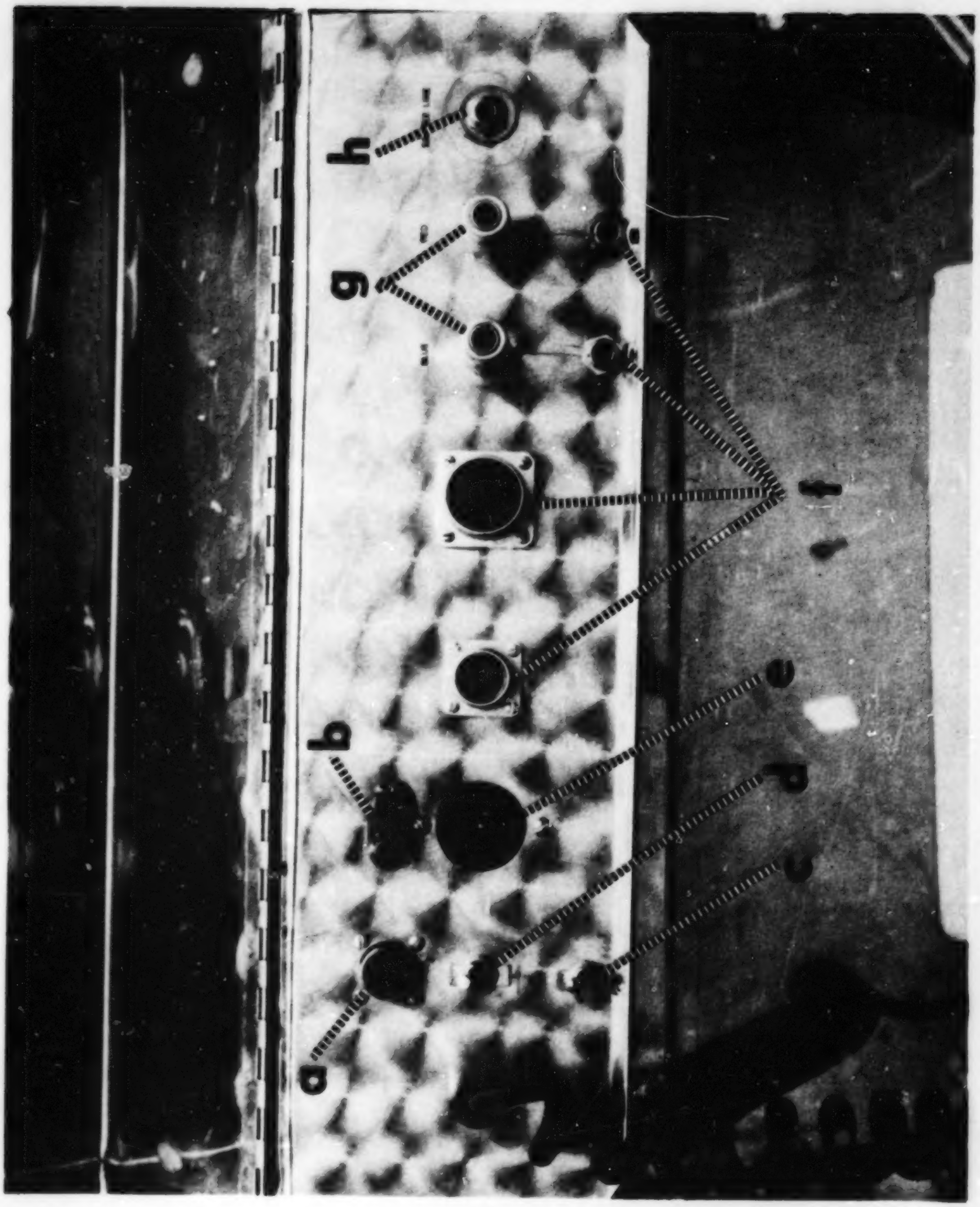

Figure A-22 Control Console Connectors

Table 2

COMPONENT PARTS

Location	Description	Part Number
	Front Face of Controller	
a	Input stage	CR280QA1045
b	Gain adjust	CR280RV32
c	Preamplifiers	CR280QA1046
d	Preamplifier supply and filter	CR280QA1047
e	Lead-Lag feedback resistors	CR280RF32
f	Lead-Lag gain block	CR280AM12B
g	Output amplifier and filter	CR280QA1048
h	1st stage supply resistor	CR280QA1049
i	Gain changer	CR280QA1050
	Back Face of Controller	
c	By-pass resistor	CR280RF32
e	Lead-Lag capacitors	CR280CF32
f	Lead-Lag input resistors and bias resistors	CR280QA1051
h	Lead-Lag supply and filter	CR280QA1052

Table 3

INLET-OUTLET CONNECTIONS

Location	Description
	Back Face of Controller
a	Input from sensor
b	Stack static reference input
d	Bias adjust inputs
f	To stabilizing volumes
g	Output to valve
i	Air supply inlet
	Control Console
a	Flow meter
b	Flow meter output jack
c	Pump power switch
d	Main power switch
e	Pump outlet
f	Umbilical cord connectors
g	Inclined manometer
h	Pneumatic supply pressure

REFERENCES

1. Whiteley & Reed, "The effect of Probe Shape on the Accuracy of Sampling Flue Gases for Dust Content".

2. V. Vitols, "Theoretical Limits of Errors Due to Anisokinetic Sampling of Particulate Matter", Journal of Air Pollution Control Association, Feb. 1966, Vol. 16.

3. Carbonar, Colin & Olivari, "The Deflection of a Jet By a Crossflowing Stream and Its Application to Aneomometry", Paper R2, Fourth Cranfield Fluidics Conference, Mar. 1970.

4. Hayes, Tanney & Templin, "The Co-flowing Jet Velocity Sensor", Paper J1, Fifth Cranfield Fluidics Conference, June 1972.

5. Smith, Martin, Durst, Hyland, Logan & Hager, "Gas Sampling Improved and Simplified with New Equipment", APC Paper #67-119.